

FUNCTIONAL CHARACTERIZATION OF CYTOSOLIC
DDX41 SENSOR IN MEDIATING ANTIVIRAL IMMUNE
RESPONSE IN BLACK TIGER SHRIMP *Penaeus monodon*



Miss Suthinee Soponpong

จุฬาลงกรณ์มหาวิทยาลัย
CHULALONGKORN UNIVERSITY

A Dissertation Submitted in Partial Fulfillment of the Requirements
for the Degree of Doctor of Philosophy in Biochemistry and Molecular
Biology

Department of Biochemistry

Faculty of Science

Chulalongkorn University

Academic Year 2019

Copyright of Chulalongkorn University

ลักษณะสมบัติเชิงหน้าที่ของไซโทไซลิกซีนเซอร် DDX41 ในการเป็นตัวกลางตอบสนองการ
ต้านไวรัสในกิ้งกูดดำ *Penaeus monodon*



วิทยานิพนธ์นี้เป็นส่วนหนึ่งของการศึกษาตามหลักสูตรปริญญาวิทยาศาสตรดุษฎีบัณฑิต
สาขาวิชาชีวเคมีและชีววิทยาโมเลกุล ภาควิชาชีวเคมี
คณะวิทยาศาสตร์ จุฬาลงกรณ์มหาวิทยาลัย
ปีการศึกษา 2562
ลิขสิทธิ์ของจุฬาลงกรณ์มหาวิทยาลัย

Thesis Title	FUNCTIONAL CHARACTERIZATION OF CYTOSOLIC DDX41 SENSOR IN MEDIATING ANTIVIRAL IMMUNE RESPONSE IN BLACK TIGER SHRIMP <i>Penaeus monodon</i>
By	Miss Suthinee Soponpong
Field of Study	Biochemistry and Molecular Biology
Thesis Advisor	Professor Anchalee Tassanakajon, Ph.D.
Thesis Co Advisor	Piti Amparyup, Ph.D. Professor Taro Kawai, Ph.D.

Accepted by the Faculty of Science, Chulalongkorn University in
Partial Fulfillment of the Requirement for the Doctor of Philosophy

..... Dean of the Faculty of Science
(Professor POLKIT SANGVANICH, Ph.D.)

DISSERTATION COMMITTEE

..... Chairman
(Associate Professor TEERAPONG BUABOOCHA,
Ph.D.)

..... Thesis Advisor
(Professor Anchalee Tassanakajon, Ph.D.)

..... Thesis Co-Advisor
(Piti Amparyup, Ph.D.)

..... Thesis Co-Advisor
(Professor Taro Kawai, Ph.D.)

..... Examiner
(Associate Professor SUPAART
SIRIKANTARAMAS, Ph.D.)

..... Examiner
(Assistant Professor SAOWARATH JANTARO,
Ph.D.)

..... External Examiner
(Assistant Professor Ratee Wongpanya, Ph.D.)

สฤณี โสภณพงษ์ : ลักษณะสมบัติเชิงหน้าที่ของไซโทโซลิกเซ็นเซอร์ DDX41 ในการเป็นตัวกลางตอบสนอง การต้านไวรัสในกึ่งกุลาคำ *Penaeus monodon*. (FUNCTIONAL CHARACTERIZATION OF CYTOSOLIC DDX41 SENSOR IN MEDIATING ANTIVIRAL IMMUNE RESPONSE IN BLACK TIGER SHRIMP *Penaeus monodon*) อ.ที่ปรึกษาหลัก : ศ. ดร.อัญชลี ทศนาขจร, อ.ที่ปรึกษาร่วม : ดร. ปิติ อ่ำพ่าย,ศ. ดร.ทาโร คาร์วายน

โปรตีน DDX41 เป็นตัวตรวจจับที่อยู่ในกลุ่มของโปรตีน DEXD ซึ่งถูกค้นพบเมื่อเร็วๆนี้ โดยทำหน้าที่เป็นตัวตรวจจับ DNA ภายในเซลล์ในสัตว์ที่มีกระดูกสันหลัง ในการศึกษาเราทำการสืบหาว่ามีตัวตรวจจับ DDX41 ในกึ่ง *Penaeus monodon* หรือไม่ โดยการหา ยีนที่เกี่ยวข้องกับการตรวจจับของ DNA จากฐานข้อมูล EST ในกึ่งกุลาคำ พบ cDNA 3 ชิ้น ซึ่งมีความเหมือนกับ DDX41 ในสิ่งมีชีวิตสาย พันธุ์ต่างๆ และเมื่อนำมาประกอบกันพบว่าเป็น ORF ของยีน DDX41ในกึ่งกุลาคำ (*PmDDX41*) ที่สมบูรณ์ ซึ่งมีขนาด 1868 คู่เบส สามารถแปลเป็นโปรตีนที่มีกรดอะมิโน 620 ตัว จากการทำ multiple sequence alignment ของโปรตีน *PmDDX41* ในกึ่งกุลาคำกับ สิ่งมีชีวิตชนิดอื่นพบว่า โปรตีนจะประกอบด้วยโดเมนอนุรักษ์จำนวน 3 โดเมนคือ โดเมน DEADc, โดเมน HELICc และ โดเมน Zinc finger โปรตีน *PmDDX41* มีความเหมือนกับโปรตีน DDX41 ในคั้ง และปู (83%) การวิเคราะห์การแสดงผลออกพบว่ายีน *PmDDX41* มีการแสดงออกในทุกเนื้อเยื่อที่มีการทดสอบ การวิเคราะห์การแสดงผลออกของยีน *PmDDX41* ในเม็ดเลือดกึ่งเมื่อมีการติดเชื้อก่อโรคโดย quantitative RT-PCR พบว่า ยีน *PmDDX41* มีการแสดงออกเพิ่มขึ้นที่เวลา 6 และ 48 ชั่วโมงหลังจากการฉีดไวรัสตัวแดงดวงขาว (WSSV) ในทางตรงข้ามพบว่า เมื่อมีการติดเชื้อ *Vibrio harveyi* พบว่า การแสดงผลออกของยีน *PmDDX41* ไม่มีการเปลี่ยนแปลง เมื่อทำการยับยั้งการแสดงผลออกของยีน *PmDDX41* พบว่ายีน *PmIKK β* , *PmIKK ϵ* , *PmPEN3* and *PmPEN5* มีการแสดงออกลดลง นอกจากนี้กึ่งที่ทำการยับยั้งการแสดงผลออกของยีน *PmDDX41* มีอัตราการตายเพิ่มขึ้นเมื่อมีการติดเชื้อไวรัส WSSV นอกเหนือจากนี้ เราพบว่าใน เม็ดเลือดกึ่งในสภาวะปกติ *PmDDX41* มีการแสดงออกในไซโทพลาสซึม แต่ในสภาวะที่มีการติดเชื้อไวรัสตัวแดงดวงขาว หรือเมื่อมีการกระตุ้น ด้วย poly(dA:dT) และ poly(I:C) *PmDDX41* มีการแสดงออกทั้งในไซโทพลาสซึมและนิวเคลียส ซึ่งผลการทดลองมีความคล้ายกันเมื่อ *PmDDX41* เมื่อถูกใส่เข้าไปในเซลล์ HEK293T นอกจากนี้เมื่อทำการทดลองด้วยวิธี immunoprecipitation พบว่า *PmDDX41* สามารถจับกับ poly(dA:dT) แต่ไม่จับกับ poly(I:C) การแสดงผลออกโปรตีน *PmDDX41* และ *MmSTING* ของหนู ในเซลล์ HEK293T พบว่าสามารถกระตุ้นการส่งสัญญาณในวิถี interferon และ NF- κ B โดยผ่านโดเมน DEADc เมื่อทำการยื่นยื่นการจับกันของ *PmDDX41* และ *MmSTING* เมื่อมีการกระตุ้นด้วย poly (dA:dT) การศึกษานี้เป็นครั้งแรกที่พบว่า *PmDDX41* ทำหน้าที่เป็นตัว ตรวจจับ DNA ในไซโทพลาสซึม ซึ่งสามารถจับกับ STING โดยใช้โดเมน DEADc เพื่อกระตุ้นการส่งสัญญาณไปยังวิถี IFN- β และ NF- κ B ซึ่งมีบทบาทในระบบภูมิคุ้มกันที่ตอบสนองต่อไวรัส

จุฬาลงกรณ์มหาวิทยาลัย
CHULALONGKORN UNIVERSITY

สาขาวิชา ชีวเคมีและชีววิทยาโมเลกุล
ปีการศึกษา 2562

ลายมือชื่อนิสิต
ลายมือชื่อ อ.ที่ปรึกษาหลัก
ลายมือชื่อ อ.ที่ปรึกษาร่วม
ลายมือชื่อ อ.ที่ปรึกษาร่วม

5672120423 : MAJOR BIOCHEMISTRY AND MOLECULAR BIOLOGY

KEYWORD: antiviral immune response, DDX41, immune signaling pathway, *Penaeus monodon*, STING

Suthinee Soponpong : FUNCTIONAL CHARACTERIZATION OF CYTOSOLIC DDX41 SENSOR IN MEDIATING ANTIVIRAL IMMUNE RESPONSE IN BLACK TIGER SHRIMP *Penaeus monodon*. Advisor: Prof. Anchalee Tassanakajon, Ph.D. Co-advisor: Piti Amparyup, Ph.D., Prof. Taro Kawai, Ph.D.

DEAD (Asp-Glu-Ala-Asp) box polypeptide 41 (DDX41), a receptor belonging to the DExD family, was recently identified as an intracellular DNA sensor in vertebrates. Here, we investigated the presence of cytosolic DNA sensing, DDX41 in shrimp *Penaeus monodon*. By searching for gene involved in DNA sensing cascade within the shrimp *P. monodon* EST database, 3 cDNA fragments exhibited similarity to DDX41 in various species were identified. Sequences assembly resulted in a complete ORF of *Penaeus monodon* DDX41 (*PmDDX41*) which has 1868-bp encoding a putative protein of 620 amino acid residues. The multiple sequence alignment of deduced amino acid sequence of *PmDDX41* with other species revealed that there are three conserved domains in the protein: DEADc domain, HELICc domain and Zinc finger domain. *PmDDX41* shares 83% similarity with DDX41 in bee and crab. The transcript of *PmDDX41* was detected in all tested tissues. Gene expression profile of *PmDDX41* in hemocyte of pathogen challenged was analyzed by quantitative RT-PCR. The results showed that the *PmDDX41* transcript of White Spot Syndrome Virus (WSSV) challenged shrimp was up-regulated at 6 and 48 hpi when compared to the control shrimp. On the contrary, after challenge with *Vibrio harveyi*, *PmDDX41* mRNA expression was not significantly changed at all time points when compared with the control PBS-injected shrimp. Knockdown of *PmDDX41* by dsRNA-mediated gene silencing resulted in a decrease of the mRNA expression level of *PmIKK β* , *PmIKK ϵ* , *PmPEN3* and *PmPEN5* genes. Moreover, *PmDDX41*-knockdown shrimp exhibited increase in the cumulative mortality after WSSV infection. In addition, *PmDDX41* was localized in the cytoplasm of shrimp hemocytes and upon WSSV infection or stimulation the nucleic acid mimics, poly(dA:dT) and poly(I:C), it was found in both the cytoplasm and nucleus of hemocytes. Similar results were observed when *PmDDX41* was transfected into human embryonic kidney 293T (HEK293T) cells. Immunoprecipitation further demonstrated that *PmDDX41* bound to biotin-labeled poly(dA:dT) but not poly(I:C). The overexpression of shrimp *PmDDX41* and mouse stimulator of interferon gene (*MmSTING*) in HEK293T cells synergistically promoted IFN- β and NF- κ B promoter activity via the DEADc domain. Co-immunoprecipitation (Co-IP) also confirmed that there was an interaction between *PmDDX41* and STING after stimulation with poly(dA:dT) but not poly(I:C). Our study is the first to demonstrate that *PmDDX41* acts as a cytosolic DNA sensor that interacts with STING via its DEADc domain to trigger the IFN- β and NF- κ B signaling pathways, thus activating antiviral innate immune responses.

Field of Study:	Biochemistry and Molecular Biology	Student's Signature
Academic Year:	2019	Advisor's Signature
		Co-advisor's Signature
		Co-advisor's Signature

ACKNOWLEDGEMENTS

On the occasion of my graduation in Ph.D. program, I would like to express my deepest gratitude to my supervisor, Prof. Dr. Anchalee Tassanakajon for support of my Ph.D. study and research, for her patience, motivation, encouragement and immense knowledge. Her great guidance helped me in all the time of research.

Beside my supervisor, I wish to express my sincere gratitude and appreciation to my co-supervisor, Dr. Piti Amparyup for his hard teaching me all things in molecular biology, improve and inspire me to do the efficient research and for his guidance and encouragement throughout of my study.

My appreciation is also expressed to Prof. Dr. Taro Kawai for warm welcome and giving me an opportunity to join his laboratory and providing me research facilities at Nara Institute of Science and Technology (NAIST), Japan and thank you so much for his valuable and excellent guidance in research which helped me to widen my research from various perspectives.

Additional, great appreciation is extended to Assoc. Prof. Dr. Teerapong Buaboocha, Assoc. Prof. Dr. Supaart Sirikantaramas, Asst. Prof. Dr. Saowarath Jantaro and Asst. Prof. Dr. Ratrie Wongpanya for serving as thesis committee, for their valuable comments and also useful suggestions.

My great appreciation is expressed to Professor Dr. Vichien Rimphanitchayakit, Assoc. Prof. Dr. Kunlaya Somboonwiwat, Assoc. Prof. Dr. Kuakarun Krusong and all colleagues at Center of Excellence for Molecular Biology and Genomics of Shrimp for giving me the helpful suggestions and precious supports. Special thanks to Dr. Warunthorn Monwan during my laboratory practice in Japan, Dr. Kantamas Apitanyasai with her technical assistance and all member at CEMs laboratory and molecular immunobiology laboratory for their encouragement and unconditional support.

I wish to acknowledge to contribution of the 100th Anniversary Chulalongkorn University Fund, joint funding of the Thailand Research Fund (TRF). I also gratefully acknowledge additional support from the 90th Anniversary of Chulalongkorn University Fund for my financial support and the Overseas Research Experience Scholarship for Graduate Student from the Graduate School, Chulalongkorn University.

Finally, and most importantly, I would like to thank my family for the great supporting me throughout my Ph.D. study. I would not have been able to complete my studies without their endless love, understanding and unconditional support along my life.

Suthinee Soponpong

1.6 Nucleic acid-induced antiviral immunity in invertebrates	14
1.6.1 Toll, IMD, and JAK/STAT pathways in antiviral immunity.....	15
1.6.1.1 Toll pathway in invertebrates	16
1.6.1.2 IMD pathway in invertebrates	19
1.6.1.3 JAK/STAT Pathway in Invertebrates	20
1.6.2 Cytosolic sensing pathway in antiviral immunity	22
1.6.2.1 RNA sensing-induced antiviral immunity by Dicer-2	22
1.6.2.2 RIG-I-like receptors (RLRs) in invertebrate antiviral immunity	25
1.6.2.3 DNA-sensing pathway in invertebrates	26
1.6.2.3.1 cGAS-STING pathway in antiviral immunity	27
1.6.2.3.2 DDX41 signaling pathway in antiviral immunity	29
1.7 Propose of this thesis research	30
MATERIALS AND METHODS.....	32
2.1 Equipment and chemicals	32
2.1.1 Equipment.....	32
2.1.2 Chemicals, reagents and biological substances	34
2.1.3 Enzymes and kits	38
2.1.4 Primary and secondary antibodies	39
2.1.5 Microorganisms	40
2.1.6 Software	40
2.2 Shrimp samples.....	41

2.3 Total RNA extraction and cDNA preparation	41
2.4 Primer design	42
2.5 Cloning and sequencing of open reading frame (ORF) cDNA of <i>PmDDX41</i> ...	44
2.6 Sequence analysis	44
2.7 Tissue distribution analysis.....	45
2.8 Gene expression analysis in response to pathogen infection and nucleic acid mimics stimulation	45
2.8.1 Microbial challenge	45
2.8.2 Nucleic acid mimics stimulation	46
2.8.3 RNA extraction and cDNA synthesis	46
2.8.4 Quantitative real time-PCR (qRT-PCR) analysis.....	46
2.9 <i>In vivo</i> Gene silencing.....	47
2.9.1 Preparation of double-stranded RNAs (dsRNAs)	47
2.9.2 Shrimp preparation and injection	48
2.9.3 Extraction of total RNA and synthesis of cDNA	48
2.9.4 Semi-quantitative RT-PCR analysis	49
2.9.5 Effect of <i>PmDDX41</i> gene silencing on the expression of other immune genes	49
2.9.6 Cumulative mortality assay	50
2.10 Protein expression of <i>PmDDX41</i> in <i>E. coli</i> system.....	50
2.10.1 Plasmid construction.....	50
2.10.2 Protein expression and western blot analysis	52

2.11 Localization of <i>PmDDX41</i> in hemocyte by immunofluorescence microscopy	52
2.12 HEK293T cells preparation	53
2.13 Luciferase activity assay of <i>PmDDX41</i>	54
2.13.1 Plasmid construction	54
2.13.2 Luciferase reporter assay	55
2.14 Localization of <i>PmDDX41</i> in HEK293T cells after stimulation with nucleic acid mimics	56
2.15 Binding activity of <i>PmDDX41</i> protein with nucleic acid mimics	56
2.15.1 Biotin labeled nucleic acids	56
2.15.2 Protein expression of <i>PmDDX41</i> in HEK293T cells	57
2.15.3 Co-immunoprecipitation	57
2.16 Luciferase reporter assay of <i>PmDDX41</i> after co-transfected with <i>MmSTING</i>	57
2.16.1 Cloning of <i>PmDDX41</i> into pCMV-5 expression vector	57
2.16.2 Luciferase assay detection after co-transfection with <i>MmSTING</i>	59
2.17 Localization of <i>PmDDX41</i> and <i>MmSTING</i> in HEK293T cells	59
2.18 Characterization of <i>PmDDX41</i> and <i>MmSTING</i> protein in HEK293T cells	60
2.18.1 Protein expression and Co-immunoprecipitation	60
2.18.2 SDS-PAGE and western blotting	60
2.19 Analysis of DNA-binding site of <i>PmDDX41</i>	61
2.19.1 IFN- β and NF- κ B luciferase activity assay	61

2.19.1.1 Construction of the expression plasmid	61
2.19.1.2 IFN- β and NF- κ B luciferase activity detection of mutated- PmDDX41	61
2.19.1.3 IFN- β and NF- κ B luciferase activity detection of mutant- PmDDX41 and MmSTING in cells.....	62
2.19.2 Localization of mutant- <i>PmDDX41</i> proteins.....	62
2.19.3 Immunofluorescence confocal microscopy of mutated- <i>PmDDX41</i> and <i>MmSTING</i>	63
2.19.4 Interaction of mutated- <i>PmDDX41</i> and <i>MmSTING</i>	63
2.19.4.1 Protein expression and Co-immunoprecipitation.....	63
2.19.4.2 SDS-PAGE and western blot analysis	64
RESULTS	65
3.1 Searching the <i>Penaeus monodon</i> EST database and cloning the open reading frame (ORF) of <i>PmDDX41</i>	65
3.2 Multiple sequence alignment and phylogenetic analysis.....	67
3.3 Tissue distribution of <i>PmDDX41</i>	71
3.4 Expression profiles of <i>PmDDX41</i> transcript after pathogen challenges	71
3.5 Expression profiles of <i>PmDDX41</i> transcript after nucleic acid mimics stimulation	73
3.6 The effect of RNAi-mediated gene silencing of <i>PmDDX41</i> on the expression of shrimp immune-related genes.....	74
3.6.1 Preparation of dsRNA <i>PmDDX41</i> and GFP	74
3.6.2 Effect of silencing of <i>PmDDX41</i> on the expression of shrimp immune- related genes	75

3.16 Interactions of <i>PmDDX41</i> domains and <i>MmSTING</i> in HEK293T cells.....	98
3.17 Co-localization of mutated- <i>PmDDX41</i> with <i>MmSTING</i> in HEK293T cells.	100
DISCUSSIONS.....	103
CONCLUSIONS.....	113
REFERENCES	116
REFERENCES	124
VITA.....	126



LIST OF TABLES

Page

Table 1 Nucleotide sequences of the primers used in this study	43
----------------------------------------------------------------------	----



LIST OF FIGURES

	Page
Fig. 1 Shrimp aquaculture production in major farming countries in Asia during 2011-2018.	2
Fig. 2 Anatomy of black tiger shrimp (<i>Penaeus monodon</i>) (Motoh, 1985).....	4
Fig. 3 White spot disease.....	5
Fig. 4 Overview of WSSV entry and environment interactions.....	8
Fig. 5 Yellow head disease.....	10
Fig. 6 Vibriosis in <i>Litopenaeus vannamei</i>	11
Fig. 7 The infected shrimp caused by early mortality syndrome or Acute Hepatopancreatic Necrosis Disease (EMS/AHPND).....	12
Fig. 8 A model of the shrimp immune system (Tassanakajon et al., 2013).	14
Fig. 9 Immune signaling pathways in insects that share the core elements of mammalian NF- κ B, IRF3, and JAK/STAT pathways.....	16
Fig. 10 Insect RNA sensing-induced antiviral immunity by Dicer-2.....	24
Fig. 11 The model of the RIG-I pathway in the Pacific oyster <i>Crassostrea gigas</i> ...26	26
Fig. 12 STING-mediated innate immune response.....	28
Fig. 13 The signaling pathway of DDX41 in innate immunity.....	30
Fig. 14 The map of pET-22b (+) expression vector (Novagen).	51
Fig. 15 The map of pcDNA3-Myc expression vector (Santa Cruz Biotechnology).	55
Fig. 16 The map of pCMV5-Flag expression vector (Sigma).	58
Fig. 17 Sequence and domain analysis of <i>PmDDX41</i>	66
Fig. 18 Sequence analysis of <i>PmDDX41</i> gene.....	68

Fig. 19 Phylogenetic tree of <i>PmDDX41</i>	69
Fig. 20 The semi-quantitative RT-PCR analysis of <i>PmDDX41</i> gene expression in shrimp tissues.	71
Fig. 21 Relative expression levels of <i>PmDDX41</i> in shrimp hemocytes at different time points after challenged with pathogens: (A) WSSV, (B) YHV and (C) <i>Vibrio harveyi</i>	72
Fig. 22 Relative expression levels of <i>PmDDX41</i> in shrimp hemocytes at different time points after injected with (A) poly(dA:dT) and (B) poly(I:C).	73
Fig. 23 The agarose gel electrophoresis of single strand RNA of <i>PmDDX41</i> and GFP and purification of dsRNA <i>PmDDX41</i> and GFP.	75
Fig. 24 Effect of gene silencing of <i>PmDDX41</i> on the expression level of the antiviral and antimicrobial peptide-associated genes.	78
Fig. 25 Percent survival of <i>PmDDX41</i> silenced shrimp challenged with WSSV.....	79
Fig. 26 PCR amplification of <i>PmDDX41</i> and plasmid DNA screening for protein expression.	80
Fig. 27 The detection of <i>PmDDX41</i> by SDS-PAGE and western blot analysis using rabbit polyclonal anti-human-DDX41.	81
Fig. 28 Localization of <i>PmDDX41</i> in shrimp hemocytes after challenged with WSSV, as visualized by fluorescence microscopy.....	82
Fig. 29 Localization of <i>PmDDX41</i> in shrimp hemocytes after stimulated with poly(dA:dT) and poly(I:C), as visualized by fluorescence microscopy.....	84
Fig. 30 The amplification of gene coding for <i>PmDDX41</i> and <i>MmDDX41</i>	85
Fig. 31 Screening of the recombinant plasmids using restriction enzymes <i>Bam</i> HI and <i>Xho</i> I and protein expression in HEK293T cells.	86
Fig. 32 Interaction of <i>PmDDX41</i> with nucleic acid mimics.	87
Fig. 33 Localization of <i>PmDDX41</i> in HEK293T cells after stimulated with poly(dA:dT) and poly(I:C), as visualized by fluorescence microscopy.	88

Fig. 34 The activation of (A) IFN- β and (B) NF- κ B promoter in HEK293T cells.	90
Fig. 35 The western blotting of <i>PmDDX41</i> and <i>MmSTING</i> protein in HEK293T cells.	92
Fig. 36 Luciferase activity assay of IFN- β (A) and NF- κ B (B) in HEK293T cells.	93
Fig. 37 Interaction of <i>PmDDX41</i> and <i>MmSTING</i> in HEK293T cells.	94
Fig. 38 Co-localization of <i>PmDDX41</i> with <i>MmSTING</i> in HEK293T cells after stimulated with poly(dA:dT) and poly(I:C), as visualized by fluorescence microscopy.....	96
Fig. 39 Activation of IFN- β and NF- κ B promoter in HEK293T cells transfected with different <i>PmDDX41</i> domains.....	97
Fig. 40 Interaction between <i>PmDDX41</i> domains and <i>MmSTING</i> in HEK293T cells.	99
Fig. 41 Co-localization of mutated- <i>PmDDX41</i> and <i>MmSTING</i> in HEK293T cells after stimulated with poly(dA:dT) and poly(I:C), as visualized by fluorescence microscopy.....	101
Fig. 42 The signaling pathway of <i>PmDDX41</i> in innate immunity.....	115

LIST OF ABBREVIATIONS

°C	degree Celsius
AHPND	acute hepatopancreatic necrosis disease
bp	base pairs
BSA	bovine serum albumin
cDNA	complementary deoxyribonucleic acid
CFU	colony forming unit
cGAS	cyclic GMP-AMP (cGAMP) synthase
DDX41	DEAD (Asp-Glu-Ala-Asp)-box polypeptide 41
dsDNA	double stranded deoxyribonucleic acid
dsRNA	double stranded ribonucleic acid
EF1- α	elongation factor 1 alpha
EMS	early mortality syndrome
EST	expressed sequence tag
g	gram
GFP	green fluorescence protein
h	hour
hpi	hours post infection
HEK293T	human embryonic kidney 293 T
IFNs	interferons
IPTG	isopropyl-beta-D-thiogalactopyranoside

IRF	interferon regulatory transcription factor
kb	kilobase
kDa	kiloDalton
LB	Luria-Bertani
LPS	lipopolysaccharide
<i>Lv</i>	<i>Litopenaeus vannamei</i>
μ M	micromolar
μ g	microgram
μ l	microliter
m	milli
M	molar
min	minute
ml	mililitre
NF- κ B	nuclear factor kappa B
O.D.	optical density
ORF	open reading frame
PAGE	polyacrylamide gel electrophoresis
PAMPs	pathogen-associated molecule patterns
PEI	polyethyleneimine
PBS	phosphate-buffered saline
PCR	polymerase chain reaction
<i>Pm</i>	<i>Penaeus monodon</i>

PRRs	pattern recognition receptors
r	recombinant
RLRs	retinoic acid-inducible gene I (RIG-I)-like receptors
RNAi	ribonucleic acid interference
RT-PCR	reverse transcription/polymerase chain reaction
SD	standard deviation
SDS	sodium dodecyl sulfate
s	second
STING	stimulator of interferon genes
TLRs	Toll-like receptors
WSSV	white spot syndrome virus
YHV	yellow head virus

CHAPTER 1

INTRODUCTION

1.1 Shrimp Aquaculture

Production of farmed shrimp has grown at the phenomenal rate of 20-30% per year. The leading shrimp producers are in the Asia-Pacific region while the major markets are in Japan, the U.S.A. and Europe. Total aquaculture production, grew steadily in Asia through 2011, with 6 percent annual growth from 2008 to 2011 (**Fig. 1**). The decline of shrimp production in Asia during 2012-2013 was due to the impact of an emerging disease, early mortality syndrome (EMS). This outbreak caused huge economic losses in Southern China then expanded to Vietnam, Malaysia and reached Thailand in 2012 (Tran et al., 2013b). Thailand is the world's leading shrimp-farming nation. It exports the most shrimp in volume and value, and is the top supplier of farmed shrimp to the United States and Japan. Traditionally, the Thai shrimp industry farmed black tiger shrimp, *Penaeus monodon*, but since 2001, it has undergone a dramatic transformation and switched to Pacific white shrimp, *Litopenaeus vannamei* (Wyban, 2007). Since the rapid expanding shrimp aquaculture in the last few decades, the sustainability for shrimp farming has been concerned. Because shrimp farming is threatened by several disease outbreaks, shrimp production has declined and questions have been raised for quality of shrimp in the market.

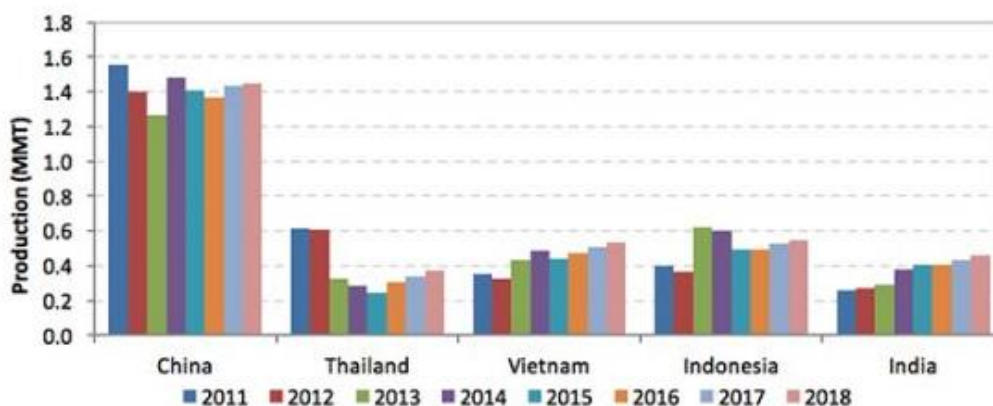


Fig. 1 Shrimp aquaculture production in major farming countries in Asia during 2011-2018.

(Sources: FAO (2011-2014) and GOAL Surveys (2012-2018))

1.2 The shrimp *Penaeus monodon* general information

The black tiger shrimp *Penaeus monodon* is an important aquaculture animal in Thailand. Its natural distribution is the Indo-Pacific, ranging from the eastern coast of Africa and the Arabian Peninsula, as far as Southeast Asia, the Pacific Ocean, and northern Australia. *P.monodon* are identified by distinct black and white or yellow stripes on the backs, tails and abdomens. They have a general shrimp body pattern including a head, tail, five pairs of swimming legs (pleopods) and five pairs of walking legs (pereopods), as well as numerous head appendages. A carapace (hard exoskeleton) encloses the cephalothorax (the head and the thorax fused together) (Fig. 2) (Bailey-Brock and Moss, 1992).

Scientific classification is identified as below (Bailey-Brock and Moss, 1992)

Kingdom Animalia

Phylum Arthropoda

Class Crustacea

Subclass Malacostraca

Order Decapoda

Suborder Natantia

Infraorder Penaeidea

Superfamily Penaeoidea

Family Penaeidae Rafinesque

Genus *Penaeus* Fabricius

จุฬาลงกรณ์มหาวิทยาลัย
CHULALONGKORN UNIVERSITY

Subgenus *Penaeus*

Species *Penaeus monodon*

Common name: Jumbo tiger prawn, Giant tiger prawn, Blue tiger prawn, Leader prawn, Panda prawn (Australia), Jar-Pazun (Burma), Bangkear (Cambodia), Ghost prawn (Hong Kong), Jinga (India, Bombay region), Udang windu (Indonesia), Ushi-ebi (Japan), Kamba ndogo (Kenya), Kalri (Pakistan), Sugpo (Phillipines), Grass shrimp (Taiwan), Kung kula-dum (Thailand), Tim sa (Vietnam).The FAO names are

Crevette gigante tigre (French), Caramon tigre gigante (Spanish) and Giant tiger prawn (English) (Noel B. Solis, 1988).

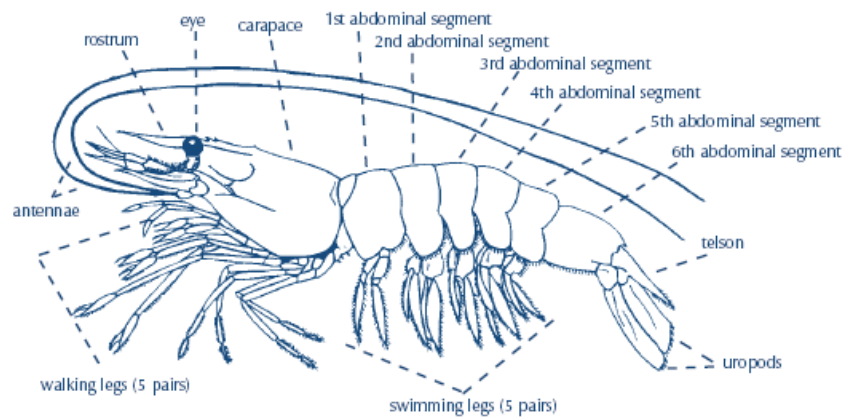


Fig. 2 Anatomy of black tiger shrimp (*Penaeus monodon*) (Motoh, 1985)

1.3 The life cycle of *Penaeus monodon*

The life cycle of shrimp consists of three larval (nauplius, protozoa and mysis), postlarvae, juvenile, sub-adult and adult. The life history of *P. monodon* has an offshore planktonic larval phase of about 14 (Silas et al., 1978) to 20 days (Kenway and Hall, 2002); an estuarine, benthic postlarval and juvenile phase of over 6 months (33 g); a coastal subadult phase of 5 to 6 months (60 g); and an inshore and offshore ocean adult and spawning phase (60 to 261 g) (Dall et al., 1990, Kenway and Hall, 2002). Mating between a recently moulted (soft-shelled) female and a hard-shelled, smaller male occurs at night in the ocean (Hudinaga, 1942). Adult *P. monodon* are found in offshore waters on sandy bottom at depths of 20–40 m. The larvae move towards the coast, entering estuaries and mangrove swamps that serve as nursery grounds. They then migrate to deeper water when they become adolescent.

Penaeus monodon has six nonfeeding naupliar stages, three protozoal stages and three mysis stages (FAO, 1985a).

1.4 Major diseases in shrimp

1.4.1 Viral diseases

1.4.1.1 White Spot Syndrome Virus (WSSV)

White spot syndrome has become the greatest threat to global crustacean aquaculture industries (Flegel, 1997; Lightner, 1996). This disease caused by the White Spot Syndrome Virus (WSSV) which belongs to the member of the Nimaviridae family (Mayo, 2002). The principle clinical sign of this disease is the development of white spots on the carapace of the infected shrimp which results from accumulated of calcium in cuticle but not all host species (Chou, 1995). The other symptoms including lower food consumption, the body surface and appendages turning to red or pink, loosing shell and lethargy. This disease caused 80-100% mortalities within 2-10 days after infection (**Fig. 3**) (Flegel, 1997; Lo, 1996).

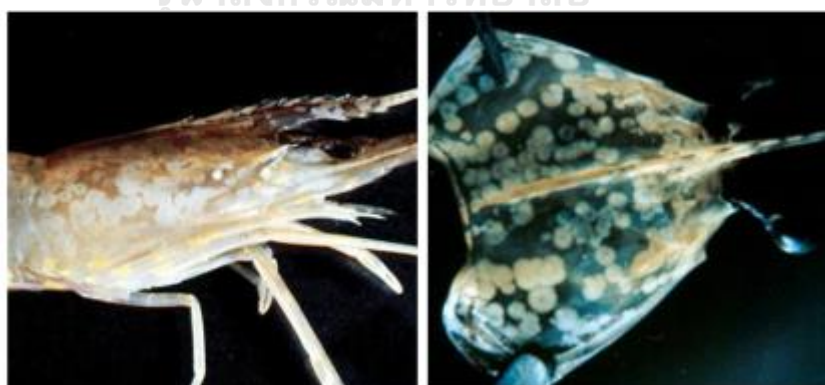


Fig. 3 White spot disease.

The white spots occur on the cuticle of infected shrimp at the late phase of infection (Lightner, 1996).

White spot syndrome virus (WSSV) is a double-stranded DNA (dsDNA) virus. WSSV has a broad host range such as shrimp, crayfish, lobsters and crab (Lo et al., 1996), and can infect various tissues including antennal gland, cuticular epidermis, gill, muscle, lymphoid organ, nervous tissue, hematopoietic tissue, connective tissues of some organs (Chang, 1996; Wang, 1997). The virions are large enveloped rod-shaped particle in the range of $80-120 \times 250-380$ nm (Durand, 1997; Nadala et al., 1998). The viral envelop has the structure of an apparently lipidic bilayer membrane. The nucleocapsid is tightly packed within the virion and surrounded by a trilaminar envelop with a tail-like appendage (Durand, 1997). The virion is formed by a complex of macromolecules specifically folded and assembled for the protection and delivery of viral genomes. Several proteins of WSSV have been characterized (Leu, 2009). For example, VP28 is most likely located on the surface of the virus particle and plays a crucial role in WSSV infection (Van Hulsten, 2001). The tegument protein VP26 was found to be useful for WSSV to move toward the nucleus by interacting with actin (Xie and Yang, 2005). The VP15 has been reported as one of the major structural proteins located in the nucleocapsid and involved in packaging of viral genome (Van Hulsten et al., 2002). VP66 is a major structural protein that forms the stacked rings of the WSSV nucleocapsid (Chai, 2013; van Hulsten et al., 2001). Up to date, several proteins from both WSSV and shrimp were characterized for their interaction upon WSSV infection.

The life cycle of WSSV has been reported and divided into three phases: entry into the host cell (directly or through host mechanisms), uncoating of the genome followed by replication and particle assembly and release (Verbruggen et al., 2016).

There are several molecules involved in this process and these molecules interaction occur between WSSV and its host (**Fig. 4**).

Initially, the virus infected into the host cells by clathrin-mediated endocytosis in a pH-dependent manner. The envelope of virus can directly penetrate into the cytosol by fusing with the plasma membrane of host cells and delivering the genomes to the replication sites in the cytosol or nucleus. Clathrin-adaptor protein 2 (AP-2), which is responsible for endocytosis at plasma membrane, consists of four subunits including α , β 2, μ 2 and σ 2, while AP-1 and AP-3 complexes participate in endocytic vesicle formation at the trans-Golgi network and at the membrane of lysosomes (Huang et al., 2015; Kaksonen and Roux, 2018; Jatuyosporn et al., 2019). During the viral maturation, the pH decreases, virus released from endosome. This stage probably involves an interaction between VP28 and Rab7. Once in the nucleus, host transcription factors bind the WSSV genome and initiate expression of viral genes. WSSV DNA replication requires host machinery and to make these available WSSV can act to halt the cell cycle in the S-phase through E2F1. A high level of viral protein production can lead to ER stress, e.g., activation of unfolded protein response (UPR) pathways. Transcription factors of the UPR can activate expression of viral genes, which in turn may inhibit translation through eIF2. WSSV replication requires essential nutrients including iron. To prevent the host from withholding iron, WSSV can inhibit the binding of iron to ferritin. WSSV can influence apoptosis signaling either through miRNA mediated inhibition of initiator caspases or through viral proteins that inhibit effector caspase activity (**Fig. 4**) (Verbruggen et al., 2016).

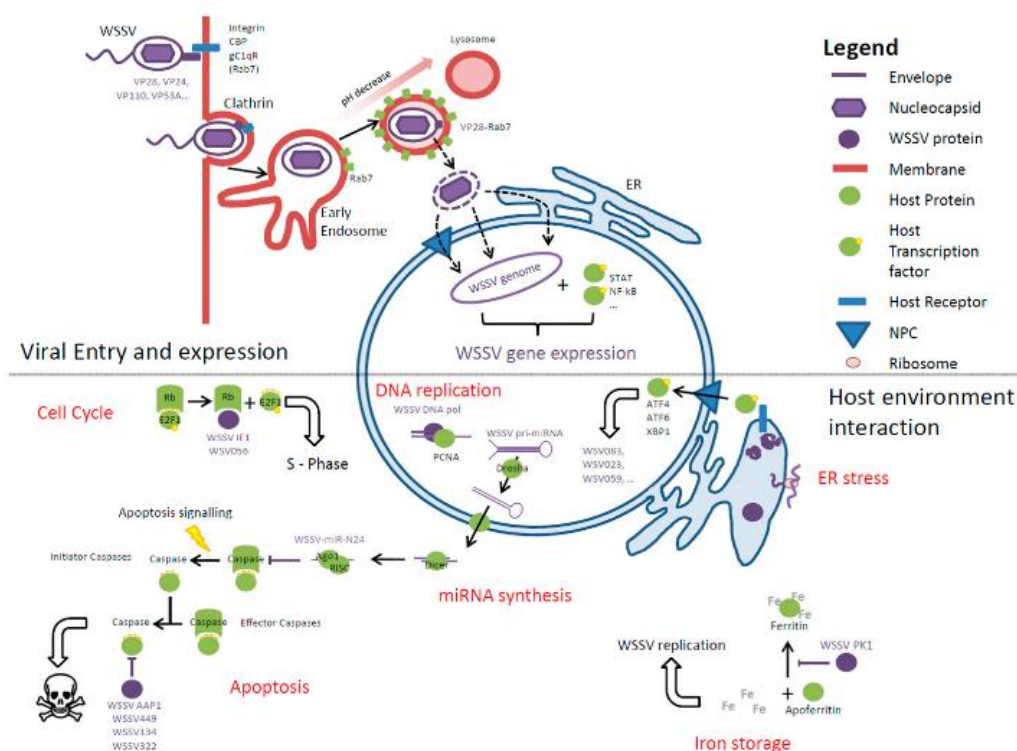


Fig. 4 Overview of WSSV entry and environment interactions. Top panel: Viral entry into the host cell. WSSV proteins interact with host receptors, which leads to induction of clathrin-mediated endocytosis. Bottom panel: Intracellular interactions between WSSV and the host cell (Verbruggen et al., 2016).

จุฬาลงกรณ์มหาวิทยาลัย
CHULALONGKORN UNIVERSITY

1.4.1.2 Yellow Head Virus (YHV)

The yellow head disease was first described as an epizootic from black tiger shrimp farms in Thailand which caused by the virus called yellow head virus (YHV). The disease is caused by a single-stranded RNA (ssRNA) virus which is a member of the genus Okavirus, family Roniviridae in the order Nidovirales (Boonyaratpalin et al., 1993; Chantanachookin et al., 1993; Senapin et al., 2010; Chen et al., 2018). Three YHV structural proteins have been discovered including two envelope glycoproteins gp116 and gp64 and a nucleocapsid protein p20 (Jitrapakdee et al.,

2003; Sittidilokratna et al., 2006). Moreover, three receptor proteins were identified from *P. monodon* including yellow head virus receptor protein (*PmYRP65*), *PmRab11* and plasmolipin 1 (*PmPLP1*) which required for YHV infection (Assavalapsakul et al., 2014; Kongprajug et al., 2017; Matjank et al., 2018). The major organ being infected by YHV is the lymphoid organ. The signs of yellow head disease are the development of yellowish cephalothorax and brown gills in the infected shrimp (Fig. 5), increase in feeding and then suddenly decline and the mortality can reach to 100% within 3-5 days of the first appearance (Boonyaratpalin, 1993; Chantanachookin, 1993; Lightner, 1996). The YHV-infected shrimp also exhibits light yellow coloration of the dorsal cephalothorax area and has a generally pale or bleached appearance (Chantanachookin et al., 1993). Lymphoid organ spheroids are commonly observed in infected shrimp. In shrimp, three types of hemocyte cells were identified as hyaline, semi-granular, and granular hemocytes. The granule-containing hemocytes are proposed to be YHV targets providing the first line of defense to viral infection and activate AMPs protein including crustins (crustin $Pm1$ and crustin $Pm4$), alpha-2-macroglobulin, and kazal-type serine proteinase inhibitor. During an early phase of YHV infection at 6 hpi, crustin $Pm1$ may participate in shrimp defense mechanism against YHV, especially on the granule-containing hemocytes (Havanapan et al., 2016). Various diagnostic methods were developed for the detection of YHV such as RT-PCR (Cowley et al., 1999), *in situ* hybridization, loop mediated isothermal amplification (RT-LAMP) (Mekata et al., 2006) and real-time RT-LAMP (Mekata et al., 2009).



Fig. 5 Yellow head disease.

The YHV-infected shrimp (left) which shows a yellowish discoloration of the cephalothorax compare to the black color of normal shrimp (right).

(Source: AGDAFF-NACA (Photo D. V. Lightner))

1.4.2 Bacterial diseases

1.4.2.1 Vibriosis

Vibriosis is one of the major diseases in shrimp aquaculture caused by bacterium *Vibrio harveyi*. The disease contributes to morbidity and mass mortality in shrimp (Austin and Zhang, 2006; Lightner, 1975). It results in almost 100% cumulative mortality which usually occurred in post-larvae and young juvenile shrimp (Flegel, 2006; Lightner et al., 1983). There have been occasional reports that Vibriosis also caused by other *Vibrio* species (Lightner, 1996). The apparent characteristics of *V. haeveyi* is a Gram-negative, motile, rod shape and luminescent bacteria (Lavilla-Pitogo, 1990). Disease transmission can occur via water or as a result of ingestion of infective material. The evident symptoms caused by *V. haeveyi* in the infected shrimp are called luminous vibriosis (disorder development of basal tissues in the digestive system) which pathogen will releases exotoxins to destroy the wall of gastrointestinal tract and the host immune cells (Peddie, 2005). High mortalities were observed particularly in juvenile shrimp, moribund shrimp appear hypoxic and often come to

the pond surface or edge, reddish discoloration and show black spots of melanization on the cephalothorax (**Fig. 6**).



Fig. 6 Vibriosis in *Litopenaeus vannamei*.

The gross signs of disease demonstrated (A) black stripes on lateral cephalothorax regions and with whitish muscle or (B) dark color of hepatopancreas with smoky body coloration. (C) Uninfected shrimp. (Longyant et al., 2008) (bar=1 cm).

1.4.2.2 Acute hepatopancreatic necrosis disease (AHPND) or early mortality syndrome (EMS)

Recently, an emerging disease known as early mortality syndrome or Acute Hepatopancreatic Necrosis Disease (EMS/AHPND) was first reported in China and subsequently in Vietnam, Thailand and Malaysia. Mortalities can reach up to 100% in shrimp post-larvae during 20-30 days of culture (Xiao et al., 2017). The causative agent of EMS/AHPND has been reported to be a *Vibrio parahaemolyticus*. Recently, the unique plasmid was identified from virulent strain of *V. parahaemolyticus*. This

plasmid encodes two genes, *PirA* and *PirB* which are homologous to the Photorhabdus insect-related (Pir) toxin genes that are lethal to insect (Han et al., 2016). However, the non-virulent strains carrying the plasmid without the *PirA* and *PirB* genes. The PCR detection methods were developed in order to detect this pathogen. AP1, AP2, AP3 and AP4 PCR primer pairs were designed based on conserved sequences of the plasmid to developed the PCR methods for detection of AHPND-related *V. parahaemolyticus* (Han et al., 2016; Kumar Jha et al., 2017). This bacterium can transmit orally, colonize in the shrimp gastrointestinal tract and produces a toxin causes tissue destruction and dysfunction of the shrimp digestive organ known as the hepatopancreas (Tran et al., 2013a). Clinical signs of this disease are slow growth, corkscrew swimming, soft texture of the exoskeleton, being reduced in size of hepatopancreas and discolored hepatopancreas (**Fig. 7**).

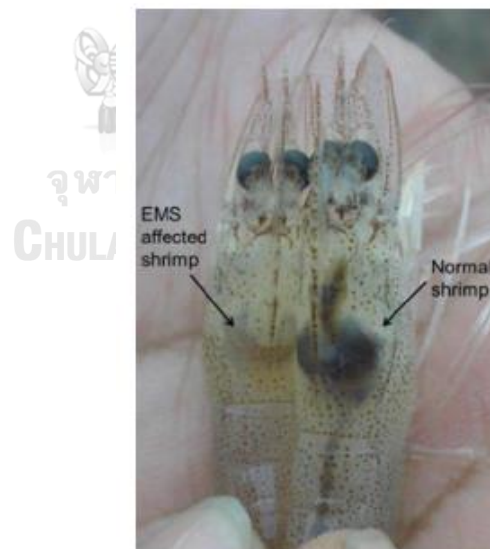


Fig. 7 The infected shrimp caused by early mortality syndrome or Acute Hepatopancreatic Necrosis Disease (EMS/AHPND). The black arrow indicated the pale hepatopancreas of EMS infected shrimp (left) compared to the brown hepatopancreas of normal shrimp (right) (Tran et al., 2013).

1.5 Shrimp innate immunity

Crustaceans, including shrimp lack an adaptive immune system, the defense mechanism relies mainly on the innate immune system (Bachère, 2004). The innate immune system is the first line of inducible host defense against invading microorganisms including bacteria, virus and fungi (Salzet, 2001). Hemocyte is considered as an immune-responsive cell that plays the most important role in immobilizing or destroying invasive microorganisms (Jiravanichpaisal et al., 2006; Johansson, 2000; Lavine and Strand, 2002; Tassanakajon et al., 2013). Hemocytes are generally classified into three types base on the presence and size of cytoplasmic granules: hyaline (agranular), semi-granular (small granular) and granular (large granula) hemocytes (Bauchau, 1980; Martin, 1985; Tsing, 1989). The functions of different hemocytes in the immune system are previously reported. The hyaline cells are involved in phagocytosis and blood clotting (Smith and Soderhall, 1983), while granular cells and semi-granular cells are generally function in apoptosis, melanization, encapsulation and nodulation (Kobayashi, 1990; Pech and Strand, 2000; Sung, 1998). The innate immune system comprises cellular and humoral immune responses (Jiravanichpaisal et al., 2007). The cellular defense performed directly by hemocytes which involved in phagocytosis, encapsulation, nodule formation and apoptosis. Otherwise, the humoral responses involve the prophenoloxidase (proPO)-activating system, the clotting cascade and the activity of immune-related proteins (Holmblad and Söderhäll, 1999; Jiravanichpaisal et al., 2007; Tassanakajon et al., 2013; Tassanakajon et al., 2018). The overview of shrimp immune system is shown in

Fig. 8.

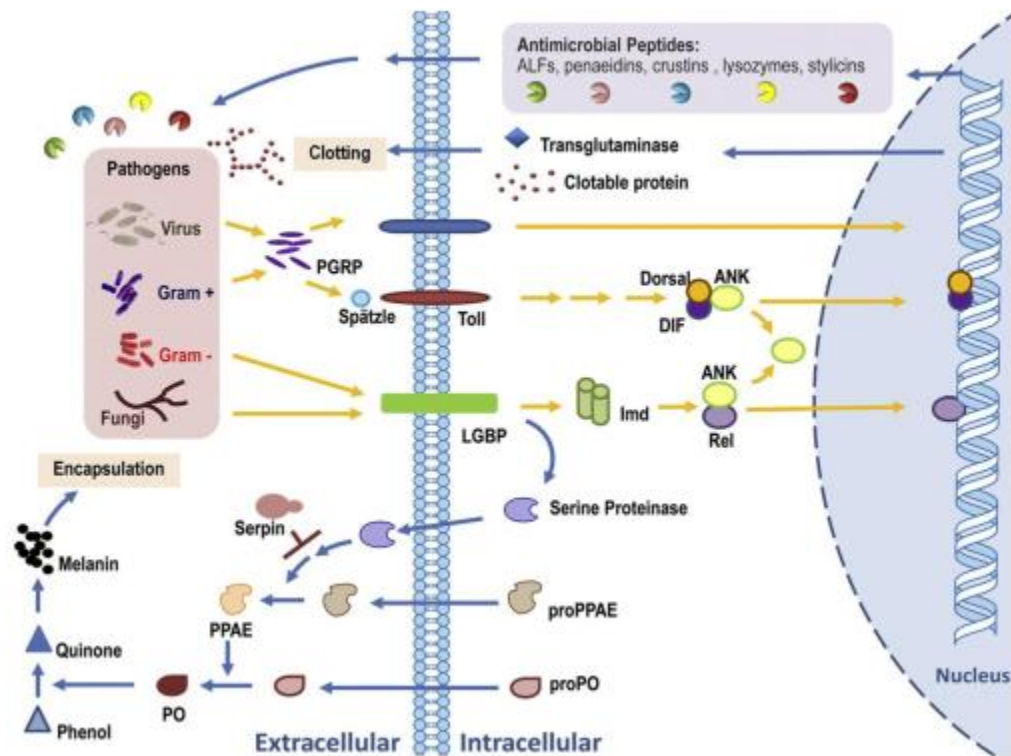


Fig. 8 A model of the shrimp immune system (Tassanakajon et al., 2013). The innate immune system is triggered upon binding of pattern recognition receptors (PRRs) to the invading pathogens and subsequently activates host signaling pathways which leads to the activation of cellular and humoral immune responses.

จุฬาลงกรณ์มหาวิทยาลัย
CHULALONGKORN UNIVERSITY

1.6 Nucleic acid-induced antiviral immunity in invertebrates

RNAi is the primary antiviral response in invertebrates such as arthropods and nematodes, whereas a protein-based IFN system mediates the major antiviral defense in vertebrates (Ding, 2010; Guo et al., 2019). Although invertebrates lack a canonical IFN response, various nucleic acids can activate non-specific antiviral responses and induce a set of immune-related genes in some invertebrates similar to IFN response in vertebrates (Wang et al., 2015a).

In shrimp, various nucleic acids, including dsRNA mimics poly(I:C) and poly(C:G), ssRNA mimics CL097 and poly C, and DNA mimic CpGDNA, activate strong antiviral responses and protects shrimp from viral infection (Wang et al., 2013b). Poly(I:C) injection upregulates a series of genes which are completely novel and different from any known genes. Meanwhile, some genes are homologous to IFN system-defined genes, such as IRFs, PKR, ADAR, and other ISGs (Wang et al., 2013b). Shrimp also has a protein-based antiviral immunity possibly mediated by Vago similar to vertebrate IFN responses. However, whether Vago upregulates dsRNA induced genes remains unknown (Chen et al., 2011; Li et al., 2015). Vago, which was first identified in insects, is a novel antiviral effector induced after viral RNA sensing by Dicer-2 that activates the JAK/STAT pathway to establish a protein-based non-specific antiviral response (Deddouche et al., 2008).

1.6.1 Toll, IMD, and JAK/STAT pathways in antiviral immunity

In insects, Toll, immune deficiency (IMD), and JAK/STAT are the major innate immune pathways controlling most immune responsive genes induced by microbial pathogens (Fig. 9) (Merkling and van Rij, 2013; Buchon et al., 2014; Myllymaki et al., 2014). These pathways regulate immune factors that modulate systemic immune responses, directly kill microbial pathogens, or participate in phagocytosis, reactive oxygen species production, and melanization cascades (Merkling and van Rij, 2013).

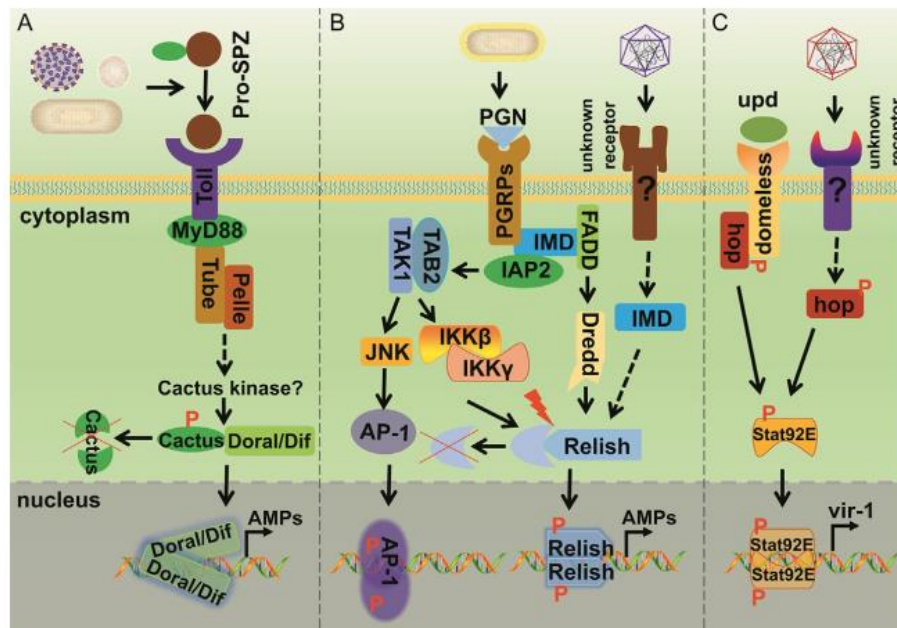


Fig. 9 Immune signaling pathways in insects that share the core elements of mammalian NF- κ B, IRF3, and JAK/STAT pathways. (A) Gram-positive bacteria and fungi infections trigger the pro-Spatzle cleavage into active Spatzle, which binds to Toll and activates the intracellular signaling cascade. (B) PGN derived from Gram-negative bacteria activates the IMD pathway and upregulates AMP expression. Viruses activate the IMD-Relish pathway via unknown receptors and unclear signal transduction mechanisms. (C) In *Drosophila*, the putative ligands of the receptor domeless, such as upd, upd2, and upd3, activate the JAK kinase hopscotch and induce Stat92E phosphorylation, thereby upregulating antiviral genes, such as virus-induced RNA-1 (vir-1) (Wang and He, 2019).

CHULALONGKORN UNIVERSITY

1.6.1.1 Toll pathway in invertebrates

The Toll pathway plays a key role in response to Gram-positive bacteria with Lys-type peptidoglycans (PGNs), possibly fungi and some viruses. The TLR family members are greatly diverse in numbers and types. For example, the nematode *C. elegans* has only one Toll receptor, whereas oysters have at least 83 TLRs. A typical V-type TLR consists of an LRRNT-(LRR)_n-LRRCT ectodomain for ligand recognition, a transmembrane region, and a cytoplasmic TIR domain for intracellular

signaling transduction (Wang et al., 2012). Meanwhile, P-type TLRs are identified in invertebrates, and they represent an ancient form of TLRs; they do not directly bind to PAMPs; the binding of these TLRs is facilitated by endogenous ligands, similar to the binding process of *Drosophila* Toll (Nie et al., 2018).

Toll, also known as Toll-1, is first characterized as a key component of antifungal immune response in *D. melanogaster*. Subsequently, numerous TLRs have been reported in mammals. V-type TLRs directly recognize PAMPs; however, some invertebrate Tolls are P-type TLRs, such as *Drosophila* Toll-1, which functions as a receptor for the secreted cytokine Spätzle but does not directly recognize pathogens (Wang et al., 2014). Infection by Gram positive bacteria, fungi, and certain viruses triggers an extracellular proteolytic cascade, resulting in the cleavage of pro-Spätzle into active Spätzle, which then binds to the transmembrane receptor Toll. Subsequently, intracellular signaling involved in MyD88, Tube, Pelle, TRAF6, Cactus, and other factors leads to the activation of NF- κ B-like transcription factors Dorsal/Dif. The activated Dorsal was translocated to the nucleus, binds to NF- κ B responsive elements, and initiates the transcription of a set of immune-related genes, including antimicrobial peptides (AMPs) (**Fig. 9**). Nine Toll proteins are found in *D. melanogaster*. Among them, Toll-9 is a V-type TLR, whereas the others belong to P-type TLRs. However, Toll-7 directly recognizes viral glycoproteins as a PRR similar to mammalian TLRs and induces antiviral autophagy (Merkling and van Rij, 2013; Wang et al., 2014).

Tolls identified in *Litopenaeus vannamei* (Wang et al., 2012; Hou et al., 2014), *Fenneropenaeus chinensis* (Yang et al., 2008), *Penaeus monodon* (Arts et al.,

2007), *Marsupenaeus japonicus* (Mekata et al., 2008), and *Procambarus clarkii* (Wang et al., 2015b) play important roles in shrimp innate immunity. *LvToll1–3* responded to *Vibrio alginolyticus* and WSSV infections in *L. vannamei* (Wang et al., 2012). *FcToll* and *MjToll* respond to various immune challenges (Mekata et al., 2008; Yang et al., 2008). *PcToll* and *PcToll2* regulate AMP expression after challenged with bacteria in *P. clarkii* (Lan et al., 2016). *LvToll* in *L. vannamei* regulates AMP expression after bacterial challenge (Hou et al., 2014).

Furthermore, *Toll2* (*LvToll2*) and *LvSpätzle* in *L. vannamei* were up-regulated after WSSV infection. *LvToll2* enhances the promoter of AMPs (Wang et al., 2012). Moreover, in kuruma shrimp, *Marsupenaeus japonicus*, the recombinant *MjToll1–3* proteins directly bind to peptidoglycan (PGN) and lipopolysaccharide (LPS) of Gram-positive bacteria and Gram-negative bacteria. The knockdown of *MjToll1–3* significantly decreases shrimp AMP induction (Sun et al., 2017). In black tiger shrimp, *Penaeus monodon*, *PmMyD88*, *PmTRAF6*, and *PmToll* are upregulated by WSSV infection and poly(I:C) stimulation and are involved in the regulation of AMP expression (Deepika et al., 2014; Feng et al., 2016). Interestingly, WSSV has developed strategies to subvert the shrimp Toll pathway and to facilitate its replication. (Qiu et al., 2014).

CpG oligodeoxynucleotides (ODNs), a kind of PAMP consisted of short synthetic ssDNAs, directly bind to TLR9 and chTLR21 in mammals and chickens, respectively, and induce the production of IFN- α and TNF- α (Sun et al., 2014). *LvToll1* and *LvToll3* exhibit affinities to CpG ODNs in a dose-dependent manner. In shrimp hemocytes, CpG ODNs can be uptaken, internalized, and distributed in the

cytoplasm with aggregated signals around the nuclei. The interaction of CpG ODNs and *LvToll1–3* is necessary for the triggering of immune responses by CpG ODNs (Sun et al., 2014). After CpG-A stimulation, the probable IFN level in shrimp plasma is upregulated, and the expression levels of IFN system-like antiviral genes are significantly induced (Jiajia Xu, 2016).

1.6.1.2 IMD pathway in invertebrates

In *Drosophila*, Gram-negative bacteria activate the IMD pathway sharing similarities with vertebrate TNFR pathway via PGN-recognition protein (PGRP)-LC and PGRP-LE receptors, as well as intracellular members, including IMD, dFadd, caspase-8 ortholog Dredd, inhibitor of apoptosis 2(IAP2), TAB2/TAK1 complex, and IKK complex (Kingsolver et al., 2013; Merklung and van Rij, 2013). Relish, another NF- κ B-like factor, is activated after its phosphorylation by the IKK complex, and the inhibitory I κ B domain is cleaved by Dredd. Activated Relish translocates into the nucleus and induces the expression of AMPs, such as diptericin and cecropin (**Fig. 9**). The IMD pathway bifurcates into the JNK pathway at the level of the TAB2/TAK1 complex, which is similar to that in mammalian TNFR pathway (Kingsolver et al., 2013; Merklung and van Rij, 2013). The mutations of Relish or PGRP-LC show high viral loads and exhibit hypersensitivity to Cricket paralysis virus (CrPV) infection in *Drosophila*. However, mutated Relish do not manifest any phenotype during viral infection, suggesting that the IMD pathway-mediated antiviral response is virus specific. IMD pathway components, such as IMD, dFADD, Dredd, dIKK β , dIKK γ , or Relish, mutate flies harboring a Sindbis virus (SINV) replicon exhibit increased genomic viral RNA accumulation, whereas normal viral RNA loads are observed in the mutants of Toll pathway members and mutants of PGRP-LC and PGRP-LE

(Avadhanula et al., 2009). PGRP-LC and PGRP-LE serve as receptors that bind to PGNs and initiate the IMD pathway after a bacterial infection occurs. (Merkling and van Rij, 2013).

In crustaceans, a similar IMD pathway is identified. Shrimp IMD pathway components, such as IMD, IKKs, IAP2, and Relish, are characterized (Wang et al., 2013a; Wang et al., 2014). Shrimp IMD pathway regulates the expression of AMPs, including penaeidins, crustins, ALFs, and lysozymes. In *P. monodon*, *PmRelish* is upregulated upon bacterial and viral challenges. The silencing of *PmRelish* decreases the expression levels of shrimp AMPs (Visetnan et al., 2015a). In *LvRelish*-knocked down shrimp, WSSV genome accumulation and vp28 expression levels markedly decrease. *LvRelish* activates the promoter of WSSV through NF- κ B-binding sites (Qiu et al., 2014). Thus, WSSV has adopted a mechanism for hijacking the shrimp Toll/IMD-NF- κ B pathways as part of their life cycle. This mechanism diverts NF- κ B immune regulatory functions to facilitate WSSV replication (Wang et al., 2014).

1.6.1.3 JAK/STAT Pathway in Invertebrates

The JAK/STAT pathway, which has an evolutionarily conserved antiviral function from arthropods to mammals, is originally identified as an antiviral effector-inducing pathway in mammals (Merkling and van Rij, 2013). This pathway plays a major role in responses to a wide range of growth factors and cytokines. Type I IFNs, including IFN- α and IFN- β , bind to IFN- α receptors composed of IFNAR1 and IFNAR2 subunits and activate Janus kinase 1 (JAK1) and tyrosine kinase 2 (TYK2), resulting in the recruitment of STAT proteins. After phosphorylation, dimerization, and nuclear translocation, STAT complexes are formed in response to stimulation,

inducing numerous IFN-stimulated response element (ISRE)-driven genes, such as ISGs, which can establish a cellular antiviral state (Ivashkiv and Donlin, 2014).

The insect JAK/STAT pathway is similar to mammalian and involved in antiviral immunity (Kingsolver et al., 2013; Merkling and van Rij, 2013). In *Drosophila*, unpaired family (upd) cytokines bind to the receptor domeless and activate the JAK kinase hopscotch, which then phosphorylates Stat92E. After the dimerization of Stat92E complexes and their translocation into the nucleus, Stat92E complexes induce the expression of genes with STAT-binding sites in their promoters, such as virus-induced RNA-1 (vir-1) and attC (Fig. 9).

In crustaceans, the core JAK/STAT pathway components, including domeless, JAK, SOCSs, and STAT, are involved in antiviral responses (Song et al., 2015; Huang et al., 2016). Shrimp STAT regulates the expression of genes with STAT-binding sites in their promoters. JAK or STAT silencing induces WSSV replication, and then the JAK/STAT pathway plays positive roles in shrimp antiviral responses. In *L. vannamei* stimulated by poly(I:C) or WSSV, *LvJAK* expression is highly induced. *LvJAK* itself and *LvSTAT* activate the *LvJAK* promoter containing multiple STAT-binding sites. *LvJAK* silencing increases mortality rate and viral load suggesting that *LvJAK* participates in defense against WSSV infection (Song et al., 2015). In addition, WSSV seems to disrupt the shrimp JAK/STAT pathway to facilitate viral replication at the early stage of infection. At the early stage of WSSV infection, shrimp STAT is induced and phosphorylated STAT level increases, resulting in the translocation of the activated STAT into the nucleus, where it induces *iel* expression (Wang et al., 2014). *L. vannamei* domeless (*Lvdomeless*), similar to IL-6

receptors in vertebrate, is upregulated after WSSV infection. *Lvdomeless* silencing decreases mortality and the number of WSSV genomic copies suggesting that WSSV hijacks *Lvdomeless* to promote viral replication (Yan et al., 2015).

1.6.2 Cytosolic sensing pathway in antiviral immunity

PRRs that recognize pathogen-derived nucleic acids are present in vesicular compartments and in the cytosol of most cell types. These PRRs include the cytosolic DNA sensor (CDS), cyclic GMP-AMP synthase (cGAS), and the cytoplasmic RNA sensor, including retinoic acid inducible gene I (RIG-I) and Dicer-2. Once PRRs were activated, they induce different signaling pathways leading to the production of a variety of antiviral molecules. Interestingly, evidence suggests that these signaling pathways are tightly interconnected to potentiate the antiviral responses.

1.6.2.1 RNA sensing-induced antiviral immunity by Dicer-2

Although the siRNA-mediated gene silencing of viral RNA plays a major role in insect antiviral defense, which represents a specific antiviral immunity, immune-related genes induced by viruses similar to those in mammals contribute to a non-specific antiviral response (Wang et al., 2014). Two main issues include the identification of viral sensors and the determination of related factors responsible for antiviral responses. Dicer-2, which is known to sense and process viral dsRNAs into siRNAs in the initiation of specific antiviral immunity, is a RNA sensor that triggers a novel signaling pathway to regulate *D. melanogaster Vago* (*DmVago*) expression (Fig. 10). Uncoupled from its function in siRNA biogenesis, viral RNA sensing by Dicer-2 triggers a novel signaling mechanism to regulate *DmVago* expression. Thus, Dicer-2 has dual functions, that is, it not only initiates an antiviral RNAi response but

also activates inducible antiviral immunity upon sensing viral RNAs. *DmDicer-2* contains an N-terminal DExD/H-box helicase domain and a C-terminal RNase III domain. The DExD/H-box helicase domain is required for dsRNA sensing, processing, and Vago induction, whereas the RNase III domain is essential for siRNA biogenesis (Deddouche et al., 2008). Dicer-2 is highly homologous to the helicase domains of vertebrate RLRs, including RIG-I and MDA-5, which sense viral RNAs, activate IFNs, and initiate systemic antiviral responses (Deddouche et al., 2008). The DExD/H helicase domain of *DmDicer-2* also senses defective viral genomes (DVGs) as PAMPs and employs them as templates to synthesize viral DNA, leading to the amplification of viral DNA-mediated antiviral RNAi response (Poirier et al., 2018). DVGs are typical PAMPs preferentially sensed by RLRs during viral infection and activate IFN. This finding establishes the conserved roles of DVGs as PAMPs and DExD/H-box helicase containing proteins Dicer-2 and RLRs as their sensors in invertebrates and vertebrates (Poirier et al., 2018).

Drosophila melanogaster Vago (*DmVago*), which encodes a secreted cysteine-rich polypeptide with 160 residues, is one of the most upregulated genes by *Drosophila C* virus (DCV) and implicated in inducible antiviral response (Deddouche et al., 2008). *DmVago* is mainly expressed in the fat body, which is the target organ of DCV. This gene is strongly induced by DCV and Sindbis virus (SINV) infection but weakly upregulated by bacterial challenge. Thus, *DmVago* has a direct role in antiviral response (Deddouche et al., 2008).

Five Vago orthologs (*LvVago1–5*) are identified in *L. vannamei* (Chen et al., 2011). *LvVago1–5* are predicted as secreted proteins containing approximately 102–

190 residues and a single von Willebrand factor type C domain with eight conserved cysteine residues similar to insect Vagos (Paradkar et al., 2012). *LvDicer-2*, *LvVago-1*, *LvVago-4*, and *LvVago-5* are significantly upregulated by WSSV infection. (Chen et al., 2011). *L. vannamei* IRF-like protein (*LvIRF*) activates the promoters of *LvVago-4* and *-5* (Li et al., 2015). In terms of protein homology, inducible expression, antiviral ability, and functional and regulatory mechanisms, *LvVago* may function as an IFN-like cytokine in shrimps. Clarifying whether *LvVago* can activate the JAK/STAT pathway may help further confirm that shrimps possess an IRF-Vago-JAK/STAT regulatory axis, which is similar to the IRF-IFN/JAK/STAT axis of vertebrates (Li et al., 2015).

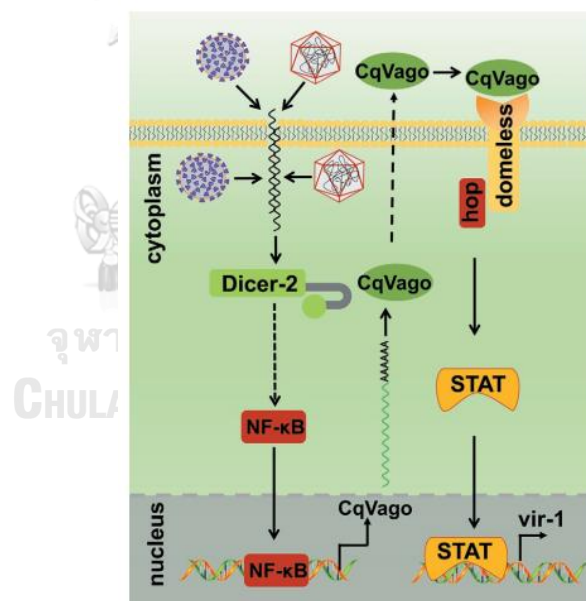


Fig. 10 Insect RNA sensing-induced antiviral immunity by Dicer-2.

Dicer-2 senses viral RNA and upregulates the novel antiviral cytokine Vago by activating NF-κB-like transcription factors. Vago activates JAK/STAT signaling and triggers systemic antiviral immunity via an unknown receptor. (Wang and He, 2019)

1.6.2.2 RIG-I-like receptors (RLRs) in invertebrate antiviral immunity

Viral RNAs are also recognized by another family of cytoplasmic receptors known as RLRs. The three members that constitute the RLR family are retinoic acid-inducible gene I (RIG-I), melanoma differentiated gene 5 (MDA5), and laboratory of genetics and physiology 2 (LGP2). RLRs are expressed in a variety of cell types, including myeloid cells, epithelial cells, fibroblasts, and cells of the central nervous system, although RLR function is not necessary for IFN production by pDCs despite their expression in this cell type (Loo and Gale, 2011). In mammals, RIG-I and MDA5 are the receptors that recognize the target RNA virus and trigger to activate cytokines and IFNs expression. RIG-I and MDA5 recognize a different class of viruses. In invertebrates, RIG-I was found in oyster genome, *Crassostrea gigas* (Zhang et al., 2015; Huang et al., 2017). CgRIG-I-1 has a typical RLR protein domain structure: the N-terminal CARDs, central RNA helicase domain, and C-terminal regulatory domain (RD) (Huang et al., 2017). Phylogenetic analysis has shown that CgRIG-I-1 is grouped into the clade of vertebrate RLRs. CgRIG-I-1 directly binds to poly(I:C) and interacts with CgMAVS via its CARDs. Subsequently, CgMAVS is activated and CgTRAF6 is recruited, and these processes activate the NF- κ B pathway. Furthermore, CgIRFs trigger the IFN- β promoter and ISRE reporter, which regulates the expression of *C. gigas* IFNLP (CgIFNLP) that possesses as an IFNs in vertebrates. (Zhang et al., 2015)

(Fig. 11).

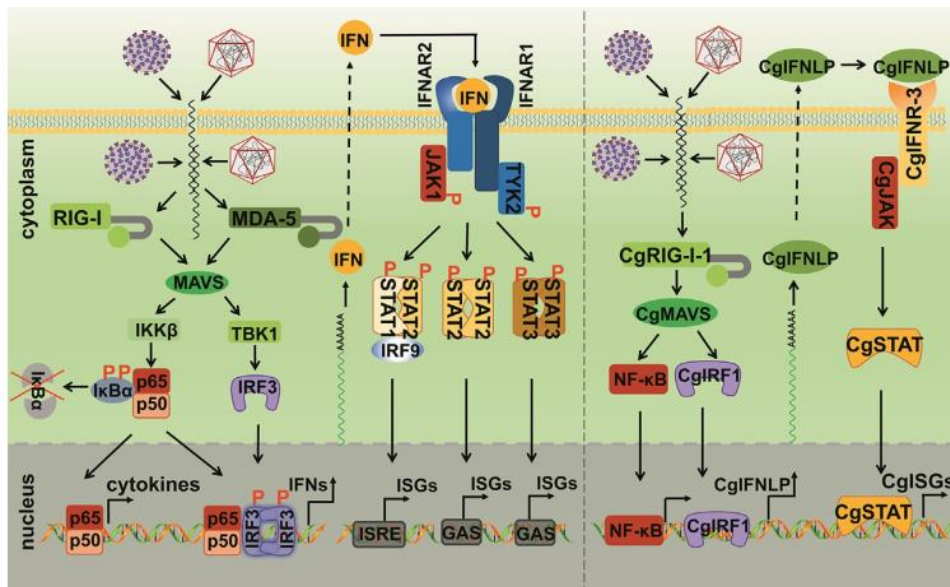


Fig. 11 The model of the RIG-I pathway in the Pacific oyster *Crassostrea gigas*. In mammals, RIG-I and MDA-5 are critical cytoplasmic dsRNA sensors in the activation of IFN response (left). Likewise, in oysters, cytoplasmic dsRNA sensing by CgRIG-I-1 activates transcription factors CgNF- κ B and CgIRF1 through CgMAVS, thereby upregulating CgIFNLP. CgIFNLP binds with the putative CgIFNLP receptor CgIFNLR-3 and activates the ISRE, STAT3, and GAS promoters through the JAK/STAT pathway (right) (Wang and He, 2019).

1.6.2.3 DNA-sensing pathway in invertebrates

The DNA sensors recognize microbial or self-DNA present in the cytoplasm as a sign of infection or cell damage and induce the production of IFN. Most of the DNA sensors recognize foreign DNA in the cytoplasm and generally utilize stimulator of interferon genes (STING; also known as TMEM173, MPYS, MITA, and ERIS) and TBK1, which are the essential components in response to intracellular DNA (Ishii et al., 2006; Ishikawa and Barber, 2008).

1.6.2.3.1 cGAS-STING pathway in antiviral immunity

In vertebrates, cGAS-STING pathway plays an important role in cytoplasmic DNA sensing and antiviral defense against viral infection (Wang et al., 2018). Cytoplasmic cGAS senses dsDNA and produces a cyclic dinucleotides (CDNs) called cGAMP, which directly binds to STING and induces the phosphorylation of TBK1 and IRF3, resulting in the activation and nuclear translocation of transcription factor IRF3, which in turn activates IFNs and downstream IFN-stimulated genes (ISGs) (Wu and Chen, 2014; Tan et al., 2018). Bacterium derived CDNs also bind to STING, activate IRF3, and induce IFN production (**Fig. 12**) Nevertheless, whether this cGAS contribute to cytoplasmic DNA sensing, cGAMP production and sensing, and antiviral immune activation still requires further investigations.

STING is activated by CDN binding via a CDN-binding domain conserved in different species. However, a previous study showed that insect STINGs, including *D. melanogaster* STING (*DmSTING*), directly binds to c-di-GMP and induces immune response partly through IMD-Relish axis (Fig. 12). *DmSTING* activates the *DmIKK* β -Relish module of the IMD pathway, induces the antiviral effectors, and participates in antiviral response during viral infections. *DmIKK* β and Relish, are required for *Drosophila* defense against the viral infection (Goto et al., 2018). The viral infection activates the immune genes through *DmIKK* β and Relish and induces *DmSTING* which results in the strong inhibition of viral replication (Fig. 12) (Goto et al., 2018). Hence, *DmSTING* functions upstream of *DmIKK* and Relish in this antiviral signaling mode. Nevertheless, the receptor that recognized the CDNs and sense the signal to *DmSTING* during viral infection still remain unknown in *Drosophila*.

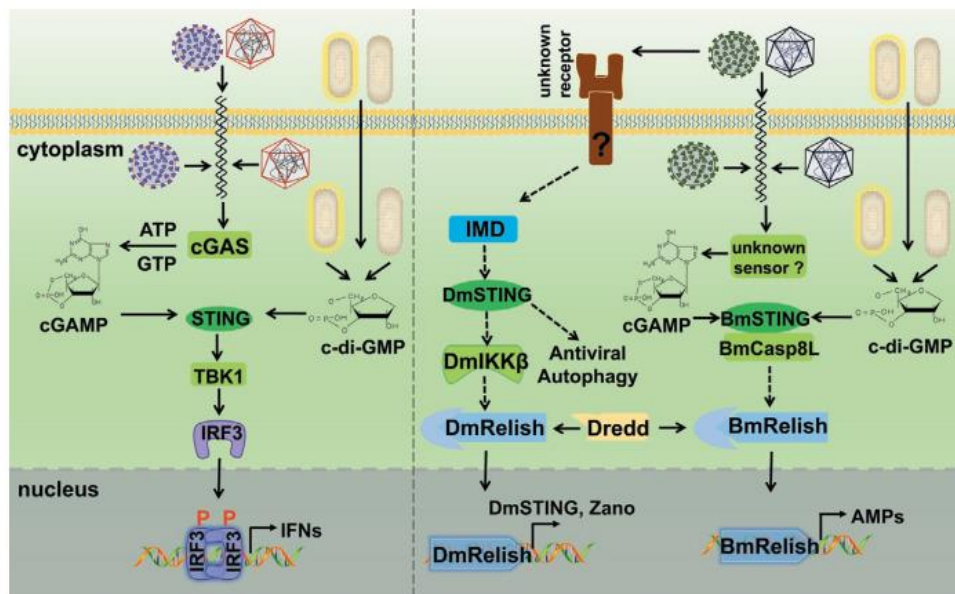


Fig. 12 STING-mediated innate immune response. The model of the STING pathway in mammals (left) and insects (right). Invertebrate STING, including oyster and insect, can directly bind with cyclic dinucleotides (CDNs) and activate immune responses. (Wang and He, 2019).

In Pacific white shrimp, a STING ortholog is identified and functionally characterized (Li et al., 2017). *LvSTING* is mainly expressed in the major immune-related tissues including hepatopancreas and intestine for AMPs induction. *LvSTING* is significantly induced in organisms challenged with *V. parahaemolyticus*, a common bacterial pathogen of shrimps. The knockdown of *LvSTING* significantly reduces the induction of *LvPenaeidin-4* by *V. parahaemolyticus* challenge, an important shrimp AMPs downstream of the Toll and IMD pathways (Li et al., 2017). Thus, the *LvSTING* regulation of *LvPenaeidin-4* expression may occur via the Toll or IMD pathway or both and via the canonical AMP regulation pathway (Li et al., 2017). *LvSTING* may be involved in innate immune regulation through the Toll or IMD pathway or both and is required for shrimp defense against bacterial infection. Further

study showed that CDNs, including c-di-GMP and cGAMP, can directly bind to and activate *LvSTING* (Li et al., 2017).

1.6.2.3.2 DDX41 signaling pathway in antiviral immunity

In addition, a new intracellular DNA sensor named DDX41 has been identified in vertebrates and has been to induce synthesis of type I interferon (Parvatiyar *et al.*, 2012). IFNs are secreted by infected cells in response to pathogens and exhibit a protective effect against acute viral and bacterial infections. Recently, DDX41 was identified in chicken cells and its function in IFN- β production was investigated. The ChDDX41 transcript was induced by the dsDNA analogue poly(dA:dT) and found to interact with chicken stimulator of interferon genes (chSTING) (Cheng *et al.*, 2017). In the Japanese flounder, *Paralichthys olivaceus*, the DDX41 gene was identified and found to be highly expressed in immune-related tissues. The Japanese flounder DDX41 has been reported to function as a cytosolic DNA sensor that is capable of inducing the expression of antiviral and inflammatory cytokines in the presence of cyclic di-GMP (Quynh *et al.*, 2015). In pigs, porcine DDX41 (poDDX41) was found to be expressed in various tissues, especially the stomach and liver. The overexpression of poDDX41 in PK-15 cells induced IFN- β by activating transcription factor 3 (IRF3) and NF- κ B (**Fig. 13**) (Zhu *et al.*, 2014). Altogether, DDX41 and cGAS are cytosolic DNA sensors which activate STING to initiate downstream signaling by activating TBK1 or IKK leading to synthesis of IFNs and NF- κ B expression.

Moreover, in *Drosophila*, a homologue of DDX41 named Abstrakt was identified and was found to share 66% identity and 80% similarity at the amino acid-

level to vertebrate DDX41. Abstract is essential for survival at all stages throughout the life cycle of the fruit fly and plays a role in controlling cell polarity and asymmetric cell division in multiple cell types (Schmucker *et al.*, 1997). Although DDX41 was identified in invertebrates, the mechanism remains poorly understood.

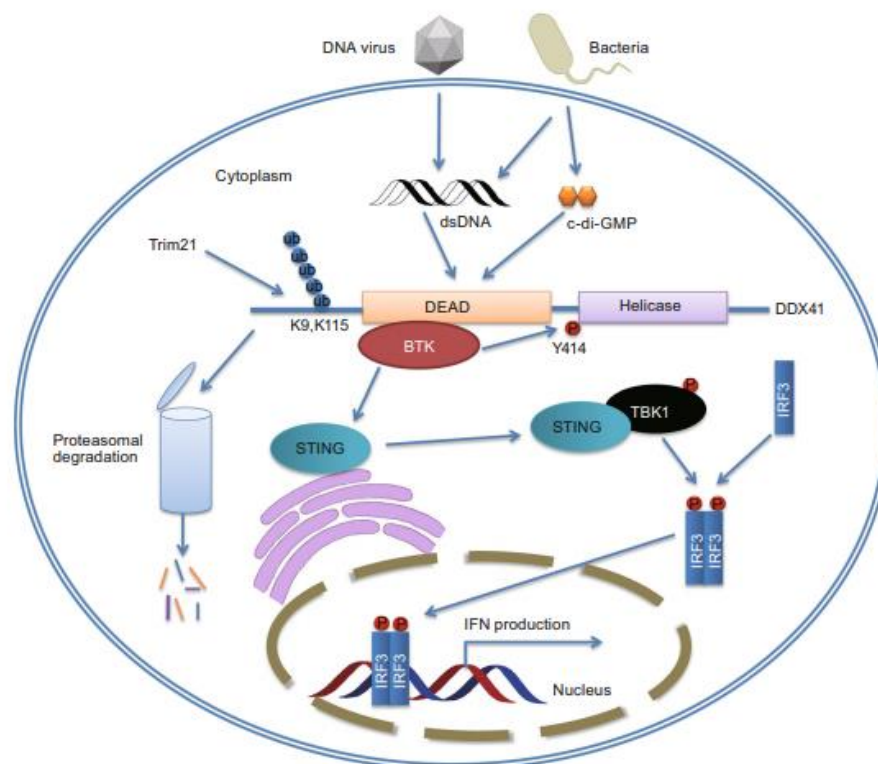


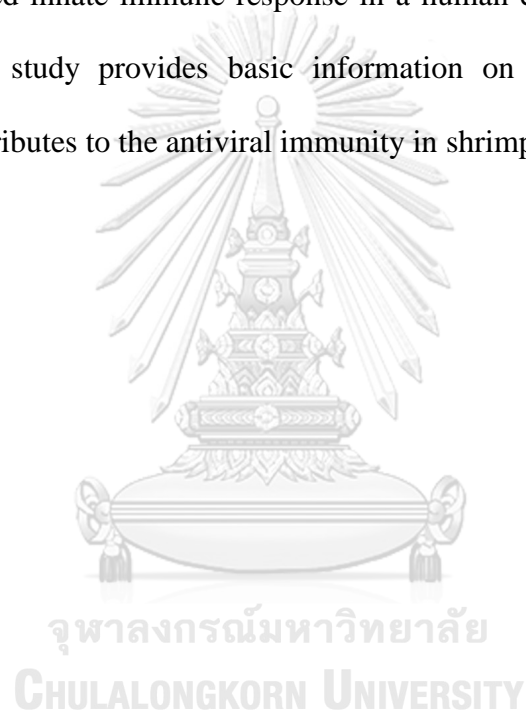
Fig. 13 The signaling pathway of DDX41 in innate immunity.

The innate immune system senses cytosolic dsDNA and bacterial cyclic dinucleotides and initiates signaling via the adaptor STING to induce type I interferon (IFN) response (Ouyang *et al.*, 2012).

1.7 Propose of this thesis research

In shrimp, the viral DNA-sensing molecules have not been studied and DDX41 has not yet been reported to date. The aims of this study were to identify and characterize the *PmDDX41* gene and investigate its involvement in the DNA-sensing

cascade in the black tiger shrimp *Penaeus monodon*. Gene expression analysis of *PmDDX41* was performed on various tissues and in response to WSSV infection. Furthermore, the function of *PmDDX41*, particularly in terms of antiviral innate immunity, was characterized using RNA interference. Moreover, I further characterized the function of *PmDDX41* as a nucleic acid sensor in shrimp and investigated how this sensor interacts with dsDNA and STING to send signals that ultimately activated innate immune response in a human embryonic kidney cell line (HEK293T). This study provides basic information on the nucleic acid sensing pathway that contributes to the antiviral immunity in shrimp.



CHAPTER 2

MATERIALS AND METHODS

2.1 Equipment and chemicals

2.1.1 Equipment

-20°C Refrigerator Freezer (SHARP), -80°C Freezer (Thermo Forma)

24-well plate Costar® (Corning Incorporation)

96-well plate Costar® (Corning Incorporation)

Amicon Ultra-4 concentrators (Vivaspin)

Autoclave LABO (SANYO)

Automatic micropipette (Gilson Medical Electrical S.A.)

Balance (METTLER TOLEDO)

Centrifuge (Thermo Scientific)

Centrifuge 5804R (Eppendorf)

Centrifuge tube CentriStar™ 15 ml, 50 ml (Corning Incorporation)

Gel documentation (SYNGENE)

Gene Pulser (BIO-RAD)

Hybridization oven (Hybrid)

Incubator (Mettmert)

Innova 4080 incubator shaker (New Brunswick Scientific)

Insulin syringes U 100 (Becton, Dickinson and Company)

Laminar Airflow Biological Safety Cabinets (NuAire, Inc.)

Microcentrifuge tube (Axygen Scientific)

Millex syringe-driven filter unit 0.22, 0.45 μM (Millipore, MERCK)

Orbital shaker SO3 (Stuart Scientific, Great Britain)

PCR Mastercycler (BIO-RAD, Eppendorf AG, Germany)

PCR Thin wall microcentrifuge tubes 0.2 ml (Axygen Scientific, USA)

PCR workstation Model # P-036 (Scientific Co., USA)

PCR strip tube white (BIO-RAD)

PCR cover strip (BIO-RAD)

PD-10 Column (GE Healthcare)

pH meter Model # SA720 (Orion)

Pipetman Classic™ (Gilson Incorporation)

Pipette tips 0.2-10, 20-200, 1000 μl (Axygen Scientific)

Power supply, Power PAC 3000 (BIO-RAD)

Spectrophotometer Spectronic 2000 (Bausch & Lomb)

Spectrophotometer DU 650 (Beckman, USA)

Sterring hot plate (Fisher Scientific)

Semi-dry Trans-Blot® (BIO-RAD)

Touch mixer Model # 232 (Fisher Scientific)

Ultra Sonicator (SONICS Vibracell)

Vertical electrophoresis system (Hofer™ miniVE)

Water bath (Mettler)

2.1.2 Chemicals, reagents and biological substances

100 mM dATP, dCTP, dGTP and dTTP (Thermo Scientific)

100 bp PlusGeneRuler™ (Thermo Scientific)

1 kb GeneRuler™ (Thermo Scientific)

2-Mercaptoethanol (Fluka)

5-bromo-4-chloro-3-indolyl- β -D-galactopyranoside (X-gal) (Fermentas)

5-bromo-4-chloro-indolyl phosphate (BCIP) (Fermentas)

Acrylamide/Bis Solution (BIO-RAD)

Agar powder (HIMEDIA)

Agarose (Research organics)

Ammonium persulfate (USB)

Ampicillin (BioBasic)

Boric acid (MERCK)

Bovine serum albumin (BSA) (SIGMA-ALDRICH)

Bromophenol blue sodium salt (USB)

Calcium chloride (MERCK)

Chloramphenicol (Sigma)

Chloroform (RCL Labscan)

Coomassie brilliant blue G-250, R-250 (BIO BASIC INC.)

Diethyl pyrocarbonate (DEPC) (Sigma)

Di-Sodium hydrogen orthophosphate anhydrous (Carlo Erba)

Dithiothreitol (DTT) (BIO BASIC INC.)

Dulbecco's modified eagle medium (DMEM) (Nacalai)

Ethanol (MERCK)

Ethidium bromide (Sigma)

Ethylene diamine tetra acetic acid disodium salt dehydrate (EDTA) (Ajax
Finechem)

Fetal bovine serum (FBS) (Life Technologies)

Formaldehyde (BDH)

Genezol reagent (Geneaid)

Glacial acetic acid (MERCK)

Glycerol (Scharlau)

Glycine (Scharlau)

Hydrochloric acid (MERCK)

Imidazole (Fluka)

Isopropanol (MERCK)

Isopropyl- β -D-thiogalactoside (IPTG) (Thermo Scientific)

Kanamycin (BIO BASIC Inc.)

Lipofectamine 2000 (Life Technologist)

Methanol (MERCK)

N, N-dimethyl formamide (Carlo Erba)

N, N-methylenebisacrylamide (Fluka)

N, N, N, N-Tetramethylethylenediamine (TEMED) (BDH)

Ni Sepharose 6 Fast Flow (GE Healthcare)

Nitrobluetetrazolium (NBT) (Fermentas)

Opti-MEM (Life Technologies)

Paraformaldehyde (SIGMA)

pEGFP vector (Clontech)

pET22b(+) vector (Novagen)

pGBKT7 vector (Clontech)

Phenol, saturated (MERCK)

Potassium chloride, KCl (Ajax Finechem)

Potassium dihydrogen orthophosphate (Ajax Finechem)

Polydeoxyadenylic-deoxythymidylic acid sodium salt (poly (dA: dT))

(Invivogen)

Polyinosinic-polycytidylic acid (poly (I:C)) Biotin (Invivogen)

Polyinosinic-polycytidylic acid (poly (I:C)) high molecular weight (HMW)

(Invivogen)

Prestained protein molecular weight marker (Fermentas)

Prolong Gold Antifade Reagent (Invitrogen)

Protein A sepharose 4 Fast Flow (GE)

Skim milk powder (HIMEDIA)

Sodium acetate (Carlo Erba)

Sodium citrate (Carlo Erba)

Sodium chloride (Ajax Finechem)

Sodium dihydrogen orthophosphate (Carlo Erba)

Sodium dodecyl sulfate (Vivantis)

Sodium hydroxide (MERCK)

Tris-(hydroxy methyl)-aminomethane (USB)

Triton® X-100 (MERCK)

Tryptone type I (HIMEDIA)

Tween™ 20 (Ajax Finechem)

Urea (SIGMA-ALDRICH)

Yeast extract powder (HIMEDIA)

2.1.3 Enzymes and kits

Advantage® 2 Polymerase Mix (Clontech)

BamHI (Biolabs® Inc.)

Biotin DecaLabel DNA Labeling Kit (Thermo Scientific)

Chemmiluminescent Nucleic Acid Detection Module Kit (Thermo Scientific)

DNase I (RNase-free) (Biolabs® Inc.)

HindIII (Biolabs® Inc.)

KOD FX DNA polymerase Mix (TOYOBO)

MEGAscript® Kit (Ambion®)

NcoI (Biolabs® Inc.)

NdeI (Biolabs® Inc.)

NotI (Biolabs® Inc.)

NucleoSpin® Extract II Kits (MACHEREY-NAGEL)

PCR-Select™ cDNA Subtraction Kit (Clontech)

Plasmid mini prep (Geneaid)

QuantiTect SYBR® Green PCR Kit (QIAGEN)

RBC T&A Cloning Vector (RBC Bioscience)

Revert Aid First Strand cDNA Synthesis kit (Thermo Scientific)

RNase A (SIGMA)

SsoFast™ Evagreen® Supermix (BIO-RAD)

T4 DNA ligase (Biolabs® Inc.)

T7 RiboMAX™ Express Large Scale RNA Production System (Promega)

Taq DNA polymerase (RBC Bioscience)

ThermoScript (Invitrogen)

XhoI (Biolabs® Inc.)

2.1.4 Primary and secondary antibodies

Alkaline phosphatase-conjugated rabbit anti-mouse IgG (Jackson

ImmunoResearch

Laboratories, Inc.)

Alkaline phosphatase-conjugated rabbit anti-rabbit IgG (Jackson

ImmunoResearch

Laboratories, Inc.)

Anti-c-Myc antibody produced in rabbit (Sigma)

Anti-DDX41 (Abcam)

Anti-Flag (Sigma)

Anti-His antiserum (GE Helthcare)

Anti-Rabbit IgG (whole molecule)–Peroxidase antibody (Sigma)

2.1.5 Microorganisms

Escherichia coli strain BL21

Escherichia coli strain DH5-α

Escherichia coli strain Rosetta (DE3)

Escherichia coli strain JM109

Human cell line HEK293T

Vibrio harveyi 639

White spot syndrome virus (WSSV)

Yellow head virus (YHV)

2.1.6 Software

Blast programs (<http://www.ncbi.nlm.nih.gov/BLAST/>)

ClustalW multiple sequence alignment program

(<http://www.ebi.ac.uk/Tools/clustalw2/>)

EMBOSS Pairwise Alignment (<http://www.ebi.ac.uk/Tools/emboss/align/>)

GENETYX 7.0.3 program (GENETYX Corporation)

GraphPad Prism 6 (GraphPad Software, Inc.)

SMART version 4.0 (<http://www.smart.emblheidelberg.de/>)

SPSS statistics 17.0 (Chicago, USA)

2.2 Shrimp samples

Healthy black tiger shrimp *Penaeus monodon* (10–15 g body weight) were kindly provided by Charoen Pokphand Foods in Chanthaburi province, Thailand. The shrimp were maintained in aerated seawater (20 ppt) at 28 °C for a week prior to the experiment. To determine the tissue expression pattern of the *PmDDX41* transcripts, eight different tissues (hemocytes, intestine, hepatopancreas, lymphoid organ, gill, heart, muscle, and eye stalk) from three shrimp were separately collected as described previously (Amparyup *et al.*, 2010). All samples were then stored at -80 °C until used for RNA extraction.

2.3 Total RNA extraction and cDNA preparation

Tissues or hemocytes from healthy or pathogen infected shrimp were collected and homogenized using GENEzol reagent (Geneaid). The total RNA was isolated according to manufacturer's protocol. In brief, 50-100 mg of sampled tissue was homogenized in 1 mL GENEzol reagent and incubated at room temperature for 5 minutes. Following the incubation, chloroform 200 µl per 1 ml GENEzol reagent was added to the homogenized sample. The sample was mixed vigorously and centrifuged at 12,000×g, 4°C for 15 minutes. The upper aqueous phase was transferred to new tube and mixed with 1 volume of isopropanol for RNA precipitation. The mixture was centrifuged at 12,000×g, 4°C for 10 minutes to collect the RNA pellet. The pellet was washed with 70% (v/v) ethanol and centrifuged at 12,000×g, 4°C for 5 minutes before air-dried for 5-10 minutes. Total RNA was resuspended with diethylpyrocarbonate-treated water (DEPC water) and treated with DNase I (RNase-free) (NEB) to remove contaminating DNA. The DNase was removed by phenol/chloroform extraction and

RNA concentration was measured using NanoDrop spectrophotometer (Thermo Scientific). The equal amounts of RNA from three individual shrimp were pooled for first strand cDNA synthesis.

One microgram of RNA was reverse transcribed to first strand cDNA using RevertAid First Strand cDNA Synthesis Kit (Thermo Scientific). As described in the manufacturer's instructions, the extracted RNA was reverse transcribed in 20 μ l reaction containing 1 μ g RNA, 1 μ l of 100 μ M Oligo(dT)18 primer, 4 μ l 5X Reaction Buffer, 1 μ l RiboLock RNase Inhibitor (20 U/ μ l), 2 μ l of 10 mM dNTP mix, 1 μ l RevertAid M-MuLV RT (200 U/ μ l) and nuclease-free water. The reaction was mixed gently, spun down and incubated at 42°C for 60 minutes followed by termination at 70°C for 5 minutes. RNA extract and first strand cDNA were stored in -80°C until used.

2.4 Primer design

All primers were designed base on nucleotide sequences of *PmDDX41*cDNA by Primer Premier 5 Software (Premier Biosoft) and SECentral program (Scientific & Education Software). The primer-dimer formation, GC content and melting temperature were carefully concerned.

2.5 Cloning and sequencing of open reading frame (ORF) cDNA of *PmDDX41*

cDNA fragments of *PmDDX41* were searched from the *P. monodon* expressed sequence tag (EST) database (<http://pmonodon.biotec.or.th>) (Tassanakajon *et al.*, 2006) and assembled. Gene-specific primers, ORF-*PmDDX41*-F and ORF-*PmDDX41*-R (Table 1), were designed from the EST sequences to amplify the ORF cDNA of *PmDDX41* and hemocyte cDNA was used as a template. The PCR reaction (25 μ l) consisted of 1 μ l of 10-fold diluted cDNA as a template, 5 μ M of each forward and reverse primer, 2.5mM dNTP and 1 U Taq polymerase (RBC Bioscience). PCR amplification was performed under the following cycling conditions: 94 °C for 1 min, followed by 35 cycles of 94 °C for 30 s, 65 °C for 30 s, and 72 °C for 30 s, with an extension step at 72 °C for 10 min. The PCR products were separated by 1.5% agarose gel electrophoresis, stained with ethidium bromide and visualized by UV-transillumination. The bands with the expected size were then excised and purified using a FavorPrep GEL/PCR Purification Kit (FAVORGEN Biotech Corp., Taiwan). The purified DNA fragments were cloned into the RBC TA Cloning Vector Kit (RBC Bioscience) and sequenced.

2.6 Sequence analysis

The cDNA and deduced amino acid sequences of *PmDDX41* were analyzed using the programs GENETYX 7.0.3 (GENETYX Corporation) and BLAST. Protein domains were analyzed using the SMART 4.0 program. A multiple sequence alignment was created with the ClustalX 2.1 program. An unrooted tree was constructed by the neighbor-joining method based on the amino acid sequences using ClustalX 2.1 and MEGA 6 software (Tamura *et al.*, 2013). Bootstrap sampling was reiterated 100 times.

2.7 Tissue distribution analysis

cDNA from various tissues was used as template for PCR amplification using the specific primers *PmDDX41-F* and *PmDDX41-R* (Table 1). A partial fragment (150 bp) of the elongation factor 1- α (EF1- α) gene was also amplified using the EF1- α -F and EF1- α -R primers (Table 1) to serve as an internal reference control for normalization. The PCR reaction (25 μ l) consisted of 1 μ l of 10-fold diluted cDNA as a template, 5 μ M of each forward and reverse primers, 2.5mM dNTP and 1 U Taq polymerase (RBC Bioscience). The PCR conditions were 94 °C for 1 min, followed by 30 cycles of 94 °C for 30 s, 65 °C for 30 s, and 72 °C for 30 s, followed by a final extension step at 72 °C for 5 min. The PCR product was analyzed by 1.8% agarose gel electrophoresis and visualized by UV-transillumination.

2.8 Gene expression analysis in response to pathogen infection and nucleic acid mimics stimulation

2.8.1 Microbial challenge

For the microbial challenge, the shrimp were divided into triplicate groups of three shrimp each. The animals were then injected with either *Vibrio harveyi* suspension ($OD_{600} = 1.9$, approximately 3.2×10^5 CFU/mL in PBS), WSSV suspension (2.64×10^5 copies/mL of WSSV in PBS), or YHV suspension (3.25×10^6 copies/mL of YHV in PBS) in the second abdominal segment (50 μ l for each shrimp). The control group was injected with phosphate-buffered saline pH 7.4 (PBS; 137 mM NaCl, 2.7 mM KCl, 4.3 mM Na_2HPO_4 , 1.4 mM KH_2PO_4).

2.8.2 Nucleic acid mimics stimulation

Shrimp (8-10 g each) were divided into triplicate groups of three shrimp and injected with 50 μ l poly(dA:dT) (2 μ g/g) or 50 μ l poly(I:C) (2 μ g/g) which was diluted in PBS. The phosphate-buffered saline was used as a control group.

2.8.3 RNA extraction and cDNA synthesis

Hemocyte cells from the experiment shrimp were randomly collected at 0, 6, 12, 24, and 48 h post-injection (hpi) for the RNA extraction. The total RNA extraction and first-strand cDNA synthesis were performed following the methods described in Section 2.2. The total RNAs from three shrimp per treatment at each time point were pooled.

2.8.4 Quantitative real time-PCR (qRT-PCR) analysis

The amplification was performed in PCR white strip tube in a 10 μ l reaction volume containing 5 μ l of SsoFastTM Evagreen[®] Supermix (Bio-RAD), 0.2 μ M of *PmDDX41-F* and *PmDDX41-R* primers and 1 μ l of 1:10 diluted cDNA template. The thermal profile for SsoFastTM Evagreen[®] Supermix (Bio-RAD) real-time PCR was 95°C for 8 min followed by 40 cycles of denaturation (95°C for 30 s), annealing (65°C for 30 s) and extension (72°C for 30 s). The specificity of PCR was verified by measuring the melting curve of the PCR product at the end of the reaction. The reaction was incubated at 95°C for 5 min and subsequently 55°C for 5 min, followed by heating for 10 s starting at 55°C with 0.5°C increments. The relative quantification was analyzed the amount of target transcript relative to an internal standard, elongation factor 1-alpha gene (EF1- α) in the same sample of shrimp hemocytes. The C_T values of pathogen-infected sample at each time point were normalized with

saline-injected samples. A mathematical model was used to determine the relative expression ratio (Pfaffl, 2001) as shown below. Data were shown as means±standard deviations (SD). Statistical analysis was performed using one-way ANOVA followed by Duncan's new multiple range test. The data was considered for statistical differences with the significance at $P<0.05$.

To calculate the relative expression according to a comparative method described by Pfaffl (2001), the following equation was used:

$$\text{Expression ratio} = \frac{(E_{\text{target}})^{\Delta C_T(\text{control-sample})}}{(E_{\text{ref}})^{\Delta C_T(\text{control-sample})}}$$

Where, E is amplification efficiency
 C_T is threshold cycle

2.9 *In vivo* Gene silencing

2.9.1 Preparation of double-stranded RNAs (dsRNAs)

Double-stranded RNAs (dsRNA) of *PmDDX41* was generated in vitro using T7 RiboMAXTM Express Large Scale RNA Production System. DNA fragment for preparation dsRNA of *PmDDX41* was amplified by PCR from a full-length *PmDDX41* containing plasmid using gene specific primers (Table 1). The primers for the dsRNA synthesis consist of the same primer sequences but flanked at the 5' end by a T7 promoter sites. Two separate PCR reactions were set up, one with

PmDDX41i-T7F1 and *PmDDX41i-R1* (Table 1) for the sense strand template, the other with *PmDDX41i-F1* and *PmDDX41i-T7R1* (Table 1) for the anti-sense strand template. In addition, the exogenous gene (GFP gene) was amplified as a negative control with pEGFP-1 vector by using GFPT7-F and GFP-R (Table 1) for the sense strand template, and GFP-F and GFPT7-R (Table 1) for the anti-sense strand template. T7 RiboMAXTM Express Large Scale RNA ProductionTM System was used to generate single stranded RNAs. Equal amount of single stranded RNAs as annealed to produce dsRNA. The quality of dsRNAs are verified by 1.8% agarose gel electrophoresis, quantified by using UV visualization following ethidium bromide staining, and UV spectrophotometer. The dsRNAs were stored at -20°C for further *in vivo* experiment.

2.9.2 Shrimp preparation and injection

The 3-5 g body weight of shrimp were used to study the RNA interference (RNAi) and maintained as above. Shrimp were divided in to 3 groups and injected with either *PmDDX41* or GFP dsRNA or 150 mM NaCl. Approximately 25µl volume containing 2 µg of dsRNA in 150 mM NaCl per 1 g of a shrimp was injected through the lateral area of the fourth abdominal segment using a 0.5 ml insulin syringe. For the control groups, GFP dsRNA or 150 mM NaCl was injected into the shrimp.

2.9.3 Extraction of total RNA and synthesis of cDNA

After 24 h, shrimp hemolymph was collected for total RNA extraction using a FavorPrep Tissue Total RNA Purification Mini Kit (FAVORGEN Biotech Corp.) according to the manufacturer's instructions. First-strand cDNA was synthesized from the total RNA (200 ng.) using a RevertAid First Strand cDNA Synthesis Kit (Thermo

Scientific.) and oligo(dT.)₁₅ primer, according to the manufacturer's instructions as describes in section 2.2. First-strand cDNA was stored at -20°C for further investigated.

2.9.4 Semi-quantitative RT-PCR analysis

The efficiency of the *PmDDX41* knockdown was analyzed by semi-quantitative RT-PCR analysis using gene-specific primers for *PmDDX41*-F and *PmDDX41*-R (Table 1). A fragment of the EF1- α gene was amplified in a separate tube and served as an internal control for normalization. The PCR reactions and thermal cycling conditions were carried out as described above (Section 2.3). After amplification, the RT-PCR products were separated using TBE-2% (w/v) agarose gel electrophoresis and visualized as stated above.

2.9.5 Effect of *PmDDX41* gene silencing on the expression of other immune genes

The effects of the dsRNA-mediated *PmDDX41* gene silencing on the transcript expression levels of the other immune genes were determined by RT-PCR amplification and the expression levels were confirmed using quantitative real-time RT-PCR with specific primers (Table 1) for the *P. monodon* shrimp signal transduction pathways (*PmIKK β* , *PmIKK ϵ* , *PmRelish*, *PmCactus*, and *PmDorsal*), antimicrobial peptides (*PmPEN3*, *PmPEN5*, *ALFPm3*, *ALFPm6*, *CrustinPm1*, and *CrustinPm7*), and IFN-like molecules (*PmVago1*, *PmVago4*, and *PmVago5*) (Table 1). Amplification of the EF1- α fragment served as the internal control for cDNA template normalization.

2.9.6 Cumulative mortality assay

Cumulative mortality experiments for the *PmDDX41*-knockdown shrimp were performed using three groups of shrimp (3–5 g) that were intramuscularly injected with either *PmDDX41* dsRNA (2 µg), GFP dsRNA (2 µg), or 150 mM NaCl (25 µL volume). Twenty-four hours after the first dsRNA injection, the shrimp were injected with the same dose of WSSV challenged (2.64×10^5 copies/mL of WSSV in PBS). The shrimp injected with GFP dsRNA or NaCl were used as the controls. The numbers of dead shrimp were recorded daily for five days post-WSSV infection. Each experiment was performed in triplicate, with each group consisting of 9–10 healthy shrimp. Statistical analysis of the cumulative mortality was performed using one-way analysis of variance (ANOVA).

2.10 Protein expression of *PmDDX41* in *E. coli* system

2.10.1 Plasmid construction

The ORF of *PmDDX41* gene was amplified from shrimp hemocyte by using specific primers *PmDDX41BamHI*-F and *PmDDX41XhoI*-R (Table 1). The PCR reaction (25 µl) consisted of 1 µl of 10-fold diluted cDNA as a template, 5 µM of each forward and reverse primer, 2.5mM dNTP and 1 U Taq polymerase (RBC Bioscience). PCR amplification was performed under the following cycling conditions: 94 °C for 1 min, followed by 35 cycles of 94 °C for 30 s, 60 °C for 30 s, and 72 °C for 30 s, with an extension step at 72 °C for 10 min. The PCR products were separated by 1.5% agarose gel electrophoresis and visualized by UV-transillumination. The bands with the expected size were then excised and purified using a FavorPrep GEL/PCR Purification Kit (FAVORGEN Biotech Corp., Taiwan).

2.10.2 Protein expression and western blot analysis

To produce the recombinant protein *PmDDX41*, the recombinant clone was grown in Luria-Bertani (LB) medium containing 100 µg/ml ampicillin at 37°C overnight with agitation at 250 rpm. The culture was diluted 1:100 in fresh LB medium and cultured until the OD₆₀₀ reached to 0.6, then the protein expression was induced by adding isopropyl-β-D-thiogalactopyranoside (IPTG) to final concentration of 1 mM. The cells were harvested at 6 h post induction by centrifugation at 10,000 × g for 10 min at 4°C, and then resuspended in 20 mM Tris-HCl (pH 8.0). The crude protein was analyzed by SDS-PAGE (15% (w/v) acrylamide) and transferred onto nitrocellulose membrane (GE-Healthcare) by semi-dry blotter (Bio-Rad) at a constant 110 mA for 90 minutes. The membrane was blocked in PBST buffer (1XPBS, pH 7.4 and 0.05% (v/v) tween 20) containing 5% of skim milk at room temperature with shaking for 1 hour. The membrane was washed with PBST 3 times for each 10 min, then probed anti-human-DDX41-rabbit (1:2000; Abcam) and incubated at room temperature for 2 h. Then, the membrane was later incubated with goat anti-rabbit IgG-AP conjugate (1: 5,000; Millipore), a secondary antibody for additional 2 h at room temperature. The positive bands were visualized by color development using NBT/BCIP solution as a substrate.

2.11 Localization of *PmDDX41* in hemocyte by immunofluorescence microscopy

To observe the localization of *PmDDX41* in shrimp hemocyte, shrimp (15 ± 1g) were injected with WSSV (10⁵ copies/mL), poly(dA:dT) (2 µg/g shrimp) or poly(I:C) (2 µg/g shrimp). The PBS buffer was injected into shrimp as a control group. After 48 h, hemolymph was collected and fixed in 4% paraformaldehyde (ratio 1:1) for 10 min at room temperature. Then, hemocyte cells were separated by using

centrifuge at $800\times g$ at 4°C for 10 min. The hemocyte were resuspended with 1X PBS pH 7.4, counted by hemocytometer and centrifuged at $1,000 \times g$ at 4°C for 10 min onto poly-L-lysine slide (Thermo Scientific) (1×10^6 cells/slide). The cells were washed with 1X PBS pH 7.4 three times, permeabilized by 1% triton X-100 in 1X PBS pH 7.4 for 5 min at room temperature and washed three times with 1X PBS pH 7.4 for 5 min. Then, the cells were blocked with 10% fetal bovine serum (FBS) in 1X PBS pH7.4 at room temperature for 1 hour. The cells were probed with 1:1000 dilution the purified rabbit polyclonal anti-human-DDX41 (Abcam) at room temperature for 3 hours and the negative control were incubated with 1% FBS in 1X PBS pH7.4. The slides were washed and probed with secondary antibody, 1:1000 dilution of goat anti-rabbit antibody conjugated with Alexa Fluor 568 in 1% FBS in 1X PBS pH 7.4 at room temperature for 1 hour. To stain the nuclear DNA, the cells were incubated with 4',6-diamidino-2-phenylindole (DAPI) before mounting with medium Prolong® Gold antifade reagent. The fluorescent staining was observed under FV1000 confocal laser scanning microscope (Olympus).

2.12 HEK293T cells preparation

HEK293T cells were cultured in DMEM medium with 10% heat-inactivated fetal bovine serum (FBS) in 5% CO_2 incubator. High molecular weight (HMW) polyinosinic-polycytidylic acid (poly (I:C)) and polydeoxyadenylic-deoxythymidylic acid sodium salt (poly (dA: dT)) were purchased from Invivogen that were each mixed with lipofectamine 2000 at ratio of 1:1 ($\mu\text{g}/\mu\text{l}$) in Opti-MEM for cell stimulation. The following antibodies were used: anti-DDX41, anti-Flag and anti-c-Myc.

2.13 Luciferase activity assay of *PmDDX41*

2.13.1 Plasmid construction

The full-length sequence of *PmDDX41* was amplified from hemocyte by using specific primers Myc_*PmDDX41*_BamHI-F and Myc_*PmDDX41*_XhoI-R (Table 1). The PCR reaction of 25 μ l consisted of 1X PCR buffer KOD FX, 4 mM dNTP, 0.3 μ M each primer, 1 μ l cDNA normal shrimp sample and 1 U KOD FX DNA Polymerase (TOYOBO). The PCR thermal cycling conditions were 94°C for 2 min, 35 cycles of 98°C for 10 sec 55°C for 30 sec and 68°C for 1 min 30 sec, and then a final extension at 68°C 7 min. The PCR products were analyzed by using 1.5% agarose gel electrophoresis. Agarose powder was dissolved in 1X TAE buffer (Tris-HCl, Acetate, EDTA), boiled the solution. Midori green advance DNA staining was added into the gel which poured into tray and the plastic comb was placed in the gel after the solution cool down. Then, the gel was completely set and PCR products were mixed with 6X dye DNA and loaded each well. The size was determined by comparing with DNA Marker (100 bp or 1 kb). Electrophoresis was performed at 100 mV 30 min and DNA fragment was detected by UV transilluminator and photographed. The expected bands were cut from agarose gel. FavorPrep GEL/PCR purification kit (FAVOGEN[®]) was used for DNA purification from gel. Briefly, the 500 μ l of PADF buffer was added to dissolved gel and melted at 55-60 °C for 10 min or until gel was completely dissolved. The solution was transferred into FADF column and then centrifuged at 11,000 xg for 30 sec at room temperature. The supernatant was removed, washed by adding 750 μ l of wash buffer and centrifuged at 11,000 xg for 30 sec and centrifuge again at full speed for 3 min to dry the column matrix. The ultrapure water 25 μ l was used as elution buffer and stored at -20°C. The

purified PCR was digested by the restriction enzymes, *Bam*HI and *Xho*I at 37°C for overnight and cloned into a pcDNA3-Myc expression vector (Santa Cruz Biotechnology) (**Fig. 15**). The reporter plasmids for IFN- β and NF- κ B and the expression vectors for IPS-1 and STING were constructed as described previously (Kawai et al., 2005).

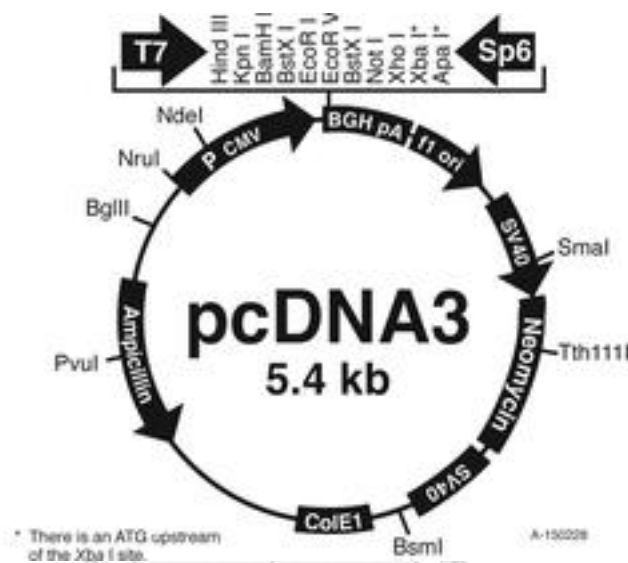


Fig. 15 The map of pcDNA3-Myc expression vector (Santa Cruz Biotechnology).

2.13.2 Luciferase reporter assay

Luciferase assay was performed to investigate the role of *Pm*DDX41-mediated IFN- β and NF- κ B expression. HEK293T cells (1×10^5 cell/ml) were plated into 24-well plates and transfected with 100 ng of reporter plasmid for IFN- β and NF- κ B and 500 ng of *Pm*DDX41-Myc expression plasmid or empty plasmid. As an internal control, 10 ng of pRL-TK (Promega) was transfected. The medium was replaced at 6 h post-transfection. After 24 h transfection, cells were stimulated with 1 μ g/ml of poly(dA:dT) and poly(I:C). After 6 h stimulation, HEK293T cells were measured the

luciferase assay with a TriStar² LB 942 Multidetector Microplate Reader (Berthold) using the Dual-Glo Luciferase System (Promega) according to the manufacturer's instructions.

2.14 Localization of *PmDDX41* in HEK293T cells after stimulation with nucleic acid mimics

To observe the localization of *PmDDX41* in cells, HEK293T cells were cultured on poly-L-Lysine-coated coverslips in 24-well plates for 6 h and transfected with 1000 ng of *PmDDX41*-c-myc expression plasmid for 16 h. Cells were stimulated with 1 µg/ml of poly(dA:dT) and poly(I:C) for 6 h and fixed with 4% paraformaldehyde for 30 min. Cells were washed 3 times with 0.02% Triton X-100 in PBS and permeabilized with PBS containing 100 mM glycine and 0.02% Triton X-100 for 30 min. Cells were blocked PBS with 10% FBS and 0.02% Triton X-100 at 4°C overnight and probed with 1:100 dilution of primary antibody; anti-c-Myc at 4°C overnight. The coverslips were washed and incubated with secondary antibody; anti-mouse and/or anti-rabbit conjugated to Alexa Fluor 568 (Invitrogen) at room temperature for 1 h. Nuclei were probed with Hoechst 33342. Stained cells were mounted with Fluoro-KEEPER Antifade Reagent (Nacalai Tesque, Japan). Fluorescence photo were obtained by LSM 700 (Carl Zeiss).

2.15 Binding activity of *PmDDX41* protein with nucleic acid mimics

2.15.1 Biotin labeled nucleic acids

Nucleic acid mimic, poly(dA:dT) was labeled with biotin using Biotin DecaLabel DNA Labeling Kit (Thermo Scientific) according to the manufacturer's instructions. Briefly, 1 ng of poly(dA:dT) was added with 10 µl of 5X reaction buffer

decanucleotide and adjusted with nuclease free-water to 44 μ l. The tube was boiled for 5-10 min and cooled it on ice. After that, the mixture was added with 5 μ l of biotin labeling mix and 5 units of Klenow fragment' exonuclease. The tube was incubated at 37°C for 20 hours. The reaction was stopped by the addition of 1 μ l of 0.5 M EDTA, pH 8.0. The labeled DNA was stored at -20°C.

2.15.2 Protein expression of PmDDX41 in HEK293T cells

To determine whether *PmDDX41* directly binds DNA, HEK293T cells (1×10^6 cell/ml) were transfected with 4 μ g of *PmDDX41*-Myc recombinant plasmid containing Myc tags using Lipofectamine 2000. After 24 h, cells were lysed by homo buffer (150 mM NaCl, 5mM EDTA pH 8.0, 25 Mm Tris-HCl pH 8.0 and 0.2% TritonX-100) and sonicated. The crude protein was harvested by centrifugation at 13,000 rpm for 15 min and kept at -20°C.

2.15.3 Co-immunoprecipitation

The *PmDDX41* protein was immunoprecipitated with 500 ng poly(dA:dT) and poly(I:C)-labeled-biotin (Invivogen) and 1:250 dilution of anti-Myc-rabbit overnight at 4°C and then added with protein A sepharose bead (GE) for 4 h at 4°C. The beads with immunoprecipitants were washed 3 times with homo buffer. Whole-protein and immunoprecipitants were immunoblotted with indicated antibodies.

2.16 Luciferase reporter assay of PmDDX41 after co-transfected with MmSTING

2.16.1 Cloning of PmDDX41 into pCMV-5 expression vector

The full-length sequence of *PmDDX41* was amplified from hemocyte using specific primers Flag_*PmDDX41*_SalI-F and Flag_*PmDDX41*_BamHI-R (Table 1). The PCR of 25 μ l consisted of 1X PCR buffer KOD FX, 4 mM dNTP, 0.3 μ M each

primer, 1 μ l cDNA normal shrimp sample and 1 U KOD FX DNA Polymerase (Toyobo). The PCR thermal cycling conditions were 94°C for 2 min, 35 cycles of 98°C for 10 sec 60°C for 30 sec and 68°C for 1 min 30 sec, and then a final extension at 68°C 7 min. The PCR products were analyzed by using 1.5% agarose gel electrophoresis. The standard method of PCR clean-up was carried out as described above. The purified PCR was digested with the restriction enzymes, *SalI* and *BamHI* at 37°C for overnight and cloned into a pCMV-5-FLAG (Sigma) expression vector (Fig. 16). The reporter plasmids for IFN- β and NF- κ B and the expression vectors for IPS-1 and *Mm*STING were constructed as described previously.

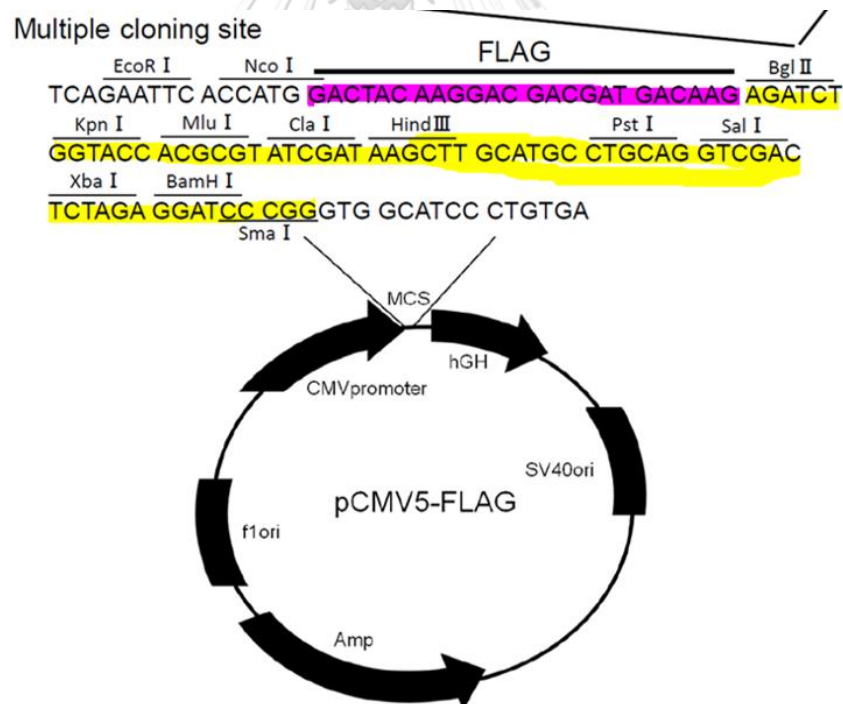


Fig. 16 The map of pCMV5-Flag expression vector (Sigma).

2.16.2 Luciferase assay detection after co-transfection with *MmSTING*

HEK293T cells (1×10^5 cell/ml) were plated into 24-well plates and transfected with 100 ng of reporter plasmid for IFN- β and NF- κ B and 500 ng of *PmDDX41*-Flag and *MmSTING*-Myc expression vector. The empty plasmid; pCMV5-FLAG was transfected as a control. As an internal control, 10 ng of pRL-TK (Promega) was transfected. After 24 h transfection, cells were stimulated with 1 μ g/ml of poly(dA:dT) and poly(I:C). After 6 h stimulation, HEK293T cells were measured the luciferase activity with a TriStar² LB 942 Multidetector Microplate Reader (Berthold) using the Dual-Glo Luciferase System (Promega) according to the manufacturer's instructions.

2.17 Localization of *PmDDX41* and *MmSTING* in HEK293T cells

PmDDX41 and *MmSTING* were observed by using immunofluorescent microscopy HEK293T cells were cultured on poly-L-Lysine-coated coverslips in 24-well plates for 6 h and co-transfected with 1000 ng of *PmDDX41*-Flag and *MmSTING*-Myc expression plasmid for 16 h. Cells were stimulated with 1 μ g/ml of poly(dA:dT) and poly(I:C) for 6 h and fixed with 4% paraformaldehyde for 30 min. The standard method of cells preparation was as described above. Cells were probed with 1:100 dilution of primary antibody; anti-flag and anti-c-Myc at 4°C overnight. The coverslips were washed and incubated with secondary antibody; anti-mouse and/or anti-rabbit conjugated to Alexa Fluor 488 (Invitrogen) or 568 (Invitrogen) at room temperature for 1 h. Nuclei were probed with Hoechst 33342. Stained cells were mounted with Fluoro-KEEPER Antifade Reagent (Nacalai Tesque). Fluorescence photo were obtained by LSM 700 (Carl Zeiss).

2.18 Characterization of *PmDDX41* and *MmSTING* protein in HEK293T cells

2.18.1 Protein expression and Co-immunoprecipitation

The recombinant plasmids, *PmDDX41*-Flag and *MmSTING*-Myc were co-transfected into HEK293T cells (1×10^6 cell/ml) which seeded into 10-cm dishes using Lipofectamine 2000. After 24 h, cells were stimulated with $1 \mu\text{g/ml}$ of poly(dA:dT) and poly(I:C) for 6 h. Cells were lysed by lysis buffer (150 mM NaCl, 5 mM EDTA pH 8.0, 25 mM Tris-HCl pH8.0 and 0.2% Triton X-100) that containing protease inhibitor cocktail (Roche). After sonication, cell lysates were immunoprecipitated with 1:500 dilution of anti-Myc-mouse overnight at 4°C and then treated with protein A sepharose bead (GE) for 4 h at 4°C . The beads with immunoprecipitates were washed 3 times with lysis buffer. Whole-cell lysates and immunoprecipitates were immunoblotted with indicated antibodies.

2.18.2 SDS-PAGE and western blotting

The beads were loaded on a reducing SDS-PAGE gel (12.5% (w/v) acrylamide resolving gel), and blotted onto a nitrocellulose membrane (GE). Membranes were then blocked in 5% (w/v) skim milk in 1X PBS and 0.05% (v/v) Tween 20 (PBST). The membrane was detected with 1:5,000 dilution anti-Flag-rabbit polyclonal antibodies as the primary antibody and the mouse-anti-Myc as internal control, washed 3 times with PBST. Then, the membrane was incubated with 1: 5,000 HRP-conjugated antibodies against rabbit and mouse IgG (sigma-aldrich) using Western Lighting Plus-ECL (PerkinElmer). HRP activity was detected by a LAS 4000 (Fujitsu Life Sciences).

2.19 Analysis of DNA-binding site of *PmDDX41*

2.19.1 IFN- β and NF- κ B luciferase activity assay

2.19.1.1 Construction of the expression plasmid

The truncated genes of *PmDDX41* containing the DEADc or HELICc domain, were amplified using the specific primers (Table 1). The PCR of 25 μ l reaction consisted of 1X KOD FX PCR buffer, 4 mM dNTP, 0.3 μ M each primer, 1 μ l cDNA normal shrimp sample and 1 U KOD FX DNA Polymerase (TOYOBO). The PCR thermal cycling conditions were 94°C for 2 min, 35 cycles of 98°C for 10 sec 58°C for 30 sec and 68°C for 1 min 30 sec, and then a final extension at 68°C 7 min. The PCR products were analyzed by 1.5% agarose gel electrophoresis. The method of PCR purification was as described above. The purified PCR was digested with the restriction enzymes, *SalI* and *BamHI* at 37°C for overnight and cloned into a pcDNA3-Myc and pCMV-5-Flag expression vectors. The reporter plasmids for IFN- β and NF- κ B and the expression vectors for IPS-1 and *MmSTING* were constructed as described previously.

2.19.1.2 IFN- β and NF- κ B luciferase activity detection of mutated-

PmDDX41

HEK293T cells (1×10^5 cell/ml) were plated into 24-well plates and transfected with 100 ng of reporter plasmid for IFN- β and NF- κ B and 500 ng of expression vector; *PmDDX41*-Myc, Dead*Pm*-Myc and Helic*Pm*-Myc or empty vector. As an internal control, 10 ng of pRL-TK (Promega) was transfected. The medium was replaced at 6 h post-transfection. After 24 h transfection, cells were stimulated with 1 μ g/ml of poly (dA:dT) and poly (I:C). After 6 h stimulation, HEK293T cells were

measured the luciferase activity with a TriStar² LB 942 Multidetector Microplate Reader (Berthold) using the Dual-Glo Luciferase System (Promega, USA) according to the manufacturer's instructions.

2.19.1.3 IFN- β and NF- κ B luciferase activity detection of mutant-*PmDDX41* and *MmSTING* in cells

HEK293T cells (1×10^5 cell/ml) were plated into 24-well plates and transfected with 100 ng of the reporter plasmid for IFN- β and NF- κ B and 500 ng of mutant-*PmDDX41*-Flag (*PmDDX41*-Flag, Dead*Pm*-Flag and Helic*Pm*-Flag) and *MmSTING*-Myc expression vector. The empty plasmid; pCMV5-FLAG was transfected as a control. As an internal control, 10 ng of pRL-TK (Promega) was transfected. The DMEM medium was replaced at 6 h post-transfection. After 24 h transfection, cells were stimulated with 1 μ g/ml of poly(dA:dT) and poly(I:C). After 6 h stimulation, HEK293T cells were measured the luciferase activity with a TriStar² LB 942 Multidetector Microplate Reader (Berthold) using the Dual-Glo Luciferase System (Promega) according to the manufacturer's instructions.

2.19.2 Localization of mutant-*PmDDX41* proteins

HEK293T cells were cultured on poly-L-Lysine-coated coverslips in 24-well plates for 6 h and transfected with 1000 ng of mutant-*PmDDX41*-Myc (*PmDDX41*-Myc, Dead*Pm*-Myc and Helic*Pm*-Myc) expression vector for 16 h. Cells were stimulated with 1 μ g/ml of poly(dA:dT) and poly(I:C) for 6 h. The cells preparation method was as described above. Cells were probed with 1:100 dilution of primary antibody; anti-Myc-mouse at 4°C overnight. The coverslips were washed and incubated with secondary antibody; anti-mouse conjugated to Alexa Fluor 568

(Invitrogen) at room temperature for 1 h. Nuclei were probed with Hoechst 33342. Stained cells were mounted with Fluoro-KEEPER Antifade Reagent (Nacalai Tesque). Fluorescence photo were obtained by LSM 700 (Carl Zeiss).

2.19.3 Immunofluorescence confocal microscopy of mutated-*PmDDX41* and *MmSTING*

To observe the co-localization of mutated-*PmDDX41* and *MmSTING* in HEK293T cells which cultured on poly-L-Lysine-coated coverslips in 24-well plates for 6 h and co-transfected with 1000 ng of mutant-*PmDDX41*-Flag and *MmSTING*-Myc expression plasmid for 16 h. Cells were stimulated with 1µg/ml of poly(dA:dT) and poly (I:C) for 6 h. The sample preparation was described above. HEK293T cells were probed with 1:100 dilution of primary antibody; anti-flag and anti-c-Myc at 4°C overnight. The coverslips were washed and incubated with secondary antibody; anti-mouse and/or anti-rabbit conjugated to Alexa Fluor 488 (Invitrogen) or 568 (Invitrogen) at room temperature for 1 h. Nuclei were probed with Hoechst 33342 for 30 min. Stained cells were mounted with Fluoro-KEEPER Antifade Reagent (Nacalai Tesque). Fluorescence photo were obtained by LSM 700 (Carl Zeiss).

2.19.4 Interaction of mutated-*PmDDX41* and *MmSTING*

2.19.4.1 Protein expression and Co-immunoprecipitation

To map the STING-binding sites of *PmDDX41*, the recombinant protein mutated-*PmDDX41*-Flag and *MmSTING*-Myc were obtained by co-transfecting HEK293T cells (1×10^6 cell/ml) with 4 µg of expression plasmid. After 24 h, cells were stimulated with 1µg/ml of poly(dA:dT) and poly(I:C) for 6 h. Cells were lysed by lysis buffer that containing protease inhibitor cocktail (Roche). After sonication,

cell lysates were immunoprecipitated with 1:500 dilution of anti-Myc-mouse overnight at 4°C and then treated with protein A sepharose bead (GE) for 4 h at 4°C. The beads with immunoprecipitants were washed 3 times with homo buffer. Whole-cell lysates and immunoprecipitants were immunoblotted with indicated antibodies.

2.19.4.2 SDS-PAGE and western blot analysis

The beads were loaded on a reducing SDS-PAGE gel (12.5% (w/v) acrylamide resolving gel), and blotted onto a nitrocellulose membrane (GE). Membranes were then blocked in 5% (w/v) BSA in 1X PBS and 0.05% (v/v) Tween 20 (PBST). The membrane was detected with 1:5,000 dilution anti-Flag-rabbit polyclonal antibodies as the primary antibody and the anti-Myc-mouse as internal control, washed 3 times with PBST. Then, the membrane was incubated with 1:5,000 HRP-conjugated antibodies against rabbit and mouse IgG (sigma-aldrich) using Western Lighting Plus-ECL (PerkinElmer). HRP activity was detected by a LAS 4000 (Fujitsu Life Sciences).

CHAPTER III

RESULTS

3.1 Searching the *Penaeus monodon* EST database and cloning the open reading frame (ORF) of *PmDDX41*

To identify a cytosolic DNA sensor in black tiger shrimp, the *Penaeus monodon* EST database (<http://pmonodon.biotech.or.th>) (Tassanakajon et al., 2006) was searched for the cDNA sequence of DDX41. A DNA sequence from three ESTs, namely, NODE_45370, NODE_133992, and NODE_285756, was assembled and identified as DDX41. The specific primers ORF-*PmDDX41*-F/-R (Table 1) were designed to amplify the ORF of *PmDDX41* cDNA from shrimp hemocytes (**Fig. 17A**). The complete ORF of *PmDDX41* consists of 1863 bp encoding a protein with 620 amino acid residues (GenBank accession number: KY608746; **Fig. 17B**). The protein has a predicted molecular mass and isoelectric point (pI) of 70 kDa and 6.84, respectively. Analysis of the conserved domain using the SMART program revealed that *PmDDX41* contains N-terminal, a DEAD-like helicase superfamily domain (DEXDc, 193–411 aa), one helicase superfamily C-terminal domain (HELICc, 439–520 aa), and one zinc finger domain (ZnF, 579–595 aa) (**Fig. 17C**). A database search using the BLASTX algorithm revealed that *PmDDX41* shared high similarity to the homolog of vertebrates DDX41 which was named Abstrakt in invertebrates (*HaAbstrakt* in *Hyaella azteca* (88% similarity), *MrAbstrakt* in *Megachile rotundata* (83% similarity), *AfAbstrakt* in *Apis florea* (83% similarity), and *DmAbstrakt* in *Drosophila melanogaster* (79% similarity)) and DDX41 in vertebrates (*LoDDX41* in *Lepisosteus oculatus* (80% similarity), *BtDDX41* in *Bos taurus* (81% similarity),

SsDDX41 in *Sus scrofa* (80% similarity), and HsDDX41 in *Homo sapiens* (80% similarity)).

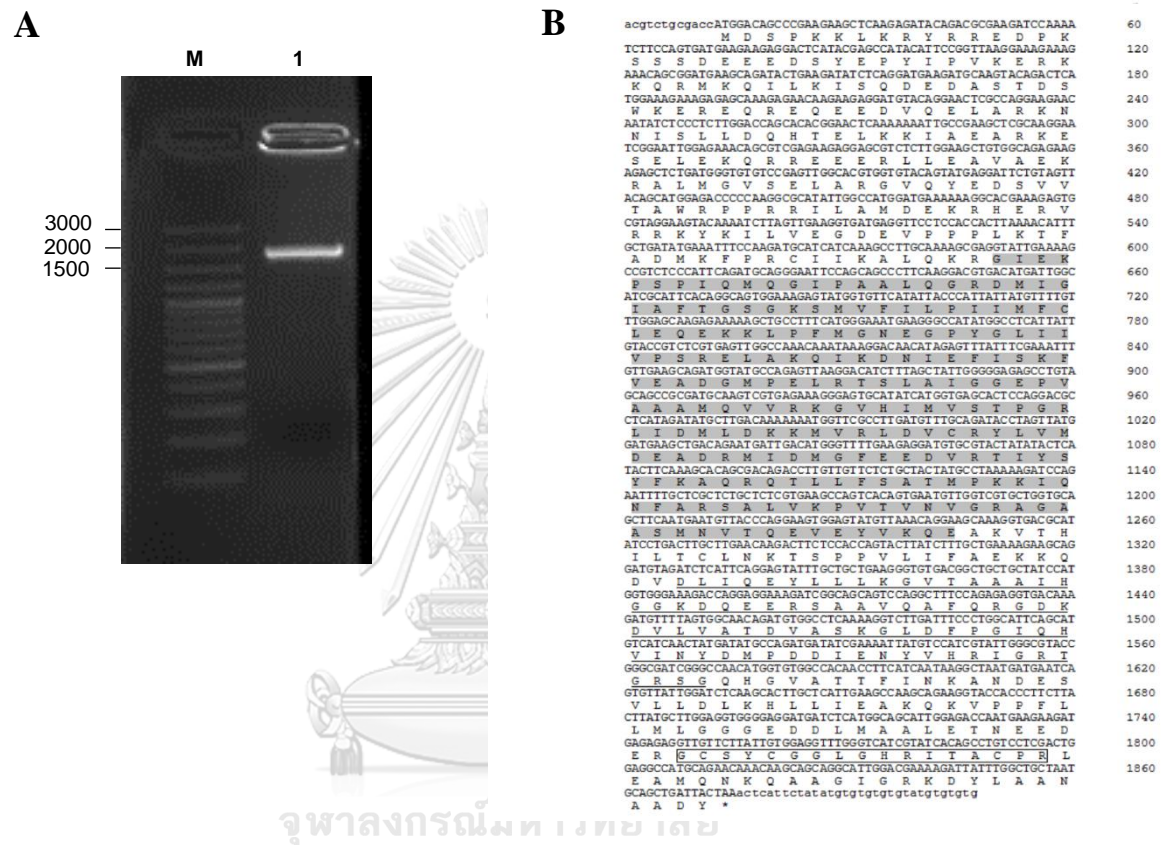


Fig. 17 Sequence and domain analysis of *PmDDX41*.

(A) *PmDDX41* was amplified from hemocytes. The PCR product was visualized under UV transilluminator following 1.5% (w/v) agarose-TBE gel electrophoresis. Lane M is GeneRuler™ 100 bp DNA ladder. Lane 1 is *PmDDX41* gene in shrimp hemocyte. (B) Nucleotide and deduced amino acid sequences of *PmDDX41* cDNA. The DEXDc domain is boxed with a gray background. The HELICc domain is underlined. The zinc finger domain is boxed. The stop codon TAA is indicated with an asterisk. (C) A schematic representation of the structural domains of *PmDDX41* analyzed using the SMART program.

3.2 Multiple sequence alignment and phylogenetic analysis

The multiple sequence alignment of the deduced amino acid sequences of *PmDDX41* with other DDX41 in vertebrates and invertebrates using ClustalW2 revealed that the protein *PmDDX41* contains three conserved domains, namely, the DEADc domain, the HELICc domain, and the zinc finger domain (**Fig. 18**).

To examine the relationship of *PmDDX41* with its homologs from other species of vertebrates and invertebrates, an unrooted neighbor-joining phylogenetic tree was drawn based on the predicted DEXDc and HELICc domains from various species. The results showed that these DDX41 proteins could be divided into two groups (**Fig. 19**). Group 1 contains DDX41 proteins from vertebrates, whereas group 2 contains Abstrakt proteins from invertebrates. *PmDDX41* clustered together with Abstrakt from amphipod crustaceans and invertebrates.


```

MrAbstrakt --MEQSEES--SRKRYRREDQKEESFFDQVDDNYVPYVVKERKKQLTKLGLGQKDDAAVGIKSSSENEKDDGD
AfAbstrakt MIMAQKEDP---FKRYRREEKESSEFFDADDNYIPYVVKERKKQLTKLGLGQKDEAAVGIKSSSENEKDDAD
DmAbstrakt -----MA---HVKKYRRESKSESEGLDNDYVYVVKERKKQMLKGLRIVGLVSTAQFK---SSSENEEDDSGG
HaAbstrakt --MS---HSMHPQTKRYRRE--SKSSDEEEDF--VFSAKERKKQLKLFKGVHEADGNKHLDDDDGKDEEPEGE
PmDDX41 -----MDSPKKLRKRYRRE--FKSSDEEEDSEYVYVVKERKKQMLKGLRISQEDAST-----DSWKEERQREQ
LoDDX41 -----METE---SRTRKRYVQEEEDAFSDEEKYVYVVKERKKQMLKGLRIRGK-----GLTEEQKDSNEQRD
BtDDX41 --MAESEPERKARATDEATGSRSEAEDEDEDYVYVVKERKKQLLQKLRKRRK-----GAAEEEQDSSEPRG
HsDDX41 --MESEPERKARATDEVLPSEAAFRMTRTRTCFMC--RYAAPQLLQKLRKRRK-----GAAEEEQDSSEPRG
GgDDX41 -----MEPGAERRRQREAAAD--GSDMSGEDEDEDYVYVVKERKKQMLKGLRIRK-----VSEEEQRDSSEPRG

MrAbstrakt DDDGQVNGRKNSSLLDQDHLKRPAPARRESAEPQLKPEEKILSVREGPALMSWENMREITDDIPICWFRARYI
AfAbstrakt DDDGQVNGRKNSSLLDQDHLKRPAPARRESAEPQLKPEEKILSVREGPALMSWENMREITDDIPICWFRARYI
DmAbstrakt AHDVETNGRKNSSLLDQDHLKRPAPARRESAEPQLKPEEKILSVREGPALMSWENMREITDDIPICWFRARYI
HaAbstrakt EEDAQLLAKNNSSLLDQDHLKRPAPARRESAEPQLKPEEKILSVREGPALMSWENMREITDDIPICWFRARYI
PmDDX41 EEDVQLAKNNSSLLDQDHLKRPAPARRESAEPQLKPEEKILSVREGPALMSWENMREITDDIPICWFRARYI
LoDDX41 DEE--AIGFRNYSLLDQDHLKRPAPARRESAEPQLKPEEKILSVREGPALMSWENMREITDDIPICWFRARYI
BtDDX41 DEDDIFLGPQSSNLLDQDHLKRPAPARRESAEPQLKPEEKILSVREGPALMSWENMREITDDIPICWFRARYI
HsDDX41 DEDDIFLGPQSSNLLDQDHLKRPAPARRESAEPQLKPEEKILSVREGPALMSWENMREITDDIPICWFRARYI
GgDDX41 DEDDIFLGPQSSNLLDQDHLKRPAPARRESAEPQLKPEEKILSVREGPALMSWENMREITDDIPICWFRARYI

MrAbstrakt LALGEARHERVVKRLILVEGDDIPEPKSRPMKFRHGLNGEQKGIKFTPIQOGHTIVUSGRDIIIGIAPTGGST
AfAbstrakt LAAEGARHERVVKRLILVEGDDVPPPKSRPMKFRHGLNGEQKGIKFTPIQOGHTIVUSGRDIIIGIAPTGGST
DmAbstrakt REMSEEREAVGKELRILVEGETPSPPKSRPMKFRHGLNGEAAKIKNFTPIQOGHTIVUSGRDIIIGIAPTGGST
HaAbstrakt MAMSNRHERVVKRYKILVEGEDVPEPKSRPMKFRHGLNGEAAKIKNFTPIQOGHTIVUSGRDIIIGIAPTGGST
PmDDX41 LAMDEKRHERVVKRYKILVEGEDVPEPKSRPMKFRHGLNGEAAKIKNFTPIQOGHTIVUSGRDIIIGIAPTGGST
LoDDX41 LSMFPAHRDVRVKRYKILVEGEGIPPKSRPMKFRHGLNGEAAKIKNFTPIQOGHTIVUSGRDIIIGIAPTGGST
BtDDX41 LSMSEERHERVVKRYKILVEGEGIPPKSRPMKFRHGLNGEAAKIKNFTPIQOGHTIVUSGRDIIIGIAPTGGST
HsDDX41 LSMSEERHERVVKRYKILVEGEGIPPKSRPMKFRHGLNGEAAKIKNFTPIQOGHTIVUSGRDIIIGIAPTGGST
GgDDX41 LAMSEARHNRVVKRYKILVEGEGIPPKSRPMKFRHGLNGEAAKIKNFTPIQOGHTIVUSGRDIIIGIAPTGGST

MrAbstrakt LVFVLEHIMFQDQEVYVAMPFVRNEGPYGLIIPSPRELAKTYDIIIRHYTNSLRQAGCEPRSCAIGGVEFSESLEYINK
AfAbstrakt LVFVLEHIMFQDQEVYVAMPFVRNEGPYGLIIPSPRELAKTYDIIIRHYTNSLRQAGCEPRSCAIGGVEFSESLEYINK
DmAbstrakt LVFVLEHIMFQDQEVYVAMPFVRNEGPYGLIIPSPRELAKTHEIIQHYSKHLQAGCEPRSCAIGGVEFSEALDVIIR
HaAbstrakt LVFVLEHIMFQDQEVYVAMPFVRNEGPYGLIIPSPRELAKIVENVEYIAQFVLDAGLPEPRVCGAIGGVEFSEALDVIIR
PmDDX41 MVFVLEHIMFQDQEKKLPFMGNEGPYGLIIPSPRELAKIKDNIETIKFVEADGMPEPRVCGAIGGVEFSEALDVIIR
LoDDX41 LVFVLEHIMFQDQEKRLPFRKRGYGLIIPSPRELAKHSIIIEYCKLLEEAGAPRCAQDGGGSKQEMVVRKH
BtDDX41 LVFVLEHIMFQDQEKRLPFRKRGYGLIIPSPRELAKHSIIIEYCKLLEEAGAPRCAQDGGGSKQEMVVRKH
HsDDX41 LVFVLEHIMFQDQEKRLPFRKRGYGLIIPSPRELAKHSIIIEYCKLLEEAGAPRCAQDGGGSKQEMVVRKH
GgDDX41 LVFVLEHIMFQDQEKRLPFRKRGYGLIIPSPRELAKHSIIIEYCKLLEEAGAPRCAQDGGGSKQEMVVRKH

DEXDc domain
MrAbstrakt GVHIMVATPGRLLDMLKRMVKSVCRYLMDIADRMIDMGFEEDVRTISSEFRGQRTLLFSATMPKKIQNFAFSALVK
AfAbstrakt GVHIMVATPGRLLDMLKRMVKSVCRYLMDIADRMIDMGFEEDVRTISSEFRGQRTLLFSATMPKKIQNFAFSALVK
DmAbstrakt GVHIMVATPGRLLDMLKRMVKSVCRYLMDIADRMIDMGFEEDVRTISSEFRGQRTLLFSATMPKKIQNFAFSALVK
HaAbstrakt GVHIMVATPGRLLDMLKRMVKSVCRYLMDIADRMIDMGFEEDVRTISSEFRGQRTLLFSATMPKKIQNFAFSALVK
LoDDX41 GVHIMVATPGRLLDMLKRMVKSVCRYLMDIADRMIDMGFEEDVRTISSEFRGQRTLLFSATMPKKIQNFAFSALVK
BtDDX41 GVHIMVATPGRLLDMLKRMVKSVCRYLMDIADRMIDMGFEEDVRTISSEFRGQRTLLFSATMPKKIQNFAFSALVK
HsDDX41 GVHIMVATPGRLLDMLKRMVKSVCRYLMDIADRMIDMGFEEDVRTISSEFRGQRTLLFSATMPKKIQNFAFSALVK
GgDDX41 GVHIMVATPGRLLDMLKRMVKSVCRYLMDIADRMIDMGFEEDVRTISSEFRGQRTLLFSATMPKKIQNFAFSALVK

MrAbstrakt PVYINVGAGAAAMNVDQVEYVKEARIVYLLDCLCKRTDPPVLIFAEKKQDVDAHEYLLLRGVBAVAIHGGKQDEERS
AfAbstrakt PVYINVGAGAAAMNVDQVEYVKEARIVYLLDCLCKRTDPPVLIFAEKKQDVDAHEYLLLRGVBAVAIHGGKQDEERS
DmAbstrakt PVYINVGAGAAAMNVDQVEYVKEARIVYLLDCLCKRTDPPVLIFAEKKQDVDAHEYLLLRGVBAVAIHGGKQDEERS
HaAbstrakt PVYINVGAGAAAMNVDQVEYVKEARVTHIPLCANKRTDPPVLIFAEKKQDVDAHEYLLLRGVBAVAIHGGKQDEERS
PmDDX41 PVYINVGAGAAAMNVDQVEYVKEARVTHIPLCANKRTDPPVLIFAEKKQDVDAHEYLLLRGVBAVAIHGGKQDEERS
LoDDX41 PVYINVGAGAAALDQVEYVKEARIVYLLDCLCKRTDPPVLIFAEKKQDVDAHEYLLLRGVBAVAIHGGKQDEERT
BtDDX41 PVYINVGAGAAALDQVEYVKEARIVYLLDCLCKRTDPPVLIFAEKKQDVDAHEYLLLRGVBAVAIHGGKQDEERT
HsDDX41 PVYINVGAGAAALDQVEYVKEARIVYLLDCLCKRTDPPVLIFAEKKQDVDAHEYLLLRGVBAVAIHGGKQDEERT
GgDDX41 PVYINVGAGAAALDQVEYVKEARIVYLLDCLCKRTDPPVLIFAEKKQDVDAHEYLLLRGVBAVAIHGGKQDEERT

HELICc domain
MrAbstrakt RSVDFRQGRKDWLVADVASKGLDFPAIQHVNYDMPEEDENYVHRIGRSGRSRTGATTEINRACDPSVLDLRLHL
AfAbstrakt RSVDFRQGRKDWLVADVASKGLDFPAIQHVNYDMPEEDENYVHRIGRSGRSRTGATTEINRACDPSVLDLRLHL
DmAbstrakt RAVDFRQGRKDWLVADVASKGLDFPAIQHVNYDMPEEDENYVHRIGRSGRSRTGATTEINRACDPSVLDLRLHL
HaAbstrakt AAIDAFKRLKDWLVADVASKGLDFPGIKHVNYDMPEEDENYVHRIGRSGRSKATTSVATTINRACDPSVLDLRLHL
PmDDX41 AAQCAFQGRKDWLVADVASKGLDFPGIQHVNYDMPEEDENYVHRIGRSGRSKATTSVATTINRACDPSVLDLRLHL
LoDDX41 KAIDAFRQGRKDWLVADVASKGLDFPAIQHVNYDMPEEDENYVHRIGRSGRSRTGATTEINRACDPSVLDLRLHL
BtDDX41 KAIDAFRQGRKDWLVADVASKGLDFPAIQHVNYDMPEEDENYVHRIGRSGRSRTGATTEINRACDPSVLDLRLHL
HsDDX41 KAIDAFRQGRKDWLVADVASKGLDFPAIQHVNYDMPEEDENYVHRIGRSGRSRTGATTEINRACDPSVLDLRLHL
GgDDX41 KAIDAFRQGRKDWLVADVASKGLDFPAIQHVNYDMPEEDENYVHRIGRSGRSRTGATTEINRACDPSVLDLRLHL

Zinc finger domain
MrAbstrakt MEAKQVFPFHEELCSENE-K----YINLGDERSGSIQGLGHRITDCELEAVQKCVSINGRDPYLAHSMVF
AfAbstrakt MEAKQVFPFHEELCSENE-T----YINLGDERSGSIQGLGHRITDCELEAVQKCVSINGRDPYLAHSMVF
DmAbstrakt LEAKQVFPFHEELPAPTEHQ----HLDGDSHGIYQGLGHRITDCELEAVQKCVSINGRDPYLAHSMVF
HaAbstrakt LEAKQVFPFHEELDNDFLAAPTSTNGDGAQSGSIQGLGHRITDCELEAVQKCVSINGRDPYLAHSMVF
PmDDX41 LEAKQVFPFHEELDGGEDDLMAA--LETNEEDERSGSIQGLGHRITDCELEAVQKCVSINGRDPYLAHSMVF
LoDDX41 LEAKQVFPFHEELVDTGDE-T----MLDIGGERGCTFQGLGHRITDCELEAVQKCVSINGRDPYLAHSMVF
BtDDX41 LEAKQVFPFHEELVHCQDE-S----MLEIGGERGCAFCQGLGHRITDCELEAVQKCVSINGRDPYLAHSMVF
HsDDX41 LEAKQVFPFHEELVHCQDE-S----MLDIGGERGCAFCQGLGHRITDCELEAVQKCVSINGRDPYLAHSMVF
GgDDX41 LEAKQVFPFHEELVHCQDE-T----MLDIGGERGCAFCQGLGHRITDCELEAVQKCVSINGRDPYLAHSMVF

```

Fig. 18 Sequence analysis of *PmDDX41* gene.

Multiple alignment of the deduced amino acid sequence of *PmDDX41* cDNA with various species including *Megachile rotundata* Abstrakt (*MrAbstrakt*), *Apis florea* Abstrakt (*AfAbstrakt*), *Drosophila melanogaster* Abstrakt (*DmAbstrakt*), *Hyaella azteca* Abstrakt (*HaAbstrakt*), *Lepisosteus oculatus* DDX41 (*LoDDX41*), *Bos taurus* DDX41 (*BtDDX41*), *Homo sapiens* DDX41 (*HsDDX41*) and *Gallus gallus* DDX41 (*GgDDX41*). The conserved residues are shaded in black.

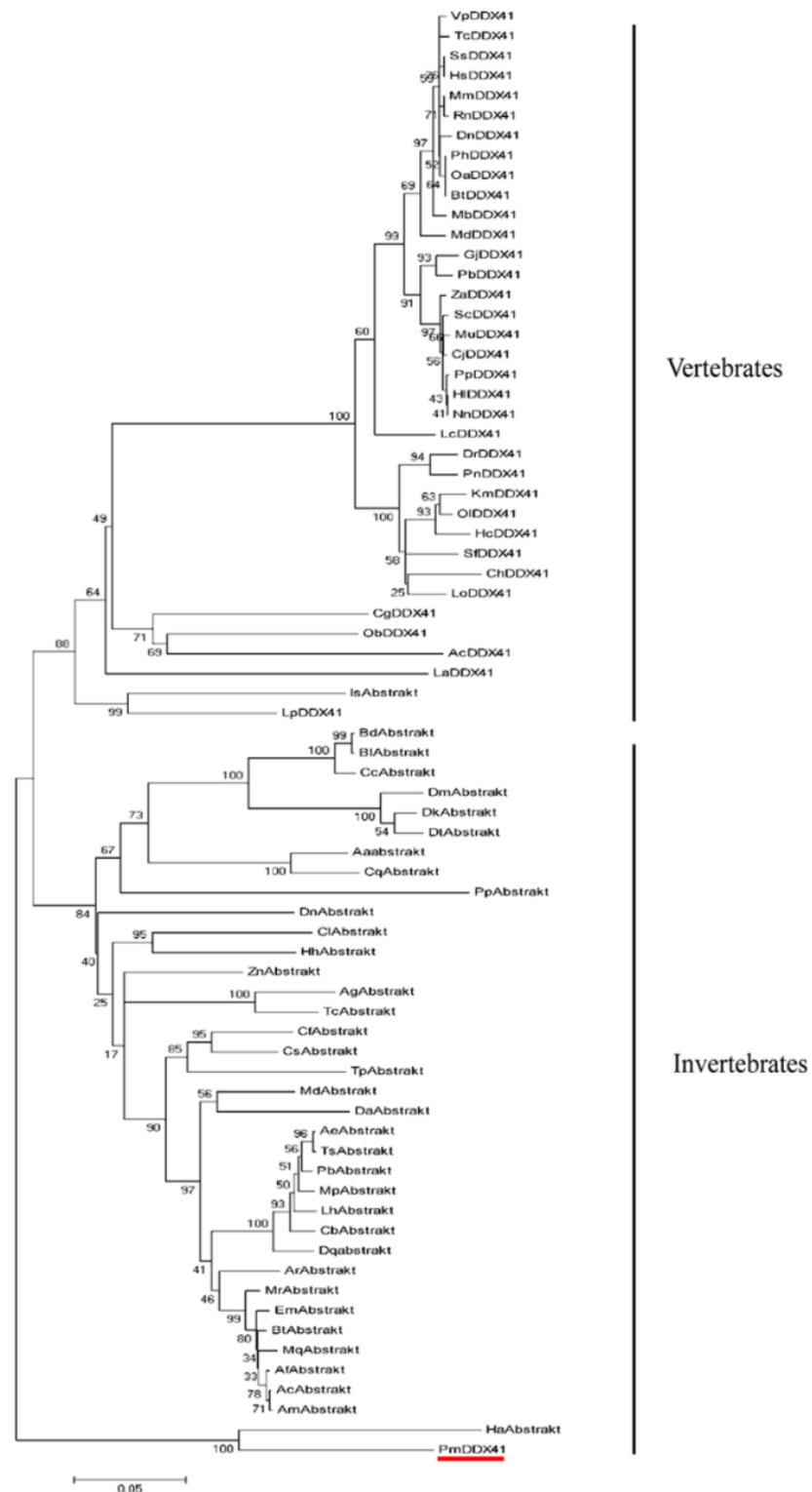


Fig. 19 Phylogenetic tree of *PmDDX41*.

Bootstrapped unrooted neighbor-joining tree of the DEXDc and HELICc domains of DDX41 from various species of vertebrates and invertebrates using the MEGA 6.0 program based on the multiple sequence alignment by ClustalX 2.1. The *PmDDX41*

protein is underlined in red. *Penaeus monodon* DDX41 (*PmDDX41*); *Hyaella azteca* (XP_018015918.1); *Megachile rotundata* (XP_003704771.1); *Eufriesea mexicana* (XP_017758091.1); *Apis florea* (XP_012345472.1); *Apis mellifera* (XP_006563505.1); *Bombus terrestris* (XP_003401085.1); *Apis cerana* (XP_016919394.1); *Melipona quadrifasciata* (KOX72336.1); *Athalia rosae* (XP_012260261.1); *Tribolium castaneum* (XP_008199686.2); *Copidosoma floridanum* (XP_014212020.1); *Zootermopsis nevadensis* (KDR18857.1); *Microplitis demolitor* (XP_008554237.1); *Halyomorpha halys* (XP_014290780.1); *Cimex lectularius* (XP_014251014.1); *Limulus polyphemus* (XP_013786635.1); *Trachymyrmex septentrionalis* (XP_018355138.1); *Acromyrmex echinator* (XP_011055156.1); *Diuraphis noxia* (XP_015375005.1); *Bactrocera latifrons* (XP_018799159.1); *Linepithema humile* (XP_012223009.1); *Aethina tumida* (XP_019876402.1); *Anoplophora glabripennis* (XP_018573118.1); *Diachasma alloeum* (XP_015112885.1); *Dinoponera quadriceps* (XP_014485147.1); *Monomorium pharaonis* (XP_012522153.1); *Ceratitis capitata* (XP_004533592.1); *Cerapachys biroi* (XP_011329703.1); *Ceratosolen solmsi marchali* (XP_011504405.1); *Pogonomyrmex barbatus* (XP_011646631.1); *Aedes albopictus* (XP_019536629.1); *Drosophila kikkawai* (XP_017036024.1); *Ixodes scapularis* (XP_002404560.1); *Trichogramma pretiosum* (XP_014223294.1); *Octopus bimaculoides* (XP_014777272.1); *Musca domestica* (XP_005190431.1); *Drosophila takahashii* (XP_016992688.1); *Drosophila melanogaster* (NP_524220.1); *Papilio polytes* (XP_013139917.1); *Culex quinquefasciatus* (XP_001865238.1); *Aplysia californica* (XP_005090184.1); *Lingula anatina* (XP_013383180.1); *Lepisosteus oculatus* (XP_006631993.1); *Melopsittacus undulatus* (XP_005147385.1); *Zonotrichia albicollis* (XP_005483802.1); *Latimeria chalumnae* (XP_005992418.1); *Serinus canaria* (XP_009089776.1); *Nipponia nippon* (XP_009470434.1); *Coturnix japonica* (XP_015731521.1); *Haliaeetus leucocephalus* (XP_010577335.1); *Picoides pubescens* (XP_009902922.1); *Oryzias latipes* (XP_004073424.1); *Kryptolebias marmoratus* (XP_017282102.1); *Danio rerio* (XP_017209912.1); *Pygocentrus nattereri* (XP_017561740.1); *Ovis aries* (XP_004008770.1); *Pantholops hodgsonii* (XP_005971040.1); *Python bivittatus* (XP_007420367.1); *Monodelphis domestica* (XP_001381058.2); *Gekko japonicus* (XP_015268030.1); *Clupea harengus* (XP_012687658.1); *Myotis brandtii* (XP_005865545.1); *Hippocampus comes* (XP_019725479.1); *Tupaia chinensis* (*TcDDX41*; XP_006158984.2); *Scleropages formosus* (XP_018597371.1); *Dasypus novemcinctus* (XP_004456590.1); *Vicugna pacos* (XP_006198995.1); *Camelus ferus* (XP_006175810.1); *Homo sapiens* (NP_057306.2); *Mus musculus* (NP_598820.2); *Rattus norvegicus* (NP_001101516.1); *Sus scrofa* (AGK93040.1); *Bos taurus* (NP_001076071.1); *Bactrocera dorsalis* (JAC51753.1); *Crassostrea gigas* (EKC40522.1)

3.3 Tissue distribution of *PmDDX41*

The transcript levels of *PmDDX41* in various shrimp tissues were determined by semi-quantitative RT-PCR using EF1- α as an internal control gene. The results showed that the *PmDDX41* transcript was expressed in all of the tested tissues, including the hemocytes, intestine, hepatopancreas, lymphoid organ, gill, heart, muscle, and eye stalk (**Fig. 20**). However, particularly high mRNA expression levels of *PmDDX41* were found in the immune-related tissues including the hepatopancreas, gill, and hemocyte.

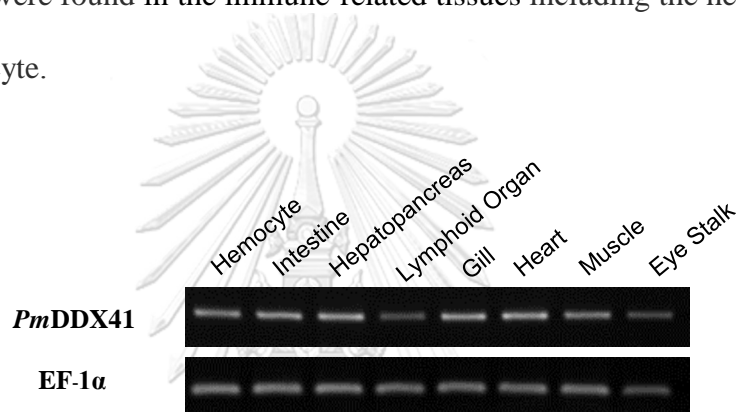


Fig. 20 The semi-quantitative RT-PCR analysis of *PmDDX41* gene expression in shrimp tissues.

The tissue distribution of *PmDDX41* was analyzed by semi-quantitative RT-PCR in the following shrimp tissues: hemocyte, intestine, hepatopancreas, lymphoid organ, gill, heart, muscle, and eye stalk. EF1- α was used as an internal control.

3.4 Expression profiles of *PmDDX41* transcript after pathogen challenges

To investigate the effects of bacterial and viral infections on *PmDDX41* gene expression, juvenile *P. monodon* were challenged with the pathogens: *V. harveyi*, WSSV, and YHV. The qRT-PCR results showed significant ($p < 0.05$) induction of the *PmDDX41* transcript by WSSV but not YHV or *V. harveyi* infection. In brief, *PmDDX41* expression had increased by 1.57- and 1.36-fold, respectively, at 6 and 48

h after infection with WSSV ($p < 0.05$) (**Fig.21A**). *PmDDX41* was significantly down-regulated by 0.33-fold at 6 h after infection in the YHV-challenged group, (**Fig. 21B**). In contrast, after injection with *V. harveyi*, no significant change was observed after injection with *V. harveyi* at any of the time points when compared with control PBS-injected shrimp ($p < 0.05$) (**Fig. 21C**).

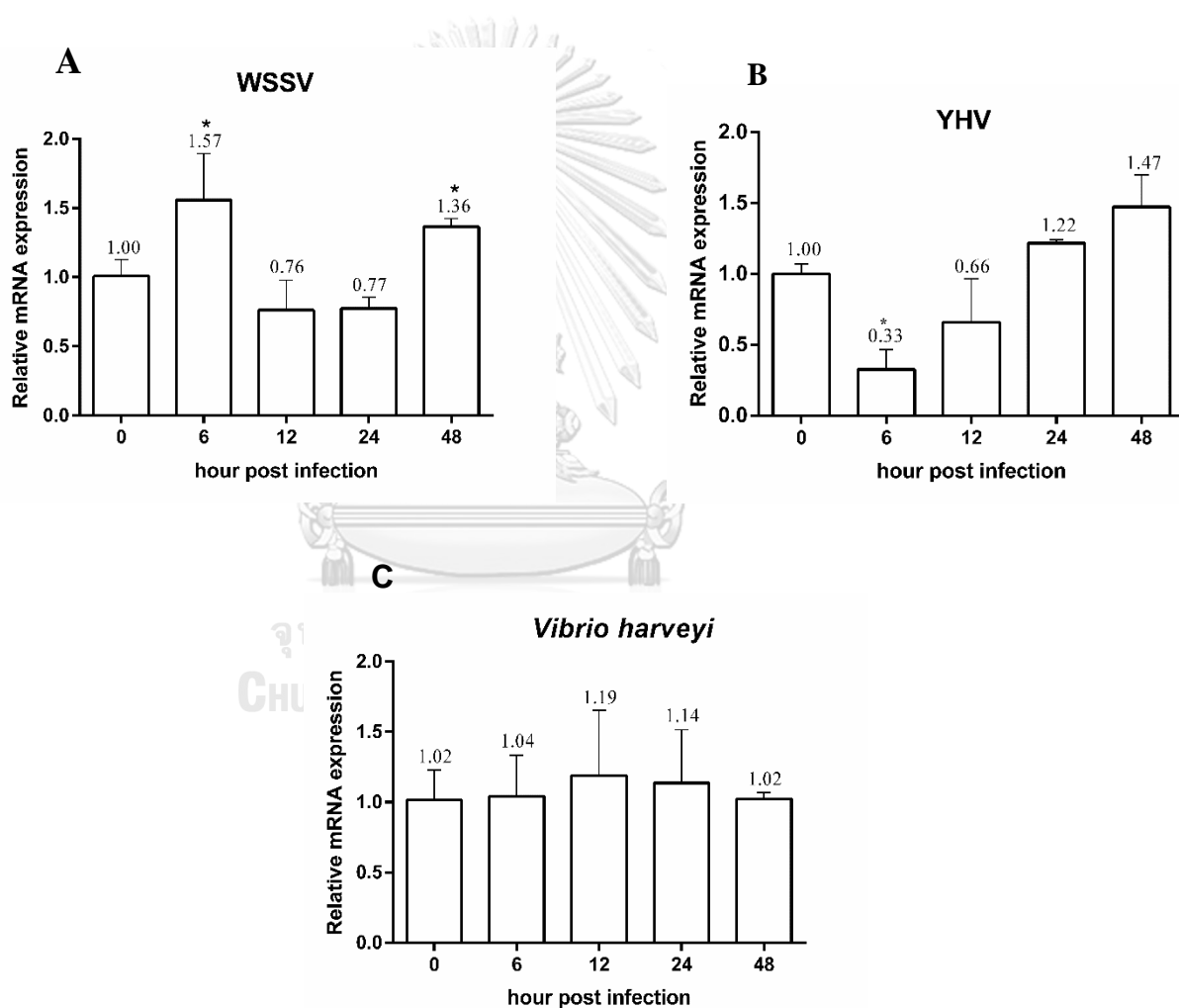


Fig. 21 Relative expression levels of *PmDDX41* in shrimp hemocytes at different time points after challenged with pathogens: (A) WSSV, (B) YHV and (C) *Vibrio harveyi*.

Expression levels were normalized with PBS-injected *P.monodon*. Relative expression is calculated according to the Pfaffl (Pfaffl, 2001) using the EF-1 α as an internal reference gene. The data are derived from three independently replicated experiments and shown as the mean \pm 1 SD (error bars). The asterisk at the above each bar indicates means with significantly different ($p < 0.05$).

3.5 Expression profiles of *PmDDX41* transcript after nucleic acid mimics stimulation

To observe the effects of nucleic acid mimics, poly(dA:dT) and poly(I:C) injection on *PmDDX41* gene expression, qRT-PCR was performed. After poly(dA:dT) injection (2 μ g/g shrimp), the expression of *PmDDX41* was significantly up-regulated by 3.37-, 3.69-, 4.14- and 6.97-fold, at 6, 12, 24 and 48 h, respectively. The *PmDDX41* transcript was highly up-regulated at 48 h (**Fig. 22A**). Moreover, after poly(I:C) injection (2 μ g/g shrimp), *PmDDX41* expression had increased by 4.43-, 3.12- and 2.67-fold, at 12, 24 and 48 h, respectively (**Fig. 22B**) ($p < 0.05$). The results suggested that *PmDDX41* could be activated by foreign nucleic acids stimulation.

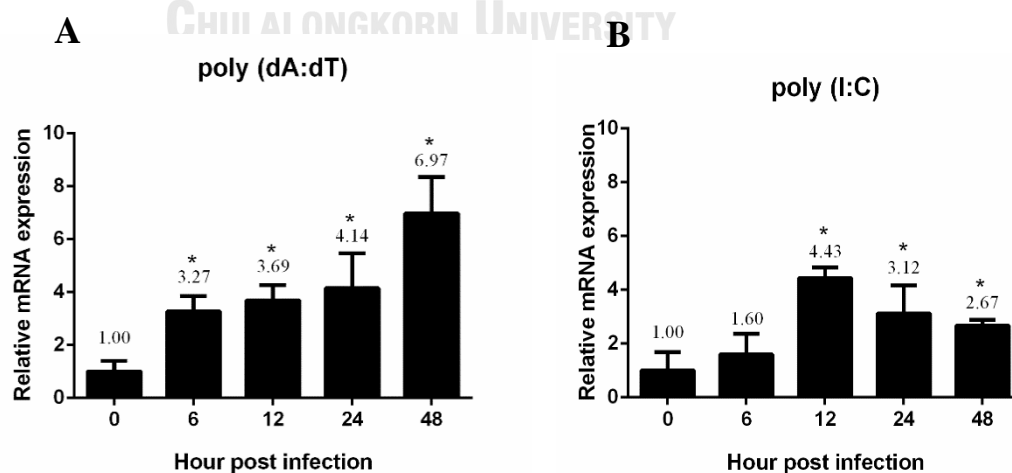


Fig. 22 Relative expression levels of *PmDDX41* in shrimp hemocytes at different time points after injected with (A) poly(dA:dT) and (B) poly(I:C).

Expression levels were normalized with PBS-injected *P. monodon*. Relative expression is calculated according to the Pfaffl (Pfaffl, 2001) using the EF-1 α as an internal reference gene. The data are derived from three independently replicated experiments and shown as the mean \pm 1 SD (error bars). The asterisk at the above each bar indicates means with significantly different ($p < 0.05$).

3.6 The effect of RNAi-mediated gene silencing of *PmDDX41* on the expression of shrimp immune-related genes

3.6.1 Preparation of dsRNA *PmDDX41* and GFP

The recombinant plasmid of full length *PmDDX41* cDNA was used as template to amplify the *PmDDX41* DNA fragment by using gene specific primers (Table 1). The primers for the dsRNA synthesis consist of the same primer sequences but flanked at the 5' end by a T7 promoter sites. The sense strand template and the anti-sense strand template were synthesized by using *PmDDX41i*-T7F1/*PmDDX41i*-R1, the other with *PmDDX41i*-F1/*PmDDX41i*-T7R1. The exogenous gene (GFP gene) was amplified using pEGFP-1 vector by using GFPT7-F and GFP-R for the sense strand template, and GFP-F and GFPT7-R for the anti-sense strand template. The expected band was cut, purified and used for synthesis dsRNA with a T7 RNA polymerase by using a T7 RiboMAXTM Express Large Scale RNA Production System (Fig. 23A). The concentration of single-stranded RNA was measured before annealing step. The major band of *PmDDX41* and GFP dsRNA were observed on 1.5% agarose gel electrophoresis after the purification of dsRNA (Fig. 23B).

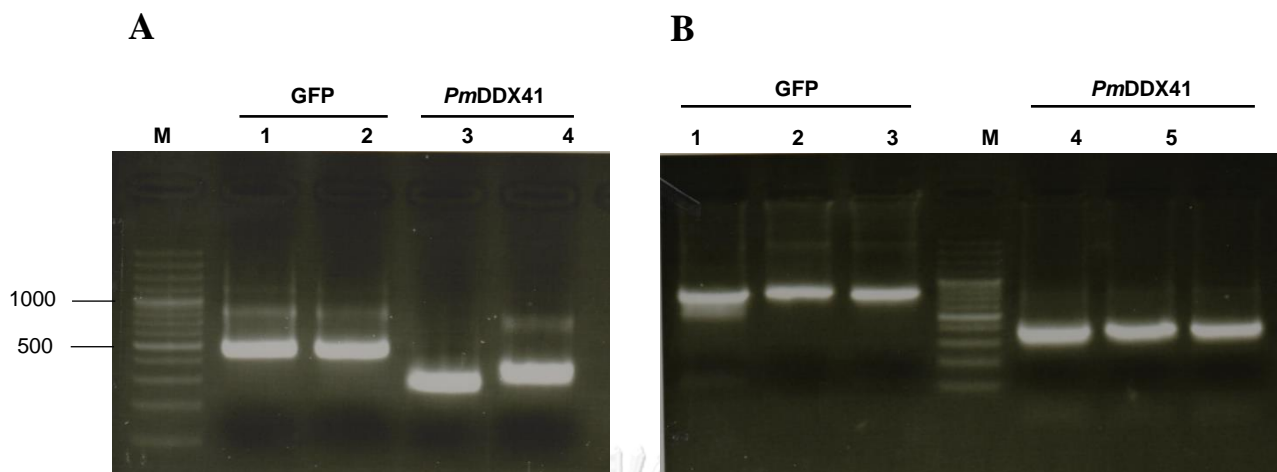


Fig. 23 The agarose gel electrophoresis of single strand RNA of *PmDDX41* and GFP and purification of dsRNA *PmDDX41* and GFP.

(A) The sense and anti-sense strands of *PmDDX41* and GFP. Lane M is GeneRuler™ 100 bp DNA ladder, Lane 1 is sense strand of GFP, Lane 2 is anti-sense strand of GFP, Lane 3 is sense strand of *PmDDX41* and Lane 4 is anti-sense strand of *PmDDX41*. (B) Purified *PmDDX41* and GFP dsRNA. Lane M is GeneRuler™ 100 bp DNA ladder. Lane 1 is dsRNA GFP after annealing, Lane 2 is dsRNA GFP after DNaseI treatment, Lane 3 is purified dsRNA GFP, Lane 4 is dsRNA *PmDDX41* after annealing, Lane 5 is dsRNA *PmDDX41* after DNaseI treatment and Lane 6 is purified dsRNA *PmDDX41*. Products were analyzed by 1.5 % agarose electrophoresis.

3.6.2 Effect of silencing of *PmDDX41* on the expression of shrimp immune-related genes

To characterize the functional role of *PmDDX41* in the innate immunity of shrimp, we used the RNA interference (RNAi) technique to knock down the *PmDDX41* transcript. Shrimp (3–5 g) were injected with *PmDDX41* dsRNA (2 µg/g shrimp), GFP dsRNA, or 150 mM NaCl, where the latter two groups were used as controls. Semi-quantitative RT-PCR was used to analyze the efficacy of the gene silencing of the targeted gene after systemic dsRNA treatment. The results revealed that the *PmDDX41* gene was successfully suppressed by the *PmDDX41* dsRNA,

while GFP dsRNA or NaCl injection had no effect on *PmDDX41* expression (**Fig. 24A**).

Furthermore, the effects of *PmDDX41* gene silencing on the expression of other immune-related genes were investigated by semi-quantitative RT-PCR. The expression levels of genes in the signal transduction pathways (*PmIKK β* , *PmIKK ϵ* , *PmRelish*, *PmCactus*, and *PmDorsal*), antimicrobial peptides (*PmPEN3*, *PmPEN5*, *ALFPm3*, *ALFPm6*, *CrustinPm1*, and *CrustinPm7*), and IFN-like molecules (*PmVago1*, *PmVago4*, and *PmVago5*) were analyzed. The results revealed that the expression levels of the *PmIKK β* , *PmIKK ϵ* , *PmRelish*, *PmCactus*, *PmDorsal*, *PmPEN3*, *PmPEN5*, and *ALFPm6* genes were decreased compared with the control groups, whereas the expression levels of the other genes (*PmVago1*, *PmVago4*, *PmVago5*, *ALFPm3*, *CrustinPm1*, and *CrustinPm7*) were unchanged (**Fig. 24A**).

To confirm the effects of silencing the *PmDDX41* gene on the expression of immune-related genes, qRT-PCR was performed. The expression levels of the signal transduction pathway genes *PmIKK β* , *PmIKK ϵ* , *PmRelish*, *PmCactus*, and *PmDorsal* were decreased to 0.26, 0.09, 0.07, 0.03, and 0.45-fold, respectively, relative to the control group. Moreover, the expression levels of the antimicrobial peptide genes *PmPEN3*, *PmPEN5*, and *ALFPm6* were decreased to 0.42, 0.72, and 0.20-fold, respectively (**Fig. 24B**).

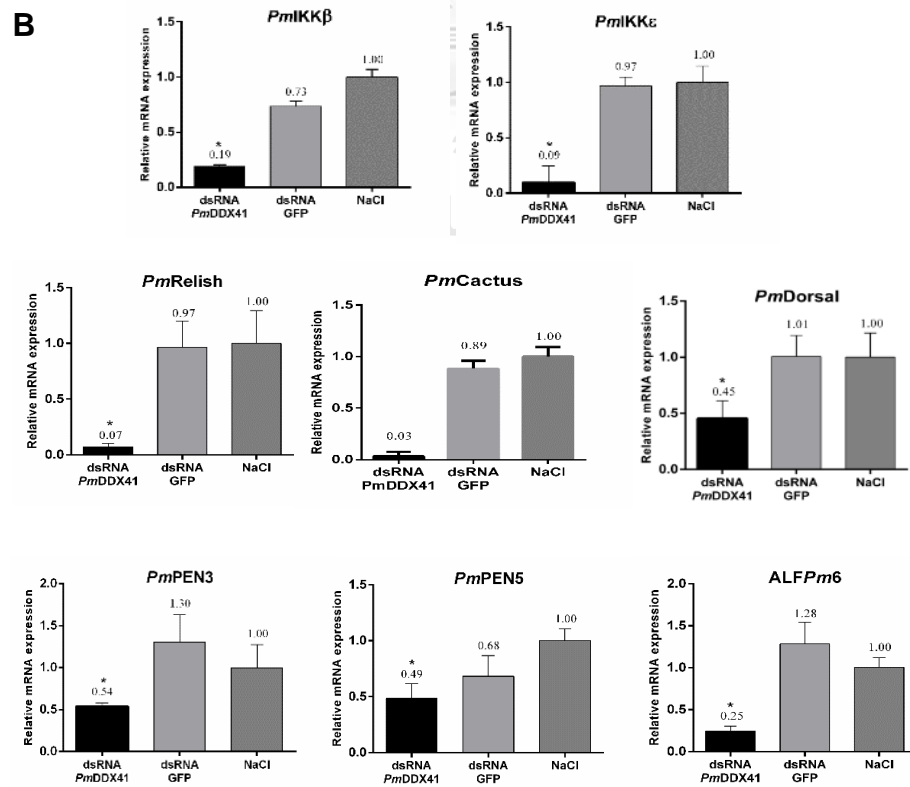
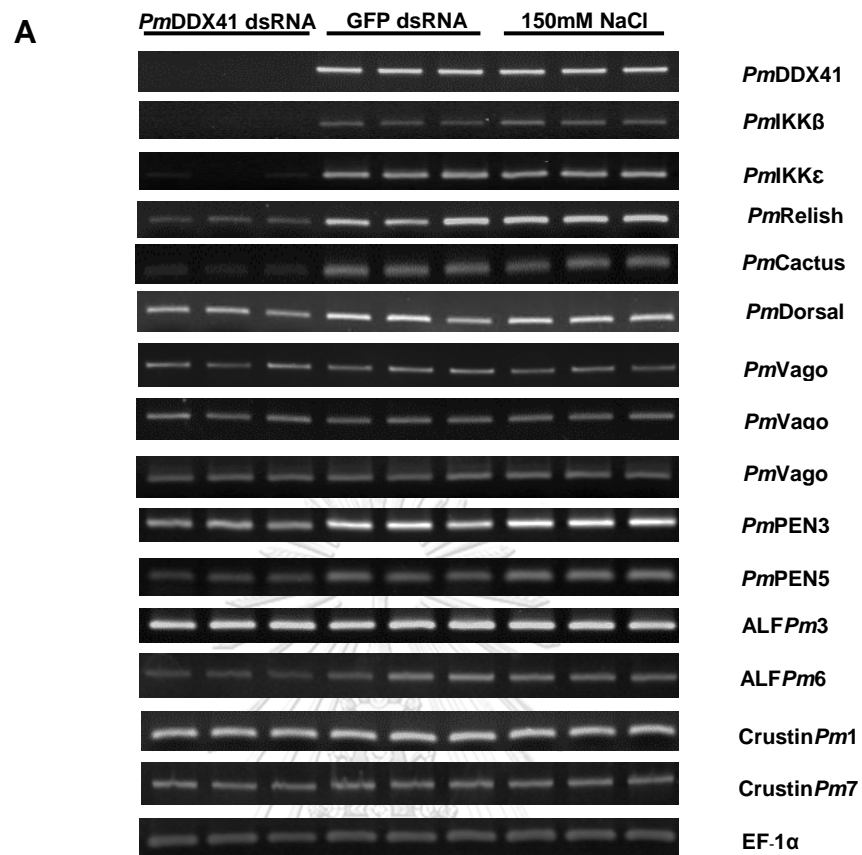


Fig. 24 Effect of gene silencing of *PmDDX41* on the expression level of the antiviral and antimicrobial peptide-associated genes.

The shrimp were injected with *PmDDX41* dsRNA, GFP dsRNA and 150 mM NaCl. After 24 hours, hemolymph was collected for (A) semi-quantitative RT-PCR analysis and (B) quantitative RT-PCR analysis. EF-1 α was used as an internal control. The effect of gene knockdown on the expression level of *P. monodon* shrimp antimicrobial peptide transcripts (*PmRelish*, *PmDorsal*, *PmPEN3*, *PmPEN5*, *ALFPm3*, *ALFPm6*, *CrustinPm1*, *CrustinPm7* and *PmMyD88*) and genes involved in the DNA sensing pathway (*PmIKK β* , *PmIKK ϵ* , *PmVago1*, *PmVago 4* and *PmVago 5*) were evaluated by semi-quantitative RT-PCR using the gene-specific primers for each gene (Table 1). The data are derived from three independently replicated experiments and shown as the mean \pm 1 SD (error bars). The asterisk at the above each bar indicates means with significantly different ($p < 0.05$).

3.7 Cumulative mortality assay of *PmDDX41* upon WSSV infection

To further address the potential role of *PmDDX41* in the shrimp defense against viral infection, the *PmDDX41*-knockdown shrimp were systemically challenged with WSSV. The shrimp were injected with 2 μ g/g shrimp of *PmDDX41* dsRNA, GFP dsRNA, or 150 mM NaCl. Twenty-four hours after the first dsRNA injection, the shrimp were injected with 2.64×10^3 copies/mL of WSSV in PBS. The survival rate was recorded over a period of five days after the challenge. For the *PmDDX41*-knockdown shrimp, all shrimp died within three days of WSSV infection, whereas in the controls injected with 150 mM NaCl or GFP dsRNA, 100% death was only observed within five days after WSSV infection. Therefore, the *PmDDX41*-knockdown shrimp exhibited a more rapid death after WSSV infection compared with the controls (**Fig. 25**), which suggests that *PmDDX41* is likely involved in the antiviral response and plays an important role in protecting shrimp from WSSV infection.

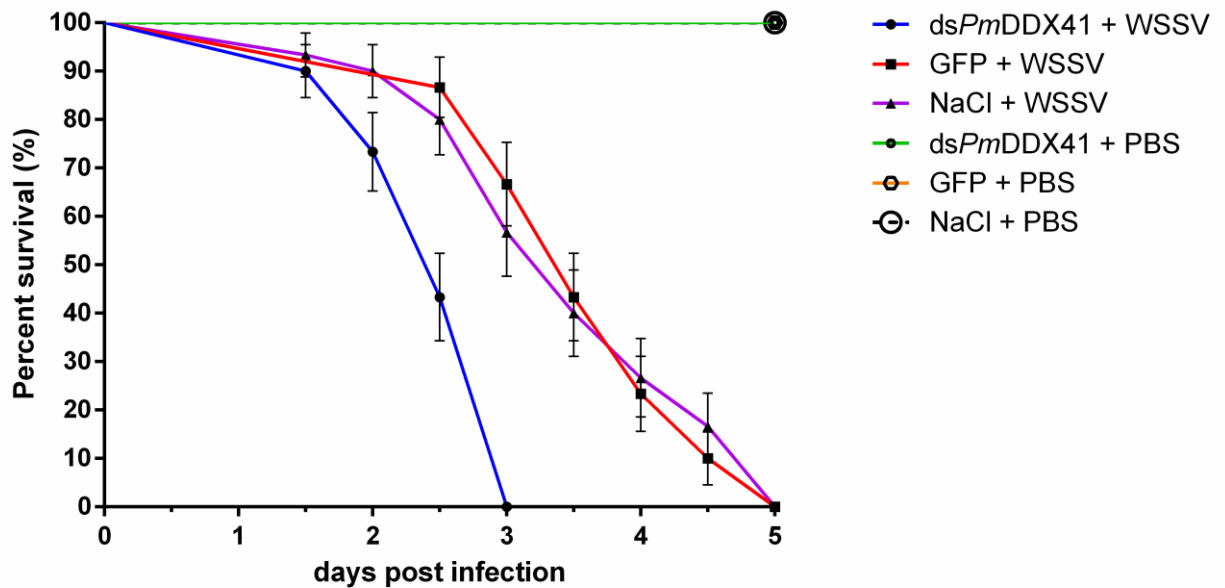


Fig. 25 Percent survival of *PmDDX41* silenced shrimp challenged with WSSV. Shrimp were injected with WSSV (2.64×10^3 copies/ml of WSSV in PBS) after the injection of *PmDDX41* dsRNA, GFP dsRNA or 150 mM NaCl 24 hours. Control groups were injected with either GFP dsRNA or 150 mM NaCl. Shrimp mortality was recorded twice a day for 5 days. The shrimp in each group were 10-15 shrimp. The data are derived from three independently replicated experiments and shown as the mean \pm 1 SD (error bars).

3.8 Immunolocalization of *PmDDX41* in shrimp hemocytes

3.8.1 Recombinant protein expression in *E. coli* system

The recombinant *PmDDX41* (r*PmDDX41*) protein was expressed in *E. coli* system for using in antibody preparation. The cDNA fragment with attached restriction recognition sites of *Bam*HI and *Xho*I for *PmDDX41* (1863 bp) was amplified and cloned into pET-22b (+) as an expression vector with hexa-histidine tag sequence to construct pET-22b (+)-*PmDDX41*-6xHis. The recombinant plasmids were prior screened using restriction digestions with *Bam*HI and *Xho*I for pET-22b

(+)-*PmDDX41*-6xHis. They were further verified by nucleotide sequencing before introduced to *E. coli* strain BL21-CodonPlus (DE3)-RIPL as an expression host (**Fig. 26**).

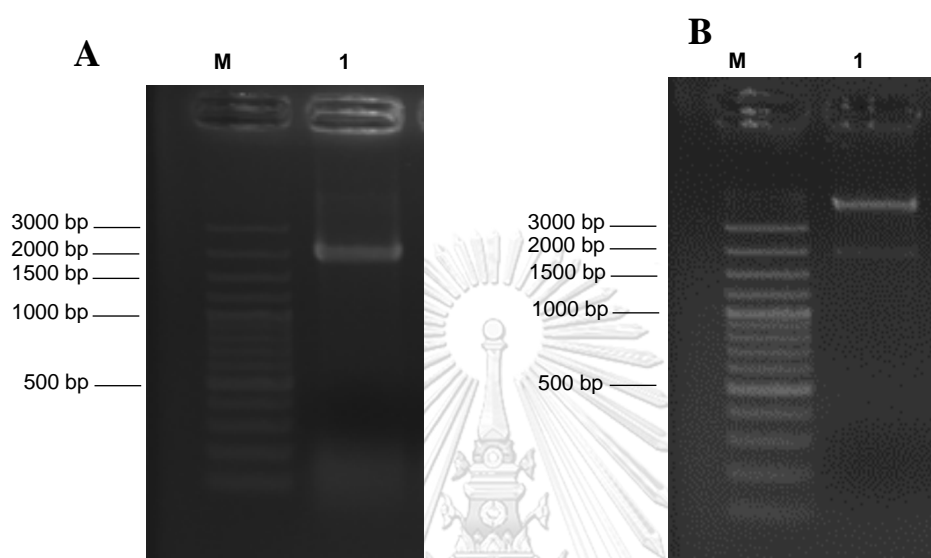


Fig. 26 PCR amplification of *PmDDX41* and plasmid DNA screening for protein expression.

(A) The ORFs of *PmDDX41* (1863 bp) was amplified in the PCR reactions with attached hexa-histidine tag sequence and cloned into pET-22b(+) to construct protein expression vectors. (B) The recombinant plasmids pET-22b(+) *PmDDX41* was digested with *Bam*HI and *Xho*I. The PCR product was visualized under UV transilluminator following 1% (w/v) agarose-TBE gel electrophoresis. Lane M is GeneRuler™ 100 bp DNA ladder. Lane 1 is *PmDDX41* gene uncut (left) and digested recombinant plasmid *PmDDX41* (right), respectively.

3.8.2 Cross-reactivity of anti-human-DDX41 with *PmDDX41*

To express the recombinant protein, a bacterium *E. coli* strain BL21-CodonPlus (DE3)-RIPL harboring pET-22b (+)-*PmDDX41*-6xHis was grown in LB medium containing ampicillin and kanamycin until the OD₆₀₀ reached approximately 0.6. Cells were harvested and induced with 1 mM IPTG for 6h. The r*PmDDX41* was

used to test the cross reactivity with commercial antibodies in western blot analysis. The crude protein of *PmDDX41* was detected in 15% SDS-PAGE with Coomassie brilliant blue staining reagent and immunostaining. The commercial anti-His-tagged and anti-human-DDX41-rabbit were used as the primary antibodies for the detection. The *rPmDDX41* with expected molecular masses of 70 kDa, was expressed at 37°C with 250 rpm shaking 6 hours post induction (**Fig. 27**). Since the commercial anti-human-DDX41 exhibited high specificity to shrimp DDX41 recombinant proteins, the large-scale protein production of the recombinant *PmDDX41* protein for antibody raising was not further carried out.

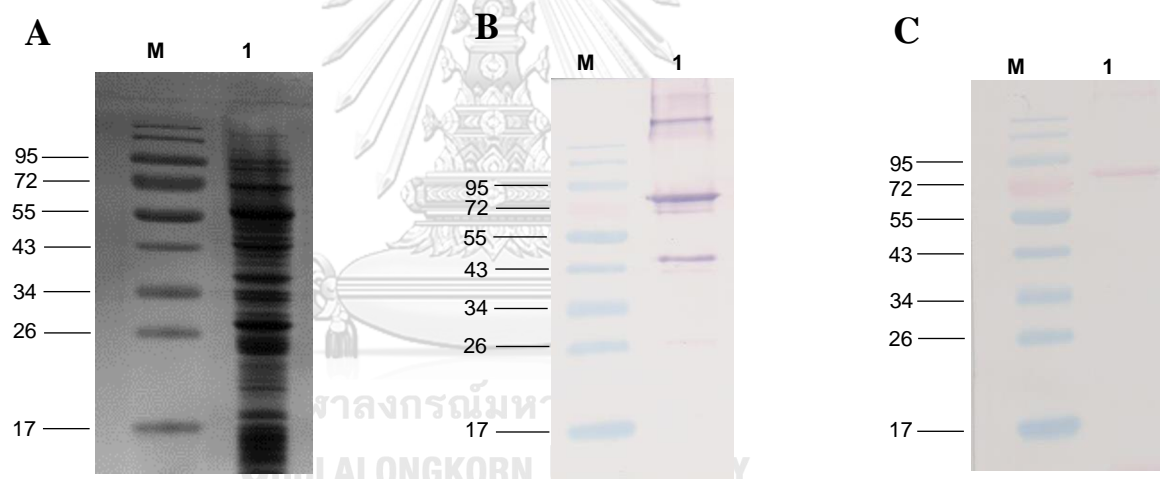


Fig. 27 The detection of *PmDDX41* by SDS-PAGE and western blot analysis using rabbit polyclonal anti-human-DDX41.

The recombinant plasmid was transformed into BL-21-CodonPlus (DE3)- RIPL and was grown in LB medium. The cells were induced with 1 mM IPTG for 6 h and harvested. (A) The crude protein *PmDDX41* was run on 15% SDS-PAGE and staining with coomassie brilliant blue and (B) *PmDDX41* protein was transferred into nitrocellulose membrane and detected by mouse monoclonal anti-His and (C) rabbit polyclonal anti-human-DDX41. Lane M is the Prestained protein marker.

3.8.3 Localization of *PmDDX41* in shrimp hemocytes after WSSV

challenged

To explore the cellular localization of *PmDDX41*, hemocytes from PBS-injected group and WSSV-injected group were collected and fixed by 4% paraformaldehyde. Hemocytes were incubated with anti-human-DDX41 antibody for immunofluorescence. As shown in **Fig. 28**, the *PmDDX41* protein in PBS-injected group was mainly distributed in cytoplasm. Interestingly, *PmDDX41* was expressed in both cytoplasm and nucleus in WSSV-injected group.

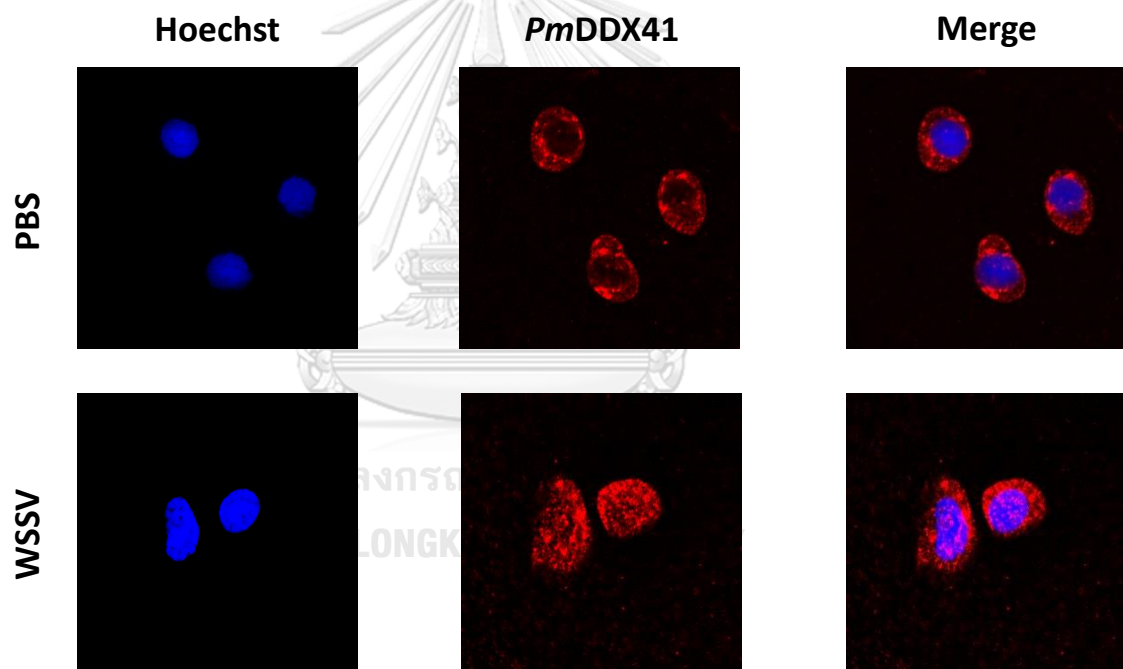


Fig. 28 Localization of *PmDDX41* in shrimp hemocytes after challenged with WSSV, as visualized by fluorescence microscopy.

Hemocyte cells were collected at 48 h post-injection and fixed with 4% paraformaldehyde. Hemocyte cells were then stained with anti-human-DDX41 antibody conjugated with Alexa Fluor 568 (red); nuclei were stained with Hoechst 33342 (blue). Images were captured by laser-scanning confocal microscopy (Zeiss LSM-700; original magnification, 63x).

3.8.4 Localization of *PmDDX41* in shrimp hemocytes after nucleic acid mimics stimulation

To observe the expression of *PmDDX41* protein in shrimp hemocytes after stimulating with nucleic acid mimic: poly(dA:dT) and poly(I:C). Hemocytes were collected and fixed by using 4% paraformaldehyde into the slide. Then, the anti-human-DDX41 was incubated and probed with Alexa 568 conjugated secondary antibody. The Hoechst 33342 was used to stain nucleus and observed under laser-scanning confocal microscopy. The results revealed that *PmDDX41* was expressed in cytoplasm and translocate into nucleus after poly(dA:dT) and poly(I:C) stimulation (Fig. 29).

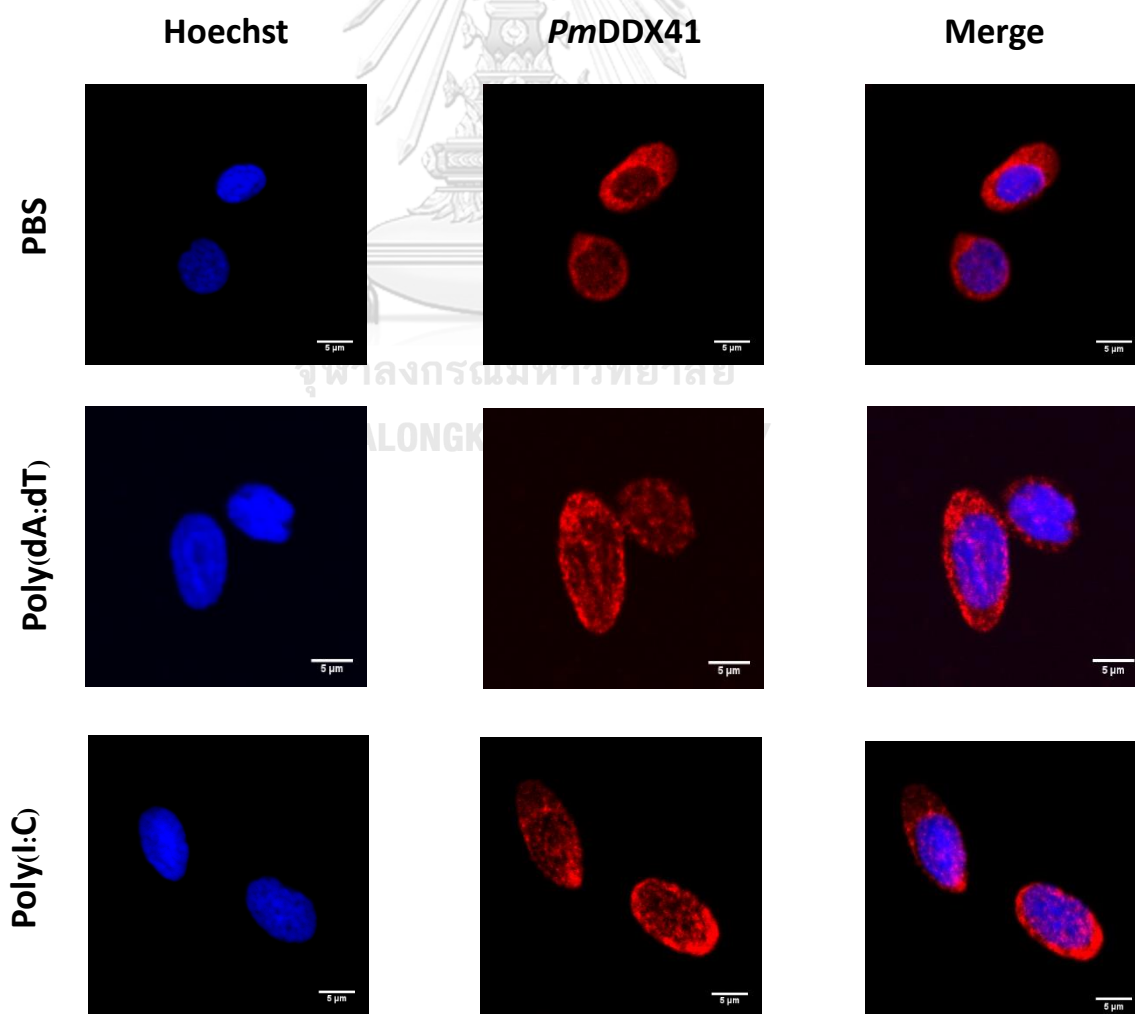


Fig. 29 Localization of *PmDDX41* in shrimp hemocytes after stimulated with poly(dA:dT) and poly(I:C), as visualized by fluorescence microscopy. Hemocyte cells were collected at 48 h post-injection and fixed with 4% paraformaldehyde. Hemocyte cells were then stained with anti-human-DDX41 antibody conjugated with Alexa Fluor 568 (red); nuclei were stained with Hoechst 33342 (blue). Images were captured by laser-scanning confocal microscopy (Zeiss LSM-700; original magnification, 63x).

3.9 Interaction of *PmDDX41* and mimic poly(dA:dT)

3.9.1 Construction and cloning of Myc-tagged-*PmDDX41* and Myc-tagged-*MmDDX41*

To determine whether *PmDDX41* directly binds DNA, the specific primers (Myc_ *PmDDX41*_ *Bam*HI_F/ Myc_ *PmDDX41*_ *Xho*I_R) were used to amplify *PmDDX41* gene from the shrimp hemocytes and cloned into pcDNA3 expression vector. Moreover, I also cloned DDX41 from mouse (*MmDDX41*) into pcDNA3 expression vector. *MmDDX41* was amplified from mouse liver by using specific primers (Myc_ *MmDDX41*_ *Bam*HI_F/ Myc_ *MmDDX41*_ *Xho*I_R) and used as control.

A single band of *PmDDX41* and *MmDDX41* were detected on UV transilluminator by 1.5% agarose gel electrophoresis with size approximate 1863 bp (**Fig. 30**). Then, the product was cloned and sequenced.

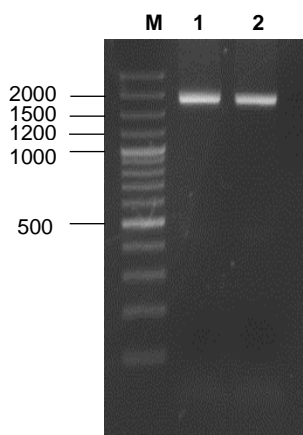


Fig. 30 The amplification of gene coding for *PmDDX41* and *MmDDX41*. *PmDDX41* and *MmDDX41* genes were amplified from shrimp hemocytes and mouse liver, respectively. Lane M is 100 bp DNA marker. Lane 1 is the PCR product of *PmDDX41* gene, Lane 2 is the PCR product of *MmDDX41* gene which detected on 1.5% agarose gel electrophoresis.

The *PmDDX41* and *MmDDX41* genes were cloned into the expression vector pcDNA3 at *BamH* I and *Xho* I sites. After ligation, the recombinant plasmids of *PmDDX41* and *MmDDX41* were transformed into *E. coli* DH5- α . Then, the recombinant plasmids were extracted, confirmed by double digestion using restriction enzyme and sequenced (**Fig. 31A**).

The recombinant plasmid *PmDDX41*-Myc-tagged and *MmDDX41*-Myc-tagged were transfected into HEK293T cells to produce the recombinant protein *PmDDX41* and *MmDDX41*. The recombinant proteins were detected by immunoblotting using anti-Myc antibody (**Fig. 31B**).

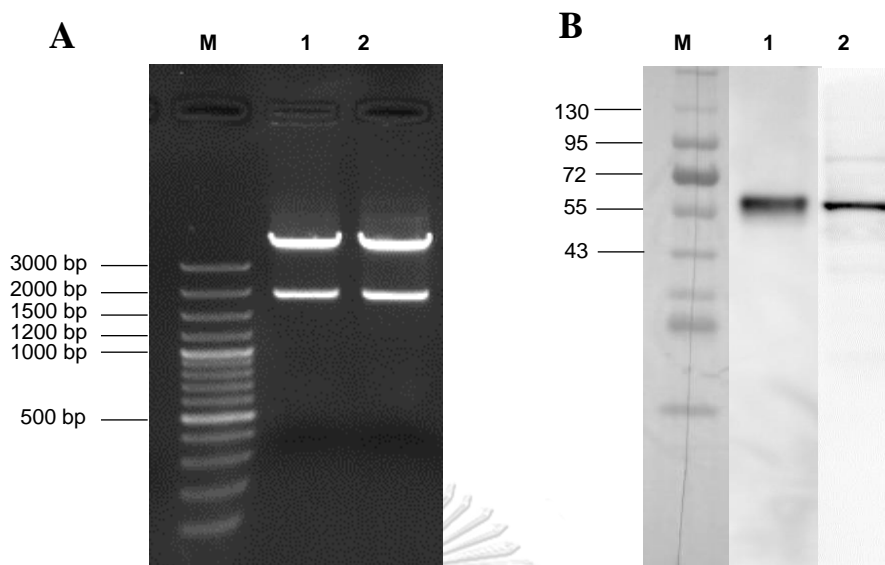


Fig. 31 Screening of the recombinant plasmids using restriction enzymes *Bam*HI and *Xho*I and protein expression in HEK293T cells.

(A) The *Pm*DDX41 and *Mm*DDX41 genes were cloned into pcDNA3, digested with *Bam*HI and *Xho*I and analyzed by 1.2% agarose electrophoresis. Lane M is 100 bp DNA ladder, Lane 1 is the recombinant plasmid Myc-tagged-*Pm*DDX41 digested with *Bam*HI and *Xho*I, Lane 2 is recombinant plasmid Myc-tagged-*Mm*DDX41 digested with *Bam*HI and *Xho*I. (B) Expression of recombinant *Pm*DDX41 and *Mm*STING protein in HEK293T cells which were transfected with 4 μ g of recombinant plasmid encoding Myc tags. *Pm*DDX41 and *Mm*DDX41 protein were analyzed by SDS-PAGE. Immunoblotting was carried out with anti-Myc (Sigma) antibody. Lane M is the Prestained protein marker. Lane 1 is overexpression of *Pm*DDX41 in HEK293T cells. Lane 2 is overexpression of *Mm*DDX41 in HEK293T cells.

3.9.2 DNA binding assay of *Pm*DDX41 and nucleic acid mimic

From previous research, DDX41 was mainly studied in vertebrates which used mammalian cells as a model. In this study, I used human embryonic kidney HEK293T cells, a widely used human model cell line naturally having minimal the expression of STING and DDX41 to study the function of *Pm*DDX41. To determine whether *Pm*DDX41 directly binds DNA, I transfected HEK293T human embryonic kidney

cells with plasmid encoding Myc-tagged *PmDDX41* recombinant protein. The Myc-tagged *MmDDX41* recombinant protein was used as a control. The recombinant protein was incubated with biotin-labeled poly (dA:dT) and poly(I:C), followed by the addition of agarose bead-linked to antibody to Myc (anti-Myc). The recombinant Myc-tagged-*PmDDX41* and Myc-tagged-*MmDDX41* were immunoprecipitated only by agarose beads plus poly(dA:dT) not poly(I:C) which indicated that DDX41 bound to DNA but not the RNA mimic (**Fig. 32**).

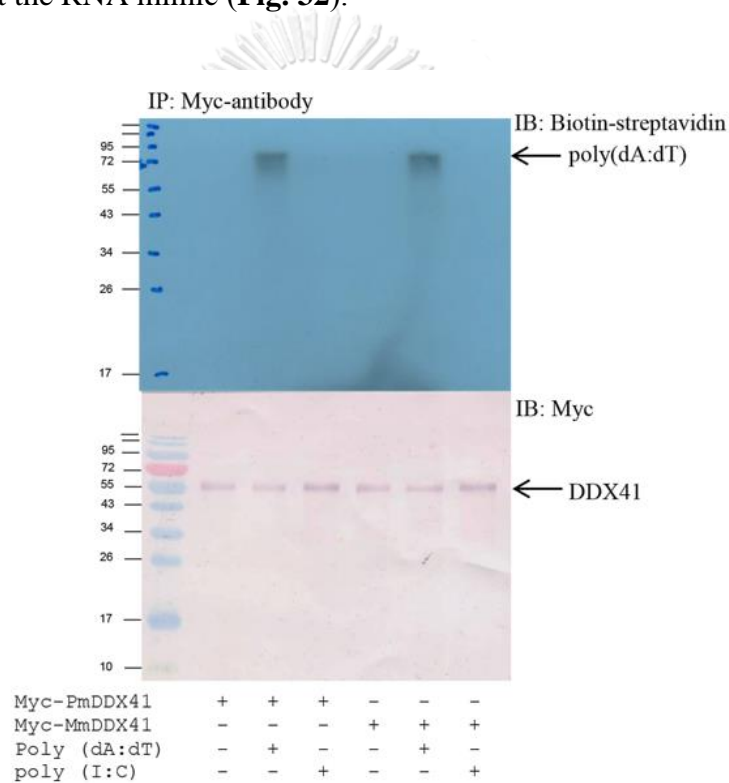


Fig. 32 Interaction of *PmDDX41* with nucleic acid mimics.

HEK293T cells were transfected with Myc-tagged-*PmDDX41* plasmid. The crude protein of *PmDDX41* was incubated with biotinylated poly(dA:dT) or poly(I:C) and immunoprecipitated with anti-Myc antibody. Western blotting was used to analyze the interaction of *PmDDX41* by probed with biotin-streptavidin detection. Myc-tagged-*MmDDX41* was used as a control.

3.10 Localization of *PmDDX41* in human embryonic kidney HEK293T cells after nucleic acid mimics stimulation

To investigate the localization of *PmDDX41* in HEK293T cells, I transfected the Myc-*PmDDX41* plasmid into HEK293T cells and stained cells with anti-Myc antibody and found that *PmDDX41* localizes exclusively in cytoplasm of HEK293T cells (**Fig. 33**). Following stimulation with transfection of poly (dA:dT) and poly(I:C), *PmDDX41* was observed in both cytoplasm and nucleus (**Fig. 33**) similar to that observed in shrimp hemocytes. These results confirmed that *PmDDX41* localized specially in cytoplasm in normal condition and it was translocated into nucleus after stimulation.

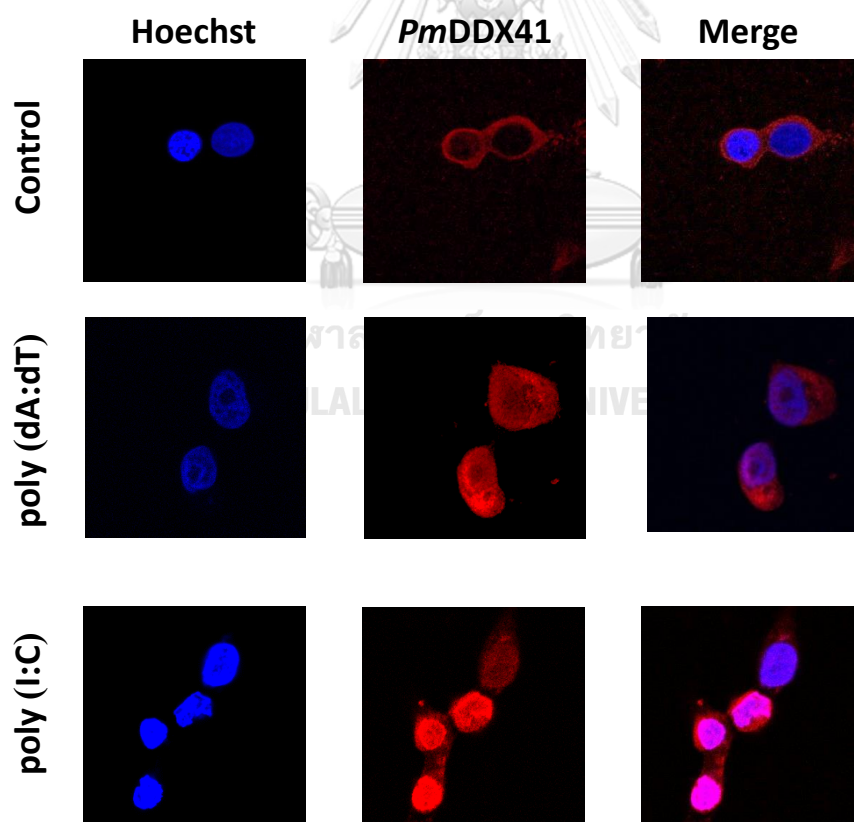


Fig. 33 Localization of *PmDDX41* in HEK293T cells after stimulated with poly(dA:dT) and poly(I:C), as visualized by fluorescence microscopy.

HEK293T cells were transfected with Myc-tagged-*PmDDX41* expression vector. After 24 h, cells were stimulated with 1 $\mu\text{g/ml}$ of poly (dA:dT) and poly(I:C) for 6 h. Cells were collected and fixed with 4% paraformaldehyde. Cells were then stained with anti-Myc antibody conjugated with Alexa Fluor 568 (red); nuclei were stained with Hoechst 33342 (blue). Images were captured by laser-scanning confocal microscopy (Zeiss LSM-700; original magnification, 63x).

3.11 Overexpression of *PmDDX41* and promoter activity assay

The IFN- β is identified as a pro-inflammatory cytokine activated in the presence of infectious diseases. The activated IFN- β stimulates the inflammatory responses in neighboring cells leading to the expression of immune-related genes involved in innate and adaptive immune responses. While, NF- κB transcription factor is a central mediator for several immune response pathways and is targeted by pathogen stimulation. To understand the involvement of *PmDDX41* in antiviral innate immunity, I constructed the expression plasmid for *PmDDX41* protein and transfected into HEK293T cells with a luciferase reporter plasmid driven by the IFN- β and NF- κB promoter. After 24 h, cells were stimulated with poly(dA:dT) and poly(I:C) for 6 h. In normal condition, *PmDDX41* could slightly increase the luciferase activity assay of IFN- β and NF- κB by 1.97 and 1.13-fold, respectively. After stimulated with poly(dA:dT), the expression of *PmDDX41* could activate the IFN- β and NF- κB promoter activity by 4.42 and 1.74-fold, respectively (**Fig. 34A, 34B**). Moreover, *MmDDX41* was used as a control to test luciferase activity assay. *MmDDX41* could increase the production of IFN- β in normal condition and stimulation with poly(dA:dT) and poly(I:C) by 5.60, 10.47 and 10.05 fold, respectively. However, *MmDDX41* could not activate the NF- κB promoter activity (**Fig. 34A, 34B**). The

results indicate that *PmDDX41* is possibly involved in the IFN- β and NF- κ B signaling pathways.

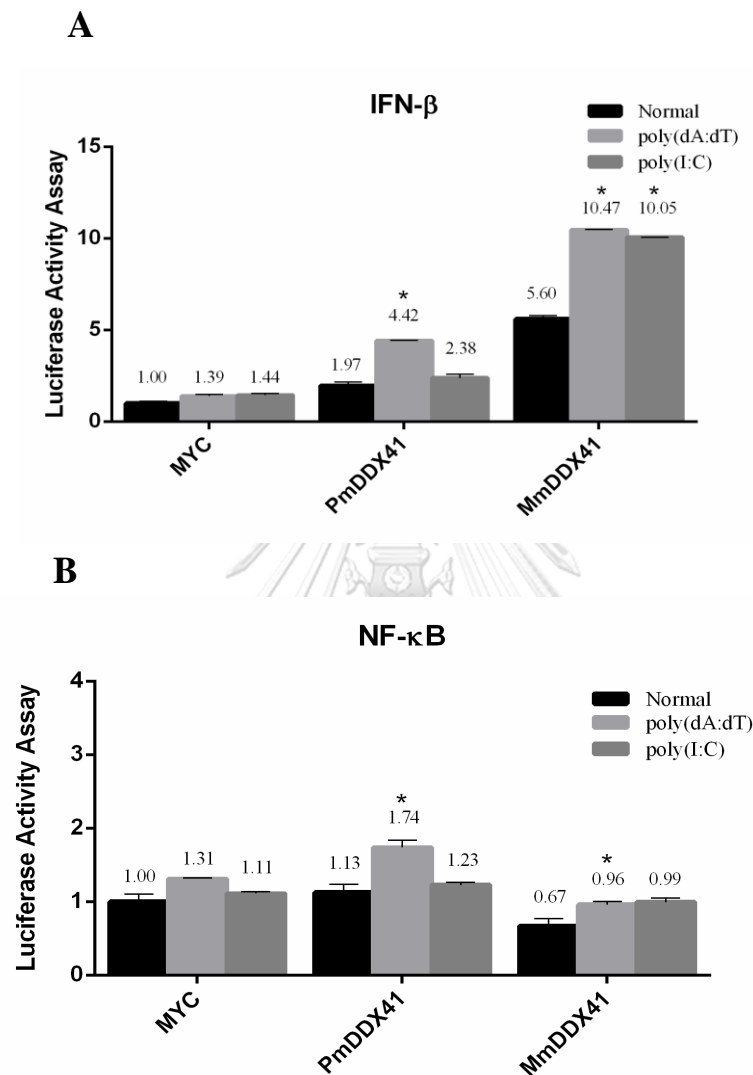


Fig. 34 The activation of (A) IFN- β and (B) NF- κ B promoter in HEK293T cells. The cells were transfected with 0.5 μ g/well Flag-tagged-*PmDDX41* and reporter plasmid for IFN- β and/or NF- κ B (IFN- β -Luc; 0.1 μ g/well, NF- κ B-Luc; 0.1 μ g/well), and renilla luciferase reporter (0.01 μ g/well). At the indicated time stimulation, the cells were stimulated with poly (dA:dT) and poly (I:C). Luciferase assay were performed after 6 h stimulation. Significant difference was ($p < 0.05$) between normal cell and stimulated cell.

3.12 Overexpression of *PmDDX41* and *MmSTING* and promoter activity assay

3.12.1 Cloning of *PmDDX41*-Flag-tagged and protein expression of *PmDDX41* and *MmSTING* in HEK293T cells

To characterize the binding activity of *PmDDX41* and *MmSTING* in nucleic acid sensing pathway, I explored the mediation of *PmDDX41* by STING, a molecule which acts as an adaptor for cytosolic nucleic acids in the innate immune response. Since STING is also conserved across different species, I used mouse STING (*MmSTING*) for investigation of *PmDDX41* in HEK293T cells. The specific primers (Flag_ *PmDDX41*_SalI_F / Flag_ *PmDDX41*_BamHI_R) were used to amplify *PmDDX41* gene from the shrimp hemocytes and cloned into pCMV5-Flag expression vector. Moreover, the recombinant plasmid *PmDDX41*-Flag-tagged or *MmSTING*-Myc-tagged were transfected into HEK293T cells to produce the recombinant protein *PmDDX41* and *MmSTING*. The recombinant proteins were detected by immunoblotting using anti-Flag or anti-Myc antibodies (**Fig. 35**).

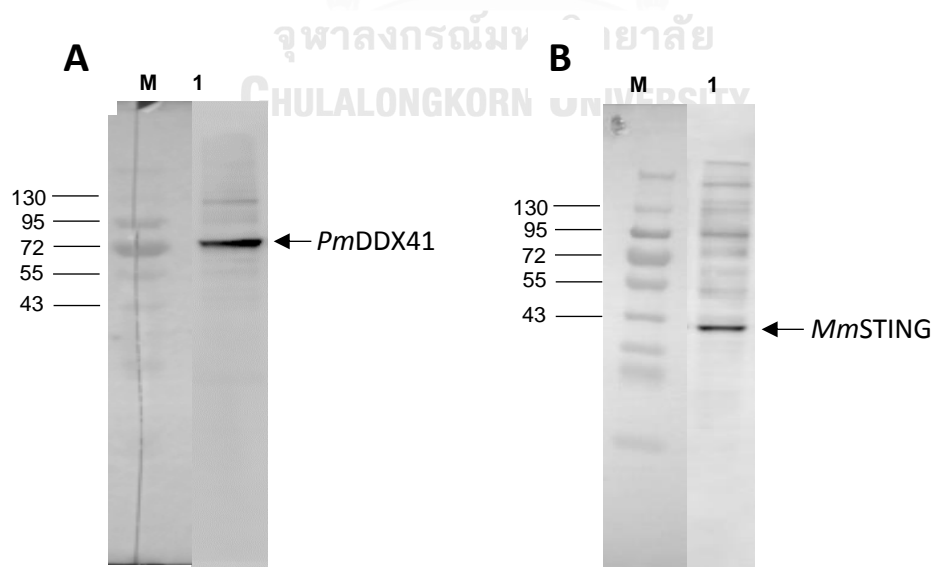


Fig. 35 The western blotting of *PmDDX41* and *MmSTING* protein in HEK293T cells.

Overexpression of (A) *PmDDX41* and (B) *MmSTING* proteins in HEK293T cells which were transfected with 4 μ g of recombinant plasmid encoding Flag or Myc tags. After 24h, cells were harvested and sonicated. *PmDDX41* and *MmSTING* proteins were separated by centrifugation and analyzed by SDS-PAGE. Immunoblotting was carried out using anti-Flag and anti-Myc antibodies. Lane M is the Prestained protein marker.

3.12.2 Dual-luciferase activity assay of *PmDDX41* and *MmSTING*

To further investigate the promoter activity of IFN- β and NF- κ B in sensing cytosolic DNA, *PmDDX41* and *MmSTING* were overexpressed in HEK293T cells containing a luciferase reporter. From **Fig. 36A and 36B**, the overexpression of *MmSTING* in HEK293T cells significantly induced the activation of IFN- β and NF- κ B promoters by 3.94- and 2.03-fold, respectively and by 5.16- and 3.49-fold when stimulated with poly(dA:dT), respectively. The co-expression of *PmDDX41* and *MmSTING* synergistically activated the activity of IFN- β and NF- κ B promoters by 4.41- and 2.89-fold, respectively and by 5.54- and 3.71-fold when stimulated with poly(dA:dT), respectively. In contrast, activation of the IFN- β and NF- κ B promoters by the overexpression of *PmDDX41*, *MmSTING* or *PmDDX41* and *MmSTING* was not induced after poly(I:C) stimulation.

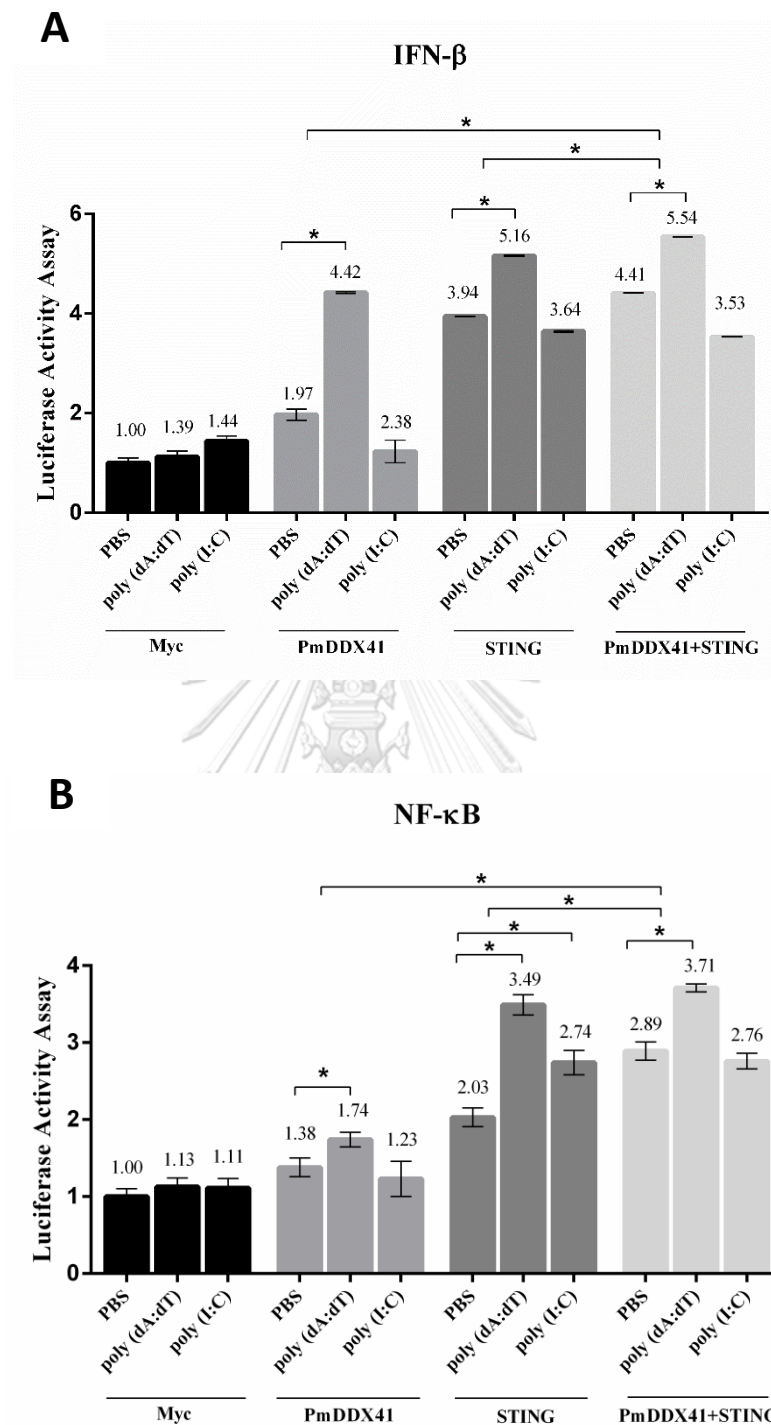


Fig. 36 Luciferase activity assay of IFN- β (A) and NF- κ B (B) in HEK293T cells. The cells were co-transfected with 0.5 μ g/well Flag-tagged-*PmDDX41* and 0.5 μ g/well Myc-tagged-*MmSTING* together with IFN- β -Luc and/or NF- κ B-Luc (IFN- β -Luc; 0.1 μ g/well, NF- κ B-Luc; 0.1 μ g/well) and pRL-TK (0.01 μ g/well). After 24 h transfection, the cells were stimulated with poly(dA:dT) and poly(I:C). Luciferase

assay was performed after 6 h stimulation. Significant difference was ($p < 0.05$) between normal cells and stimulated cells.

3.13 Interaction of *PmDDX41* with *MmSTING*

To verify whether *PmDDX41* binds with *MmSTING* after stimulation with nucleic acid mimics, co-immunoprecipitation (Co-IP) was performed. HEK293T cells were co-transfected with Flag-*PmDDX41* and Myc-*MmSTING*. The Flag-tagged or Myc-tagged protein was detected using an anti-Flag antibody or anti-Myc antibody, respectively by western blotting. The cell lysates were precipitated with anti-Myc antibody in conjugated with protein A-sepharose before detected by antibody. The results showed that *PmDDX41* could interacted with *MmSTING* after poly (dA:dT) stimulation (**Fig. 37**). These results indicate that *PmDDX41* was associated with *MmSTING* in transfected cells after stimulation with mimic DNA.

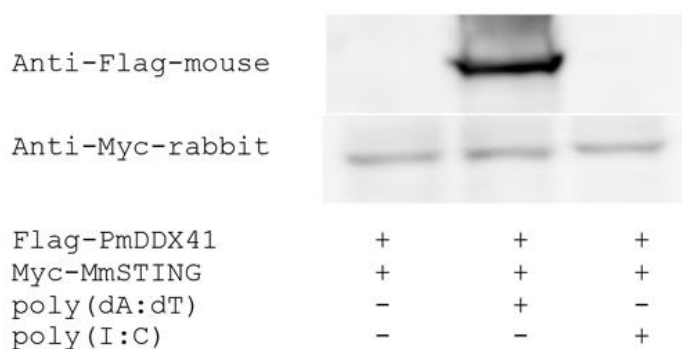


Fig. 37 Interaction of *PmDDX41* and *MmSTING* in HEK293T cells.

HEK293T cells were co-transfected to express Flag-tagged full-length *PmDDX41* and Myc-tagged *MmSTING*. After 24 h, cells were stimulated with poly(dA:dT) and poly(I:C). The protein was incubated with anti-Myc tagged overnight and agarose beads were added into the protein for 6 hours. Western blotting was used to analyze the interaction of *PmDDX41* and *MmSTING* by using anti-Flag and anti-Myc antibodies.

3.14 Co-localization of *PmDDX41* with *MmSTING* in HEK293T cells

To verify whether *PmDDX41* is one of the DNA sensors which STING relied in DNA sensing, I investigated co-localization of *PmDDX41* and *MmSTING* in HEK293T cells. It was found that *PmDDX41* was co-localized with *MmSTING* in cytoplasm which indicated that *PmDDX41*-*MmSTING* complex was located in cytoplasm which indicated that *PmDDX41*-*MmSTING* complex was located in cytosol (**Fig. 38**). Furthermore, after stimulation with poly(dA:dT) or poly(I:C), there was the lower expression of *PmDDX41* in cytoplasm and higher expression of *PmDDX41* in nucleus, while *MmSTING* was located only in the cytoplasm (**Fig. 38**). The results indicate that only *PmDDX41* not *MmSTING* was translocated from cytoplasm to nucleus after stimulation.

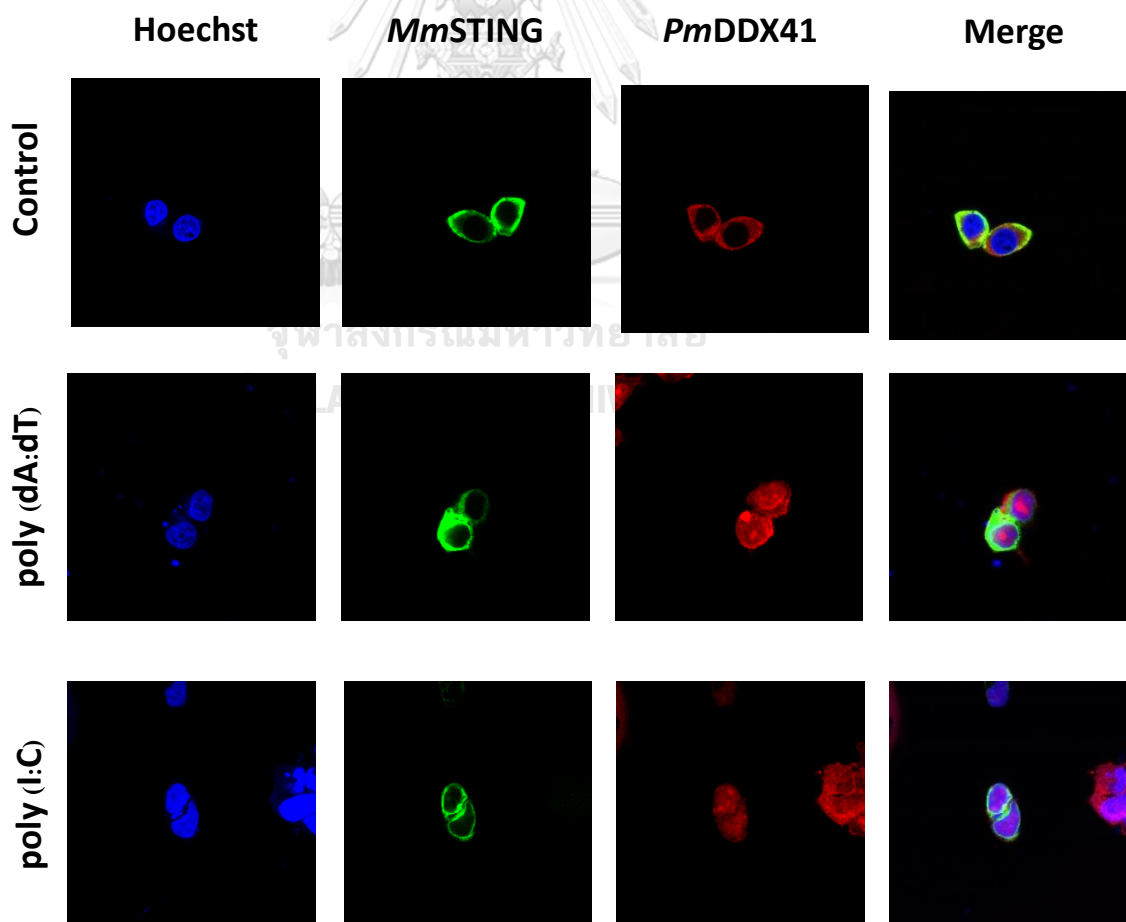


Fig. 38 Co-localization of *PmDDX41* with *MmSTING* in HEK293T cells after stimulated with poly(dA:dT) and poly(I:C), as visualized by fluorescence microscopy. HEK293T cells were co-transfected with Flag-tagged-*PmDDX41* expression vector and Myc-tagged-*MmSTING*. After 24 h, cells were stimulated with 1 µg/ml of poly(dA:dT) and poly(I:C) for 6 h. Cells were collected and fixed with 4% paraformaldehyde. Cells were then stained with anti-Flag and anti-Myc antibodies conjugated with Alexa Fluor 568 (red) and Alexa Fluor 488 (green), respectively. Nuclei were stained with Hoechst 33342 (blue). Images were captured by laser-scanning confocal microscopy (Zeiss LSM-700; original magnification, 63x).

3.15 The function of *PmDDX41* domains in *MmSTING*-dependent innate immune signaling pathways

From previous studies, *PmDDX41* contains three conserved domains including DEADc domain, HELICc domain and zinc finger domain. To further investigate the functional roles of different *PmDDX41* domains in the DNA sensing signaling pathway, I constructed deletion mutant plasmids lacking the HELICc domain and the DEADc domain (**Fig. 39A**). I then transfected these mutant plasmids into HEK293T cells with a luciferase reporter plasmid driven by the IFN-β or NF-κB promoter. I found that the co-transfection of *PmDDX41* or DEADc domain (*DeadPm*) with *MmSTING*, significantly activated ($p < 0.05$) the promoter activity of IFN-β and NF-κB compared to cells overexpressing *MmSTING* under both stimulated with poly(dA:dT) and poly(I:C) and non-stimulated conditions (**Fig. 39B, 39C**). There was no significant activation of these reporters in cells co-expressing the HELICc domain and *MmSTING* compared to cells overexpressing *MmSTING*. These results indicated that the DEADc domain of *PmDDX41* is responsible for activation of the *PmDDX41*–*MmSTING*-mediated IFN-β and NF-κB signaling pathways.

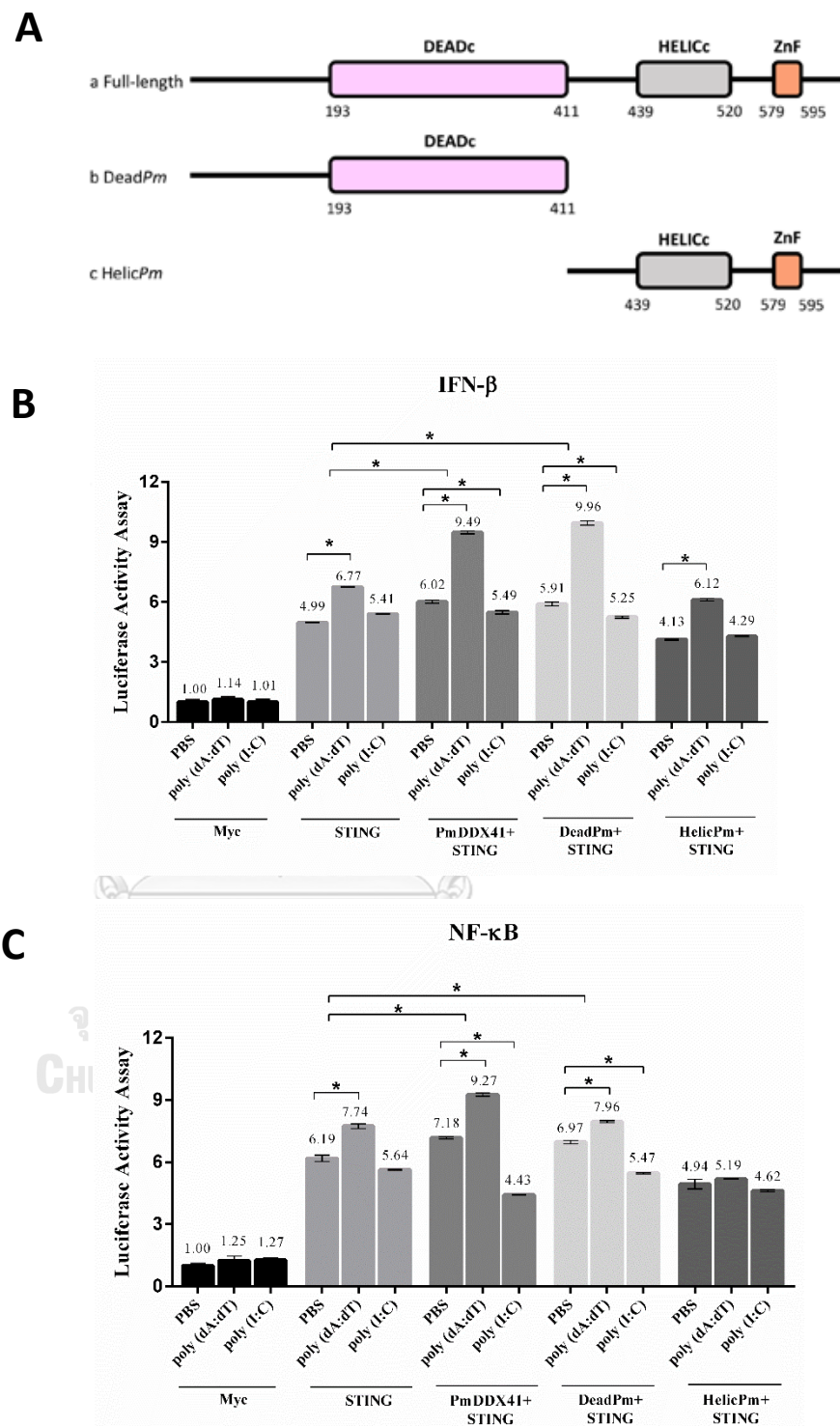


Fig. 39 Activation of IFN- β and NF- κ B promoter in HEK293T cells transfected with different *PmDDX41* domains.

(A) Schematic diagram of full-length and mutated *PmDDX41* fragments. (B,C) HEK293T cells were co-transfected with 0.5 μ g/well of full-length or mutated

PmDDX41 expression vector, or empty vector, and with 0.5 $\mu\text{g}/\text{well}$ of Myc-tagged-*MmSTING* together with IFN- β -Luc and/or NF- κ B-Luc (IFN- β -Luc; 0.1 $\mu\text{g}/\text{well}$, NF- κ B-Luc; 0.1 $\mu\text{g}/\text{well}$) and the renilla luciferase reporter, pRL-TK (0.01 $\mu\text{g}/\text{well}$). After 24 h transfection, the cells were stimulated with poly(dA:dT) and poly(I:C). Luciferase assay was performed after 6 h stimulation. Significant difference was ($p < 0.05$) between normal cells and stimulated cells.

3.16 Interactions of *PmDDX41* domains and *MmSTING* in HEK293T cells

In determine the binding site specificity of *PmDDX41*, I performed a Co-IP assay in HEK293T cells overexpressing Myc-tagged-*MmSTING* and Flag-tagged-DDX41 or Flag-tagged-Dead*Pm* or Flag-tagged-HELICc*Pm*. This experiment aimed to evaluate interactions between *MmSTING* and *PmDDX41* under normal conditions, and following stimulation by poly(dA:dT) or poly(I:C). I found that *PmDDX41* and the DEADc domain could bind only to *MmSTING* after poly(dA:dT) stimulation but not after poly(I:C) stimulation (**Fig. 40**). These results suggest that *PmDDX41* binds to *MmSTING* through the DEADc domain and then stimulates the DNA sensing pathway.

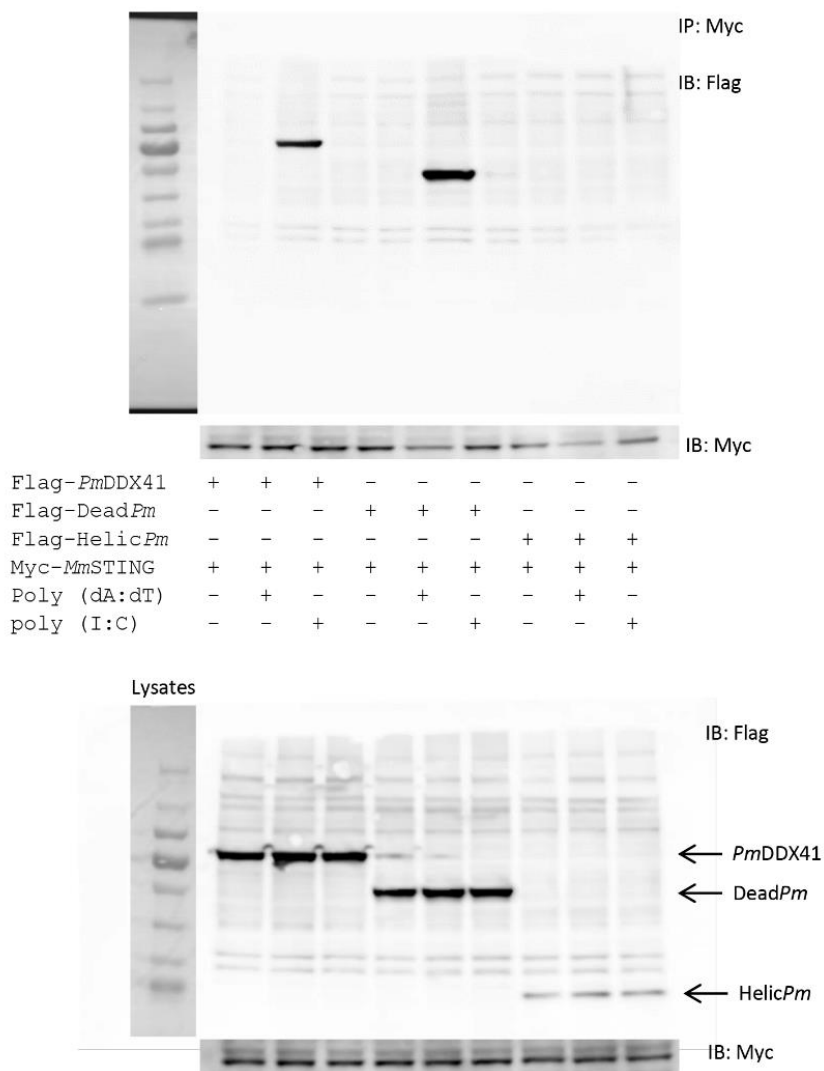
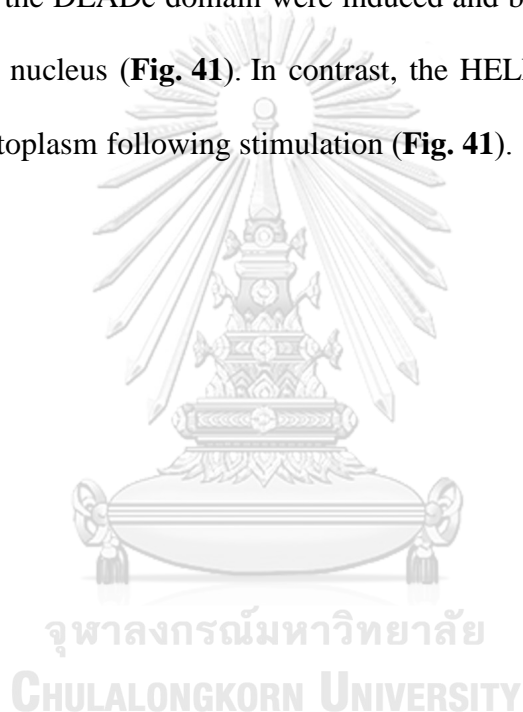


Fig. 40 Interaction between *PmDDX41* domains and *MmSTING* in HEK293T cells. HEK293T cells were co-transfected with Flag-tagged-mutated-*PmDDX41* and Myc-tagged-*MmSTING* for 24 h. Cells were then stimulated with poly(dA:dT) and poly(I:C) for 6 h. Proteins were then extracted. The protein was immunoprecipitated with anti-Myc antibody (IP: Myc). Western blotting was then performed by using anti-Flag (IB: Flag) or anti-Myc (IB: Myc) antibodies. Expression of the transfected plasmids were analyzed with anti-Flag and anti-Myc antibodies in whole cell lysates.

3.17 Co-localization of mutated-*PmDDX41* with *MmSTING* in HEK293T cells

To examine the co-localization of mutated-*PmDDX41* lacking HELICc domain, DEADc domain with *MmSTING*, fluorescence microscopy was performed. Immunofluorescence analysis also showed that in normal condition, *PmDDX41*, the DEADc domain protein and the HELICc domain protein were localized with *MmSTING* in the cytoplasm. Following stimulation with poly(dA:dT), the expression of *PmDDX41* and the DEADc domain were induced and both proteins were found in the cytoplasm and nucleus (**Fig. 41**). In contrast, the HELICc domain of *PmDDX41* remained in the cytoplasm following stimulation (**Fig. 41**).



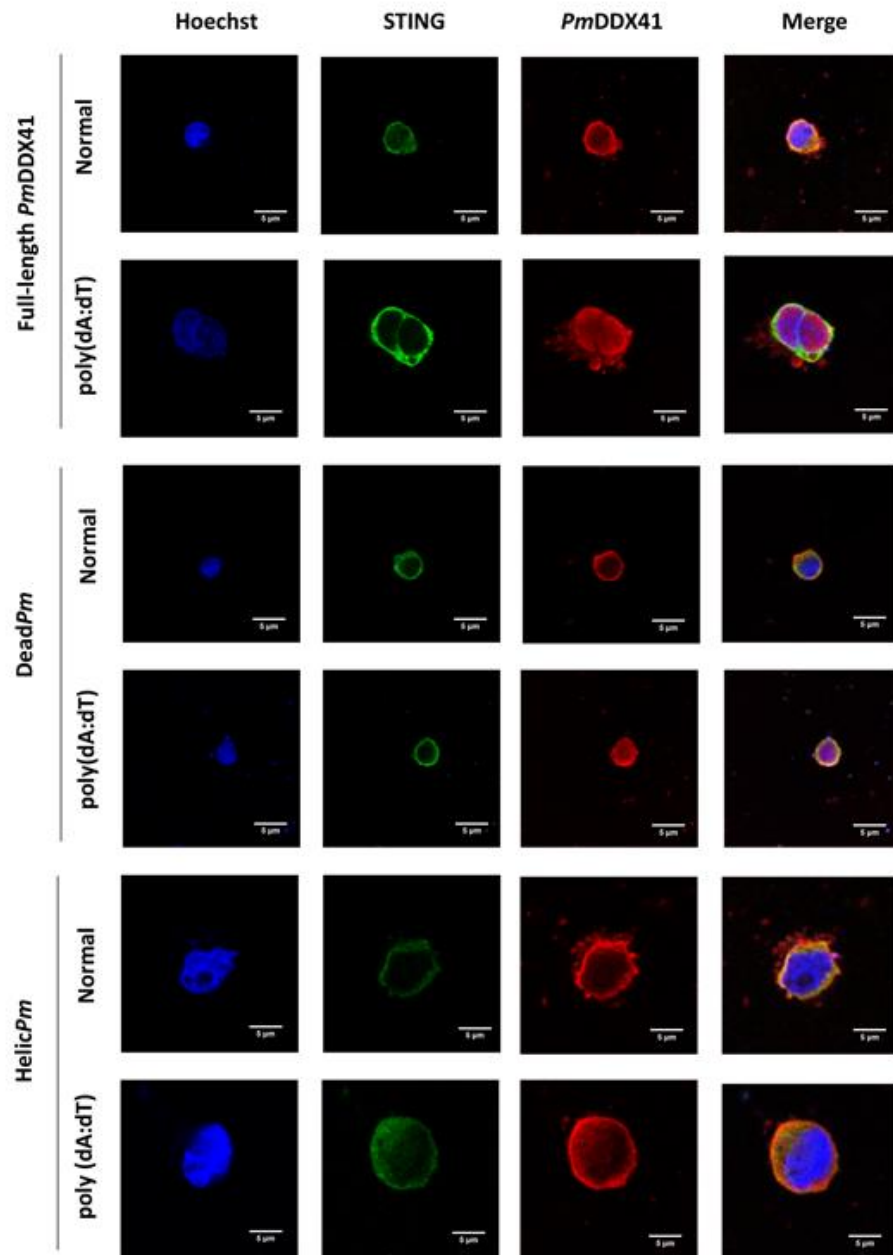


Fig. 41 Co-localization of mutated-*PmDDX41* and *MmSTING* in HEK293T cells after stimulated with poly(dA:dT) and poly(I:C), as visualized by fluorescence microscopy.

HEK293T cells were co-transfected with Flag-tagged-*PmDDX41* expression vector and Myc-tagged-*MmSTING*. After 24 h, cells were stimulated with 1 $\mu\text{g/ml}$ of poly(dA:dT) and poly(I:C) for 6 h. Cells were collected and fixed with 4% paraformaldehyde. Cells were then stained with anti-Flag and anti-Myc antibodies conjugated with Alexa Fluor 568 (red) and Alexa Fluor 488 (green), respectively.

Nuclei were stained with Hoechst 33342 (blue). Images were captured by laser-scanning confocal microscopy (Zeiss LSM-700; original magnification, 63x).



CHAPTER IV

DISCUSSIONS

Microbial nucleic acids, such as DNA or RNA that are detected in the cytoplasm of host cells can induce host immune responses in the infected cells. In previous studies, it has shown that host contain sensor molecules that sense these nucleic acids and trigger various immune responses (Kawai and Akira, 2010; Unterholzner et al., 2010; Parvatiyar et al., 2012; Broz and Monack, 2013). A number of cytosolic sensors for microbial DNA or RNA have been identified (Takaoka et al., 2007; Zhang et al., 2011; Ablasser et al., 2013; Sun et al., 2013). In recent years, it has been reported that several DExD/H-box helicases contribute to antiviral immunity in vertebrates, either by acting as sensors for viral nucleic acids or by facilitating downstream signaling events (Ahmad and Hur, 2015). DDX41 is defined as a member of the DExD/H-box helicase superfamily to be involved in intracellular DNA sensor which triggered the innate immune response against the viral infection in mammalian cells (Jiang et al., 2017). Knocking down of DDX41 in mouse splenic mDC line D2SC leading to 90% decrease of IFN- β responses to poly(dA:dT) (Zhang et al., 2011).

In this study, the first DDX41 from the shrimp *Penaeus monodon* (*PmDDX41*) was identified and characterized according to its role in innate immunity against viral infection. The ORF of the *PmDDX41* cDNA was composed of 1863 bp encoding a polypeptide of 620 amino acid residues. According to the SMART program, *PmDDX41* contains three signature domains, namely, the DEXDc, HELICc, and zinc finger domains which contribute to the function of the protein (Zhang et al., 2011; Ma

et al., 2018). From the phylogenetic tree, *PmDDX41* clustered together with invertebrate Abstrakt genes, with the closest similarity to the amphipod Abstrakt. Abstrakt in *Drosophila* is the homolog of DDX41, which shares 66% identity and 80% similarity at the amino acid level. The gene was initially identified by a very specific phenotype, the failure of the Bolwig nerve to fasciculate and project normally (Schmucker et al., 1997). The Abstrakt gene is essential for survival at all stages throughout the life cycle of the fly (Irion and Leptin, 1999). These results supported that DDX41 family members were structurally conserved from vertebrate to invertebrate evolution.

Tissue distribution analysis revealed that the *PmDDX41* transcript was expressed in various shrimp tissues, including hemocytes, intestine, hepatopancreas, lymphoid organ, gill, heart, muscle, and eye stalk. However, particularly high mRNA expression levels of *PmDDX41* were found in immune-related tissues including the hepatopancreas, gill, and hemocytes. These tissues play an important role in metabolism and immunity in crustaceans (He et al., 2015). DDX41 in chickens was found to be expressed in various tissues and mostly expressed in the digestive crop (Cheng et al., 2017). The porcine DDX41 was expressed in all of the tested tissues, especially the stomach and liver and reported to be involved in the dsDNA- and dsDNA-virus-mediated type I IFN signaling pathway in porcine kidney cells (Zhu et al., 2014). DDX41 was identified as a PRR in mouse dendritic cells (DCs) that sensed the dsDNA, cyclic di-GMP, and cyclic di-AMP and reported to form a complex with STING and activate type I interferon via interferon regulatory factors (IRF3 and IRF7) (Zhang et al., 2011; Parvatiyar et al., 2012). More recently, an IRF has been

characterized in the Pacific white shrimp and found to be involved in the IFN-like system in shrimp (Li et al., 2015).

To further investigate the role of *PmDDX41* in the shrimp immune response, the shrimp were challenged with three major pathogens (WSSV, *V. harveyi*, and YHV) and analyzed for hemocyte *PmDDX41* expression patterns. The results revealed that *PmDDX41* was up-regulated after challenge with the dsDNA virus WSSV but down-regulated after challenge with the ssRNA virus YHV, and no significant change was observed after challenge with the bacterium *V. harveyi*. Moreover, I found that *PmDDX41* was up-regulated after nucleic acid mimics (poly(dA:dT) and poly(I:C)) injection but it should be noted that *PmDDX41* transcript level was higher expressed in poly(dA:dT) than poly(I:C) injection. In chickens, the *chDDX41* transcript was slightly up-regulated by the dsDNA analogue poly(dA:dT) but not by the dsRNA analogue poly(I:C) or RNA virus (Cheng et al., 2017). In terms of vertebrates, *DDX41* expression was induced in the olive flounder by Ranavirus stimulation in monocyte-like cells (Quynh et al., 2015). *DDX41* was found to recognize a dsDNA virus in innate immunity in vertebrates (Zhang et al., 2011). Our results suggest that *PmDDX41* might be involved in the immune response to the dsDNA virus. Further investigation using co-immunoprecipitation (Co-IP), revealed that *PmDDX41* protein could bind to poly(dA:dT) not poly(I:C). Similarly, mouse *DDX41* binds to poly(dA:dT) and poly(dG:dC) but not poly(I:C) (Zhang et al., 2011). The results indicated that *PmDDX41* is possibly function as a cytosolic DNA sensor.

WSSV is one of the most common and destructive pathogens in shrimp aquaculture, and shrimp mortality can reach 100% within 3–10 days after infection

(Wang *et al.*, 1999). To evaluate the role of *PmDDX41* in the shrimp immune response to WSSV, I knocked down *PmDDX41* prior to WSSV infection and determined the survival rate of the knockdown shrimp compared to the control shrimp. The results showed that 100% death was observed within three days for the *PmDDX41*-silenced shrimp, compared with five days for the control shrimp, which indicates that *PmDDX41* plays an important role in the shrimp antiviral response to WSSV infection. To further validate the effects of *PmDDX41* knockdown in the shrimp antiviral immune response, I observed the expression levels of genes involved in signal transduction pathways, antimicrobial peptides, and IFN-like molecules. It was found that the expression levels of genes involved in the signal transduction pathways (*PmIKK β* , *PmIKK ϵ* , *PmRelish*, and *PmDorsal*) and antimicrobial peptides (*PmPEN3*, *PmPEN5*, and *ALFPm6*) were reduced in the *PmDDX41*-knockdown shrimp. In vertebrates, the knockdown of DDX41 via short-hairpin RNA inhibited the immune response to cyclic di-GMP and resulted in defective activation of the DNA-sensing pathway by decreasing IFN- β (Parvatiyar *et al.*, 2012). In the Pacific white shrimp *Litopenaeus vannamei*, IKK β and IKK ϵ are the central regulators of the NF- κ B signaling pathway and represent a point of convergence for most of the signal transduction pathways that lead to NF- κ B activation (Vallabhapurapu and Karin, 2009). In addition, the levels of the shrimp antimicrobial peptides (*LvPEN2*, *LvPEN3*, and *LvPEN4*) were significantly decreased in *LvIKK β* - and *LvIKK ϵ* -silenced *L.vannamei*. The IMD pathway, which is involved in the sensing of RNA viruses and Gram-negative bacteria and mediated by the IKK complex to activate the NF- κ B transcription factor Relish, has been studied in shrimp (Wang and Wang, 2013). The activated Relish is translocated into the nucleus to induce the expression of shrimp

antimicrobial peptides (penaeidins, crustins, and antilipopolysaccharide factor) (Tassanakajon *et al.*, 2013). After knockdown of the *PmRelish* gene in shrimp, it was found that the *PmPEN5* transcript was suppressed, while *PmPEN3* was slightly upregulated. These results indicate that *PmPEN5* and *PmPEN3* are regulated by *PmRelish* (Visetnan *et al.*, 2015b).

It is well known that DEAD-box helicases are essential in various cellular processes including mRNA export, transcriptional and translational regulation, and ribosome biogenesis (Rocak and Linder, 2004). More recent studies have suggested that vertebrate DDX41 could recognize the bacterial secondary messengers cyclic di-GMP or cyclic di-AMP to activate the type I IFN immune response, and that DDX41 senses intracellular DNA mediated by the adaptor STING in dendritic cells (Bowie, 2012; Parvatiyar *et al.*, 2012; Miyabe *et al.*, 2014). Interestingly, another recently identified DNA sensor, cGAS, also recognizes microbial DNA to generate the second messenger cGAMP to initiate the STING pathway and subsequent IFN production (Ablasser *et al.*, 2013; Sun *et al.*, 2013; Diner and Vance, 2014). In arthropods, the Vago, a virally activated secreted peptide, is considered to be a cytokine functionally similar to IFN. Recently, it has been reported that the shrimp Vago might function as an IFN-like molecule and shrimp might possess an antiviral mechanism similar to the IFN system (Li *et al.*, 2015). In this study, the expression of *PmVagos* was not changed in the *PmDDX41*-knockdown shrimp. Thus, it is interesting to speculate whether shrimp DDX41 functions in concert with or engages directly with the STING innate immune-sensing pathway to induce the production of antiviral molecules.

To provide the experimental evidence for this notion, the localization of *PmDDX41* was observed in shrimp hemocytes. The results demonstrated that

PmDDX41 was located in cytoplasm and translocated to the nucleus after WSSV infection, poly(dA:dT) or poly(I:C) stimulation. From previous studies, DDX41 protein in duck was mainly distributed in the cytoplasm (Li et al., 2018). The results suggest that *PmDDX41* is a cytoplasmic DNA sensor mediating innate immune response in host cell, but the nuclear function of DDX41 remains unclear.

Due to the limitation of using shrimp cell line, the human embryonic kidney, HEK293T cells, which naturally has a low or lacks the expression of endogenous DDX41 and STING was used as a model system cell lines for further functional study of *PmDDX41* (Ma et al., 2018). In spite of the functional conservation of DDX41, it was initially found to be a cytosolic protein in HEK293T cells and D2SC cells (Zhang et al., 2011; Parvatiyar et al., 2012). In this study, we found that *PmDDX41* mostly distributed in the cytoplasm of HEK293T cells when the cells were not stimulated. After stimulation with poly(dA:dT) and poly(I:C), *PmDDX41* was observed in the nucleus. Similar results were seen in duck DDX41 (Li et al., 2018), while *DrDDX41* from zebrafish was transported from nucleus to cytoplasm under stimulation condition (Ma et al., 2018). These observations suggested that *PmDDX41* was a trafficking protein that acted as a cytosolic sensor and translocated into nucleus in response to stimulation. The evidence of trafficking protein requires further investigation.

It was known that stimulator of IFN genes (STING), which is also called MPYS, MITA, ERIS and TRIM173, was discovered using a cDNA expression library designed to isolate molecules that activated the IFN- β promoter (Ishikawa and Barber, 2008). Moreover, STING is a central adaptor protein connecting various innate immune signaling pathways through associated with IKK β or TBK1 to activate type I

interferon. However, the upstream receptor for the initiation of the STING-IFN- β signaling pathway remains uncertain. In this study, the role of *PmDDX41* in STING-mediated signaling pathways was investigated in HEK293T cells. Overexpression of both *PmDDX41* and the membrane-associated adaptor STING together had a synergistic effect in promoting IFN- β and NF- κ B promoter activity. In mouse fibroblast cell line L929, overexpression of DDX41 and STING lead to more activation of IFN- β promoter (Zhang et al., 2011). To further investigate the potential interaction between *PmDDX41* and *MmSTING* in HEK293T cells, Co-immunoprecipitation assay was performed. The results showed that *PmDDX41* interacts with STING after poly(dA:dT) stimulation. Similarly, it has been reported that *DrDDX41* binds to *DrSTING* after stimulation with poly(dA:dT) (Ma et al., 2018) and it might form a complex with STING under DNA stimulation condition. Moreover, *PmDDX41* localized together with *MmSTING* in cytoplasm but following the nucleic mimics stimulation, *PmDDX41* was translocated into nucleus, while STING remained in cytoplasm. In vertebrates, DDX41-STING complex was located in cytosol and after stimulation with poly(dA:dT), there was lower expression of DDX41 and STING in endoplasmic reticulum and mitochondria and higher expression of DDX41 and STING in endosomes (Zhang et al., 2011). In murine embryonic fibroblasts, STING was relocalized with TBK1 from the endoplasmic reticulum to endosome (Ishikawa et al., 2009).

Base on predicted domains of *PmDDX41*, two mutants containing the different domains of *PmDDX41* were constructed to identify the DNA binding site of *PmDDX41* and investigate their role in mediating IFN- β and NF- κ B signaling pathway. The activity of IFN- β and NF- κ B promoter were significantly enhanced by

co-transfection with full-length of *PmDDX41* or *DeadPm* and *MmSTING*. Interestingly, wild-type *PmDDX41* and its mutants containing the DEADc domain could interact with *MmSTING* after stimulation with poly(dA:dT). From previous studies, mouse DDX41 acts as a cytosolic sensor in mDCs, and can bind with synthetic double-stranded DNA (dsDNA) through DEADc domain in vitro (Paludan and Bowie, 2013). Recently, Li et al. reported that duck STING overexpression activated NF- κ B and induced the transcription of IFN- β in DEFs cells (Li et al., 2018). These results indicate that the DEADc domain of *PmDDX41* is responsible for their interaction.

From previous studies, Liu and Wang (2016) have reported that knockdown of DDX41 expression blocked the activation of TBK1 and the transcription factors NF- κ B and IRF3 by DNA but not RNA. STING functions as a key scaffolding and adaptor protein to facilitate the signal transduction initiating from upstream cytosolic dsDNA receptors to the downstream effectors TBK1 and IRF3, leading to the activation of type I interferon (Liu and Wang, 2016). These results suggested that after viral infection, the viral DNA releases the dsDNA to the cells which was detected by a cytosolic DNA sensor, DDX41 and then activate STING. The activated STING interacts with TBK1 to form the complex and required for phosphorylation and nuclear translocation of IRF3, ultimately leading to expression of IFN- β . These results suggested that *PmDDX41* is involved in antiviral immune response via a DNA sensing pathway that is triggered through I κ B kinase complex and leading to activation of immune-related genes in Toll and IMD pathways. In addition, they identified two IKK homologs, *LvIKK β* and *LvIKK ϵ* from Pacific white shrimp that are related to NF- κ B signaling pathway. IKK α/β and TBK1/IKK ϵ are the central

regulators of NF- κ B signaling pathway in mammals. *LvIKK β* also strongly induced NF- κ B activity in HEK293T cells, while *LvIKK β* but not *LvIKK ϵ* can be activated antimicrobial peptides (AMPs) receptors of shrimp, such as the Penaeidins. Moreover, the silencing of *LvIKK β* or *LvIKK ϵ* using RNA interference (RNAi) decreases the expression of *Litopenaeus vannamei* AMPs, including *LvPEN2*, *LvPEN3*, *LvPEN4*, *Lvlysozyme*, *LvCrustin1* and *LvCrustin2*. It indicated that IKK-NF- κ B signaling pathway could activate the shrimp AMPs expression. In crustaceans, STING ortholog has recently been identified and functionally characterized in shrimp (*LvSTING*) (Li et al., 2017). The knockdown of *LvSTING* significantly decreased the induction of *LvPEN4* after challenged with *Vibrio parahaemolyticus* which an important shrimp AMP downstream of Toll and IMD pathway (Li et al., 2017).

In summary, the first DDX41 from shrimp, *PmDDX41*, was identified and demonstrated that it shares high sequence identity with DDX41 from various organisms including human and mouse. The transcript of *PmDDX41* was up-regulated after infection with the dsDNA virus WSSV, suggesting that *PmDDX41* might play a role in the immune response to DNA viruses. Gene silencing of *PmDDX41* resulted in the more rapid death of WSSV-infected shrimp and a reduction in the levels of several immune transcripts related to the signaling pathway and antimicrobial peptides. Furthermore, *PmDDX41* is likely play a key role in the innate immune response against WSSV infection by binding to the viral DNA via the DEADc domain in the cytosol. *PmDDX41* interacts with a *MmSTING* adaptor in the cytoplasm and initiates a signal by activating downstream regulators, thus leading to the production of antiviral genes, including cytokine-like molecules and AMPs (**Fig. 42**). This research extends our knowledge with regards to the role of *PmDDX41* as a

cytosolic DNA sensor in the innate immune response to viral infection in the shrimp

P. monodon.



CHAPTER V

CONCLUSIONS

1. *Penaeus monodon* DEAD (Asp-Glu-Ala-Asp)-box polypeptide 41 (*PmDDX41*) was identified. The complete open reading frame (ORF) of *PmDDX41* contains 1863-bp encoding a putative protein of 620 amino acids which contains 3 conserved domains, DEADc, HELICc and zinc finger domains.
2. The transcript of *PmDDX41* was detected in all tested tissues and was up-regulated upon infection with a DNA virus, white spot syndrome virus (WSSV) and stimulation with nucleic acid mimic poly(dA:dT).
3. The suppression of *PmDDX41* by dsRNA-mediated gene silencing resulted in a more rapid death of WSSV-infected shrimp and a significant decrease in the mRNA expression levels of several immune-related genes (*PmIKK β* , *PmIKK ϵ* , *PmRelish*, *PmCactus*, *PmDorsal*, *PmPEN3*, *PmPEN5*, and ALFPm6).
4. Cellular localization using immunofluorescence staining revealed that *PmDDX41* was localized in cytoplasm and translocated into nucleus upon WSSV infection and poly(dA:dT) and poly(I:C) injection.
5. The overexpression analysis of *PmDDX41* and adaptor *MmSTING* in HEK293T cells could promote the activation of IFN- β and NF- κ B signaling pathways in a STING-dependent manner. Moreover, *PmDDX41* could interact with *MmSTING* under stimulation with poly(dA:dT). In normal condition, both were localized in cytoplasm of HEK293T cells but *PmDDX41* translocated to the nucleus upon WSSV infection while *MmSTING* remained in the cytoplasm.

6. The DEADc domain of *PmDDX41* is required for the activation of *PmDDX41*-*MmSTING* to mediate IFN- β and NF- κ B signaling pathways. By using Co-IP assay, DEADc domain was shown to contribute to the association of *PmDDX41* and *MmSTING* after poly(dA:dT) stimulation. These results suggest that *PmDDX41* is involved in antiviral response probably via DNA sensing pathway which forms a complex with STING and sending a signal to activate the immune responses of shrimp.

7. Taken together the results suggest that after WSSV infection, the virus releases the dsDNA which is detected by *PmDDX41*. Subsequently, *PmDDX41* binds to viral DNA and forms complex with STING and sends the signal through TBK/IKK-IRF3 to activate the interferon response. Moreover, IKK complex activates the NF- κ B transcription factor *PmRelish* leading to activation of antimicrobial peptides synthesis (Fig. 42).

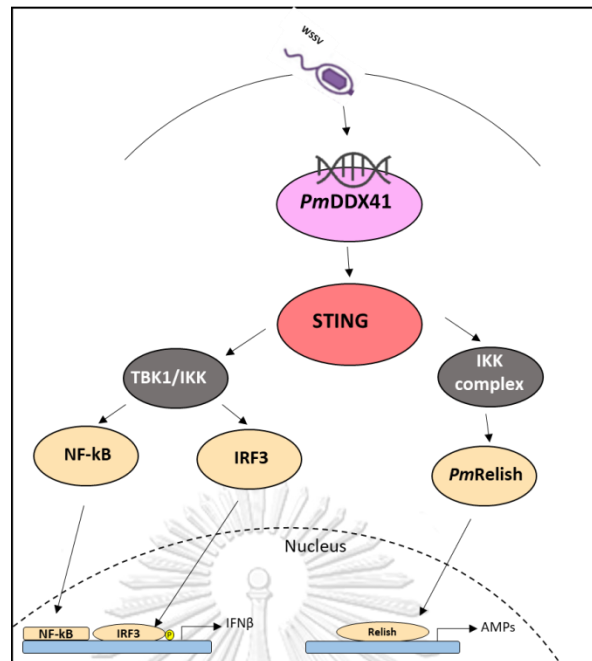


Fig. 42 The signaling pathway of *PmDDX41* in innate immunity. *PmDDX41* recognizes nucleic acid dsDNA and mediates innate immune response through the STING leading to the activation of the downstream production including type I interferons and antimicrobial peptides.

REFERENCES

- Ablasser, A., Goldeck, M., Cavlar, T., Deimling, T., Witte, G., Rohl, I., et al. (2013). cGAS produces a 2'-5'-linked cyclic dinucleotide second messenger that activates STING. *Nature* 498 (7454), 380-384.
- Ahmad, S., and Hur, S. (2015). Helicases in antiviral immunity: dual properties as sensors and effectors. *Trends Biochem Sci* 40 (10), 576-585.
- Amparyup, P., Wiriyaukaradecha, K., Charoensapsri, W., and Tassanakajon, A. (2010). A clip domain serine proteinase plays a role in antibacterial defense but is not required for prophenoloxidase activation in shrimp. *Dev Comp Immunol* 34 (2), 168-176.
- Arts, J.A., Cornelissen, F.H., Cijssouw, T., Hermsen, T., Savelkoul, H.F., and Stet, R.J. (2007). Molecular cloning and expression of a Toll receptor in the giant tiger shrimp, *Penaeus monodon*. *Fish Shellfish Immunol* 23 (3), 504-513.
- Assavalapsakul, W., Kiem, H.K., Smith, D.R., and Panyim, S. (2014). Silencing of *PmYPR65* receptor prevents yellow head virus infection in *Penaeus monodon*. *Virus Res* 189, 133-135.
- Avadhanula, V., Weasner, B.P., Hardy, G.G., Kumar, J.P., and Hardy, R.W. (2009). A novel system for the launch of alphavirus RNA synthesis reveals a role for the Imd pathway in arthropod antiviral response. *PLoS Pathog* 5 (9), e1000582.
- Bailey-Brock, J.H., and Moss, S.M. (1992). "CHAPTER 2 - PENAEID TAXONOMY, BIOLOGY AND ZOOGEOGRAPHY," in *Marine Shrimp Culture*, eds. A.W. Fast & L.J. Lester. (Amsterdam: Elsevier), 9-27.
- Boonyaratpalin, S., Supamattaya, K., Kasornchandra, J., Direkbusarakom, S., Aekpanithanpong, U., and Chantanachooklin, C. (1993). Non-occluded baculo-like virus, the causative agent of yellow head disease in the black tiger shrimp (*Penaeus monodon*). *Fish Pathology* 28, 103-109.
- Bowie, A.G. (2012). Innate sensing of bacterial cyclic dinucleotides: more than just STING. *Nat Immunol* 13 (12), 1137-1139.
- Broz, P., and Monack, D.M. (2013). Newly described pattern recognition receptors team up against intracellular pathogens. *Nat Rev Immunol* 13 (8), 551-565.
- Buchon, N., Silverman, N., and Cherry, S. (2014). Immunity in *Drosophila melanogaster* from microbial recognition to whole-organism physiology. *Nat Rev Immunol* 14 (12), 796-810.
- Chantanachookin, C., Boonyaratpalin, S., Kasornchandra, J., Direkbusarakom, S., Ekpanithanpong, U., Supamataya, K., et al. (1993). Histology and ultrastructure reveal a new granulosis-like virus in *Penaeus monodon* affected by yellow-head disease. *Diseases of Aquatic Organisms* 17, 145-157.
- Chen, H., Sun, H., You, F., Sun, W., Zhou, X., Chen, L., et al. (2011). Activation of STAT6 by STING is critical for antiviral innate immunity. *Cell* 147 (2), 436-446.
- Chen, J., Wang, W., Wang, X., Zhang, Q., Ren, Y., Song, J., et al. (2018). First detection of yellow head virus genotype 3 (YHV-3) in cultured *Penaeus monodon*, mainland China. *J Fish Dis* 41 (9), 1449-1451.
- Cheng, Y., Liu, Y., Wang, Y., Niu, Q., Gao, Q., Fu, Q., et al. (2017). Chicken DNA virus sensor DDX41 activates IFN-beta signaling pathway dependent on STING. *Dev Comp Immunol* 76, 334-342.

- Cowley, J.A., Dimmock, C.M., Wongteerasupaya, C., Boonsaeng, V., Panyim, S., and Walker, P.J. (1999). Yellow head virus from Thailand and gill-associated virus from Australia are closely related but distinct prawn viruses. *Dis Aquat Organ* 36 (2), 153-157.
- Deddouche, S., Matt, N., Budd, A., Mueller, S., Kemp, C., Galiana-Arnoux, D., et al. (2008). The DExD/H-box helicase Dicer-2 mediates the induction of antiviral activity in *Drosophila*. *Nat Immunol* 9 (12), 1425-1432.
- Deepika, A., Sreedharan, K., Paria, A., Makesh, M., and Rajendran, K.V. (2014). Toll-pathway in tiger shrimp (*Penaeus monodon*) responds to white spot syndrome virus infection: evidence through molecular characterisation and expression profiles of MyD88, TRAF6 and TLR genes. *Fish Shellfish Immunol* 41(2), 441-454.
- Diner, E.J., and Vance, R.E. (2014). Taking the STING out of cytosolic DNA sensing. *Trends Immunol* 35 (1), 1-2.
- Ding, S.W. (2010). RNA-based antiviral immunity. *Nat Rev Immunol* 10(9), 632-644.
- Feng, J., Zhao, L., Jin, M., Li, T., Wu, L., Chen, Y., et al. (2016). Toll receptor response to white spot syndrome virus challenge in giant freshwater prawns (*Macrobrachium rosenbergii*). *Fish Shellfish Immunol* 57, 148-159.
- Goto, A., Okado, K., Martins, N., Cai, H., Barbier, V., Lamiable, O., et al. (2018). The kinase IKKbeta regulates a STING- and NF-kappaB-dependent antiviral response pathway in *Drosophila*. *Immunity* 49 (2), 225-234.
- Guo, Z., Li, Y., and Ding, S. (2019). Small RNA-based antimicrobial immunity. *Nature Reviews Immunology* 19 (1), 31-44.
- Han, J., Tang, K., Aranguren, F., and Piamsomboon, P. (2016). Characterization and pathogenicity of acute hepatopancreatic necrosis disease natural mutants, pirABvp (-) *V. parahaemolyticus*, and pirABvp (+) *V. campbellii* strains. *Aquaculture* 470.
- Havanapan, P.O., Taengchaiyaphum, S., Ketterman, A.J., and Krittanai, C. (2016). Yellow head virus infection in black tiger shrimp reveals specific interaction with granule-containing hemocytes and crustinPm1 as a responsive protein. *Dev Comp Immunol* 54(1), 126-136.
- He, Y., Ju, C., and Zhang, X. (2015). Roles of small RNAs in the immune defense mechanisms of crustaceans. *Mol Immunol* 68 (2), 399-403.
- Holmblad, T., and Söderhäll, K. (1999). Cell adhesion molecules and antioxidative enzymes in a crustacean, possible role in immunity. *Aquaculture* 72, 111-123.
- Hou, F., He, S., Liu, Y., Zhu, X., Sun, C., and Liu, X. (2014). RNAi knock-down of shrimp *Litopenaeus vannamei* Toll gene and immune deficiency gene reveals their difference in regulating antimicrobial peptides transcription. *Dev Comp Immunol* 44 (2), 255-260.
- Huang, B., Zhang, L., Du, Y., Xu, F., Li, L., and Zhang, G. (2017). Characterization of the Mollusc RIG-I/MAVS pathway reveals an archaic antiviral signalling framework in invertebrates. *Sci Rep* 7(1), 8217.
- Huang, J., Li, F., Wu, J., and Yang, F. (2015). White spot syndrome virus enters crayfish hematopoietic tissue cells via clathrin-mediated endocytosis. *Virology* 486, 35-43.
- Huang, Y., Wang, W., and Ren, Q. (2016). Two host microRNAs influence WSSV replication via STAT gene regulation. *Sci Rep* 6, 23643.

- Irion, U., and Leptin, M. (1999). Developmental and cell biological functions of the *Drosophila* DEAD-box protein abstract. *Curr Biol* 9 (23), 1373-1381.
- Ishii, K.J., Coban, C., Kato, H., Takahashi, K., Torii, Y., Takeshita, F., et al. (2006). A Toll-like receptor-independent antiviral response induced by double-stranded B-form DNA. *Nat Immunol* 7 (1), 40-48.
- Ishikawa, H., and Barber, G.N. (2008). STING is an endoplasmic reticulum adaptor that facilitates innate immune signalling. *Nature* 455 (7213), 674-678.
- Ishikawa, H., Ma, Z., and Barber, G.N. (2009). STING regulates intracellular DNA-mediated, type I interferon-dependent innate immunity. *Nature* 461 (7265), 788-792.
- Ivashkiv, L.B., and Donlin, L.T. (2014). Regulation of type I interferon responses. *Nat Rev Immunol* 14 (1), 36-49.
- Jatuyosporn, T., Laohawutthichai, P., Supungul, P., Sotelo-Mundo, R.R., Ochoa, A., Tassanakajon, A., et al. (2019). Role of clathrin assembly protein-2 beta subunit during white spot syndrome virus infection in black tiger shrimp *Penaeus monodon*. *Sci Rep* 9 (1), 13489.
- Jiajia Xu, D.Z., Mintao Sun, Liping Wang, Zhen-yu Jia, Rui Liu, Liqiong Song (2016). A-type CpG ODN with higher binding affinity to *LvToll1* could probably activate downstream IFN system-like antiviral response in shrimp *Litopenaeus vannamei*. *Invertebrate Survival Journal* 13, 397-410.
- Jiang, Y., Zhu, Y., Liu, Z.J., and Ouyang, S. (2017). The emerging roles of the DDX41 protein in immunity and diseases. *Protein Cell* 8 (2), 83-89.
- Jiravanichpaisal, P., Lee, S.Y., Kim, Y.A., Andren, T., and Soderhall, I. (2007). Antibacterial peptides in hemocytes and hematopoietic tissue from freshwater crayfish *Pacifastacus leniusculus*: characterization and expression pattern. *Dev Comp Immunol* 31 (5), 441-455.
- Kaksonen, M., and Roux, A. (2018). Mechanisms of clathrin-mediated endocytosis. *Nat Rev Mol Cell Biol* 19 (5), 313-326.
- Kawai, T., and Akira, S. (2010). The role of pattern-recognition receptors in innate immunity: update on Toll-like receptors. *Nat Immunol* 11 (5), 373-384.
- Kawai, T., Takahashi, K., Sato, S., Coban, C., Kumar, H., Kato, H., et al. (2005). IPS-1, an adaptor triggering RIG-I- and Mda5-mediated type I interferon induction. *Nat Immunol* 6 (10), 981-988.
- Kingsolver, M.B., Huang, Z., and Hardy, R.W. (2013). Insect antiviral innate immunity: pathways, effectors, and connections. *J Mol Biol* 425 (24), 4921-4936.
- Kongprajug, A., Panyim, S., and Ongvarrasopone, C. (2017). Suppression of *PmRab11* inhibits YHV infection in *Penaeus monodon*. *Fish Shellfish Immunol* 66, 433-444.
- Kumar Jha, R., Yousep Babikian, H., Yousef Babikian, H., Van Khoa, L., Wisoyo, D., Srisombat, S., et al. (2017). Efficacy of natural herbal formulation against acute hepatopancreatic necrosis disease (AHPND) causing *Vibrio parahaemolyticus* in *Penaeus vannamei*. *Veterinary Medicine* 2, 1-6.
- Lan, J.F., Zhao, L.J., Wei, S., Wang, Y., Lin, L., and Li, X.C. (2016). *PcToll2* positively regulates the expression of antimicrobial peptides by promoting *PcATF4* translocation into the nucleus. *Fish Shellfish Immunol* 58, 59-66.

- Li, C., Li, H., Chen, Y., Chen, Y., Wang, S., Weng, S.P., et al. (2015). Activation of Vago by interferon regulatory factor (IRF) suggests an interferon system-like antiviral mechanism in shrimp. *Sci Rep* 5, 15078.
- Li, H., Wang, S., Lu, K., Yin, B., Xiao, B., Li, S., et al. (2017). An invertebrate STING from shrimp activates an innate immune defense against bacterial infection. *FEBS Lett* 591 (7), 1010-1017.
- Li, Y., Li, H., Su, N., Liu, D., Luo, R., and Jin, H. (2018). Molecular cloning and functional characterization of duck DDX41. *Dev Comp Immunol* 88, 183-189.
- Lightner, D.V. (1996). Epizootiology, distribution and the impact on international trade of two penaeid shrimp viruses in the Americas. *Rev Sci Tech* 15 (2), 579-601.
- Liu, X., and Wang, C. (2016). The emerging roles of the STING adaptor protein in immunity and diseases. *Immunology* 147 (3), 285-291.
- Lo, F., Leu, H., Ho, H., Chen, C., Peng, S., Chen, Y., et al. (1996). Detection of baculovirus associated with white spot syndrome in penaeid shrimps using polymerase chain reaction. *Diseases of Aquatic Organisms* 25, 133-141.
- Longyant, S., Rukpratanporn, S., Chaivisuthangkura, P., Suksawad, P., Srisuk, C., Sithigorngul, W., et al. (2008). Identification of *Vibrio* spp. in vibriosis *Penaeus vannamei* using developed monoclonal antibodies. *Journal of Invertebrate Pathology* 98 (1), 63-68.
- Loo, Y.M., and Gale, M., Jr. (2011). Immune signaling by RIG-I-like receptors. *Immunity* 34 (5), 680-692.
- Ma, J.X., Li, J.Y., Fan, D.D., Feng, W., Lin, A.F., Xiang, L.X., et al. (2018). Identification of DEAD-box RNA helicase DDX41 as a trafficking protein that involves in multiple innate immune signaling pathways in a zebrafish Model. *Front Immunol* 9, 1327.
- Matjank, W., Ponprateep, S., Rimphanitchayakit, V., Tassanakajon, A., Somboonwiwat, K., and Vatanavicharn, T. (2018). Plasmolipin, *PmPLP1*, from *Penaeus monodon* is a potential receptor for yellow head virus infection. *Dev Comp Immunol* 88, 137-143.
- Mekata, T., Kono, T., Savan, R., Sakai, M., Kasornchandra, J., Yoshida, T., et al. (2006). Detection of yellow head virus in shrimp by loop-mediated isothermal amplification (LAMP). *J Virol Methods* 135 (2), 151-156.
- Mekata, T., Kono, T., Yoshida, T., Sakai, M., and Itami, T. (2008). Identification of cDNA encoding Toll receptor, *MjToll* gene from kuruma shrimp, *Marsupenaeus japonicus*. *Fish Shellfish Immunol* 24 (1), 122-133.
- Mekata, T., Sudhakaran, R., Kono, T., K, U.t., Supamattaya, K., Suzuki, Y., et al. (2009). Real-time reverse transcription loop-mediated isothermal amplification for rapid detection of yellow head virus in shrimp. *J Virol Methods* 162 (2), 81-87.
- Merkling, S.H., and van Rij, R.P. (2013). Beyond RNAi: antiviral defense strategies in *Drosophila* and mosquito. *J Insect Physiol* 59 (2), 159-170.
- Miyabe, H., Hyodo, M., Nakamura, T., Sato, Y., Hayakawa, Y., and Harashima, H. (2014). A new adjuvant delivery system 'cyclic di-GMP/YSK05 liposome' for cancer immunotherapy. *J Control Release* 184, 20-27.
- Motoh, H. (1985). Biology and ecology of *Penaeus monodon*. *Aquaculture Department*.

- Myllymaki, H., Valanne, S., and Ramet, M. (2014). The *Drosophila* imd signaling pathway. *J Immunol* 192 (8), 3455-3462.
- Nie, L., Cai, S.Y., Shao, J.Z., and Chen, J. (2018). Toll-Like Receptors, associated biological roles, and signaling networks in non-mammals. *Front Immunol* 9, 1523.
- Ouyang, S., Song, X., Wang, Y., Ru, H., Shaw, N., Jiang, Y., et al. (2012). Structural analysis of the STING adaptor protein reveals a hydrophobic dimer interface and mode of cyclic di-GMP binding. *Immunity* 36 (6), 1073-1086.
- Paludan, S.R., and Bowie, A.G. (2013). Immune sensing of DNA. *Immunity* 38 (5), 870-880.
- Paradkar, P.N., Trinidad, L., Voysey, R., Duchemin, J.B., and Walker, P.J. (2012). Secreted Vago restricts west nile virus infection in *Culex* mosquito cells by activating the Jak-STAT pathway. *Proc Natl Acad Sci U S A* 109 (46), 18915-18920.
- Parvatiyar, K., Zhang, Z., Teles, R.M., Ouyang, S., Jiang, Y., Iyer, S.S., et al. (2012). The helicase DDX41 recognizes the bacterial secondary messengers cyclic di-GMP and cyclic di-AMP to activate a type I interferon immune response. *Nat Immunol* 13 (12), 1155-1161.
- Poirier, E.Z., Goic, B., Tome-Poderti, L., Frangeul, L., Boussier, J., Gausson, V., et al. (2018). Dicer-2-dependent generation of viral DNA from defective genomes of RNA viruses modulates antiviral immunity in insects. *Cell Host Microbe* 23 (3), 353-365.
- Qiu, W., Zhang, S., Chen, Y.G., Wang, P.H., Xu, X.P., Li, C.Z., et al. (2014). *Litopenaeus vannamei* NF-kappaB is required for WSSV replication. *Dev Comp Immunol* 45 (1), 156-162.
- Quynh, N.T., Hikima, J., Kim, Y.R., Fagutao, F.F., Kim, M.S., Aoki, T., et al. (2015). The cytosolic sensor, DDX41, activates antiviral and inflammatory immunity in response to stimulation with double-stranded DNA adherent cells of the olive flounder, *Paralichthys olivaceus*. *Fish Shellfish Immunol* 44 (2), 576-583.
- Rocak, S., and Linder, P. (2004). DEAD-box proteins: the driving forces behind RNA metabolism. *Nat Rev Mol Cell Biol* 5 (3), 232-241.
- Schmucker, D., Jackle, H., and Gaul, U. (1997). Genetic analysis of the larval optic nerve projection in *Drosophila*. *Development* 124 (5), 937-948.
- Senapin, S., Thaowbut, Y., Gangnonngiw, W., Chuchird, N., Sriurairatana, S., and Flegel, T.W. (2010). Impact of yellow head virus outbreaks in the whiteleg shrimp, *Penaeus vannamei* in Thailand. *J Fish Dis* 33 (5), 421-430.
- Song, X., Zhang, Z., Wang, S., Li, H., Zuo, H., Xu, X., et al. (2015). A Janus Kinase in the JAK/STAT signaling pathway from *Litopenaeus vannamei* is involved in antiviral immune response. *Fish Shellfish Immunol* 44 (2), 662-673.
- Sun, J.J., Xu, S., He, Z.H., Shi, X.Z., Zhao, X.F., and Wang, J.X. (2017). Activation of toll pathway is different between kuruma shrimp and *Drosophila*. *Front Immunol* 8, 1151.
- Sun, L., Wu, J., Du, F., Chen, X., and Chen, Z.J. (2013). Cyclic GMP-AMP synthase is a cytosolic DNA sensor that activates the type I interferon pathway. *Science* 339 (6121), 786-791.

- Sun, R., Wang, M., Wang, L., Yue, F., Yi, Q., Huang, M., et al. (2014). The immune responses triggered by CpG ODNs in shrimp *Litopenaeus vannamei* are associated with *LvTolls*. *Dev Comp Immunol* 43 (1), 15-22.
- Takaoka, A., Wang, Z., Choi, M.K., Yanai, H., Negishi, H., Ban, T., et al. (2007). DAI (DLM-1/ZBP1) is a cytosolic DNA sensor and an activator of innate immune response. *Nature* 448 (7152), 501-505.
- Tamura, K., Stecher, G., Peterson, D., Filipinski, A., and Kumar, S. (2013). MEGA6: molecular evolutionary genetics analysis version 6.0. *Mol Biol Evol* 30 (12), 2725-2729.
- Tan, X., Sun, L., Chen, J., and Chen, Z.J. (2018). Detection of microbial infections through innate immune sensing of nucleic acids. *Annu Rev Microbiol* 72, 447-478.
- Tassanakajon, A., Klinbunga, S., Paunglarp, N., Rimphanitchayakit, V., Udomkit, A., Jitrapakdee, S., et al. (2006). *Penaeus monodon* gene discovery project: the generation of an EST collection and establishment of a database. *Gene* 384, 104-112.
- Tassanakajon, A., Rimphanitchayakit, V., Visetnan, S., Amparyup, P., Somboonwiwat, K., Charoensapsri, W., et al. (2018). Shrimp humoral responses against pathogens: antimicrobial peptides and melanization. *Dev Comp Immunol* 80, 81-93.
- Tassanakajon, A., Somboonwiwat, K., Supungul, P., and Tang, S. (2013). Discovery of immune molecules and their crucial functions in shrimp immunity. *Fish Shellfish Immunol* 34 (4), 954-967.
- Tran, L., Nunan, L., M Redman, R., L Mohney, L., Pantoja, C., Fitzsimmons, K., et al. (2013). Determination of the infectious nature of the agent of acute hepatopancreatic necrosis syndrome affecting penaeid shrimp. *Diseases of aquatic organisms* 105, 45-55.
- Unterholzner, L., Keating, S.E., Baran, M., Horan, K.A., Jensen, S.B., Sharma, S., et al. (2010). IFI16 is an innate immune sensor for intracellular DNA. *Nat Immunol* 11 (11), 997-1004.
- Vallabhapurapu, S., and Karin, M. (2009). Regulation and function of NF-kappaB transcription factors in the immune system. *Annu Rev Immunol* 27, 693-733.
- Verbruggen, B., Bickley, L.K., van Aerle, R., Bateman, K.S., Stentiford, G.D., Santos, E.M., et al. (2016). Molecular mechanisms of white spot syndrome virus infection and perspectives on treatments. *Viruses* 8 (1).
- Visetnan, S., Supungul, P., Hirono, I., Tassanakajon, A., and Rimphanitchayakit, V. (2015). Activation of *PmRelish* from *Penaeus monodon* by yellow head virus. *Fish Shellfish Immunol* 42(2), 335-344.
- Wang, D., Li, S., and Li, F. (2013a). Screening of genes regulated by Relish in Chinese shrimp *Fenneropenaeus chinensis*. *Dev Comp Immunol* 41 (2), 209-216.
- Wang, P.H., Fung, S.Y., Gao, W.W., Deng, J.J., Cheng, Y., Chaudhary, V., et al. (2018). A novel transcript isoform of STING that sequesters cGAMP and dominantly inhibits innate nucleic acid sensing. *Nucleic Acids Res* 46 (8), 4054-4071.
- Wang, P.H., and He, J.G. (2019). Nucleic acid sensing in invertebrate antiviral immunity. *Int Rev Cell Mol Biol* 345, 287-360.

- Wang, P.H., Huang, T., Zhang, X., and He, J.G. (2014). Antiviral defense in shrimp: from innate immunity to viral infection. *Antiviral Res* 108, 129-141.
- Wang, P.H., Liang, J.P., Gu, Z.H., Wan, D.H., Weng, S.P., Yu, X.Q., et al. (2012). Molecular cloning, characterization and expression analysis of two novel Tolls (*LvToll2* and *LvToll3*) and three putative Spatzle-like Toll ligands (*LvSpz1-3*) from *Litopenaeus vannamei*. *Dev Comp Immunol* 36 (2), 359-371.
- Wang, P.H., Weng, S.P., and He, J.G. (2015a). Nucleic acid-induced antiviral immunity in invertebrates: an evolutionary perspective. *Dev Comp Immunol* 48 (2), 291-296.
- Wang, P.H., Yang, L.S., Gu, Z.H., Weng, S.P., Yu, X.Q., and He, J.G. (2013b). Nucleic acid-induced antiviral immunity in shrimp. *Antiviral Res* 99 (3), 270-280.
- Wang, X.W., and Wang, J.X. (2013). Pattern recognition receptors acting in innate immune system of shrimp against pathogen infections. *Fish Shellfish Immunol* 34 (4), 981-989.
- Wang, Y.G., Hassan, M.D., Shariff, M., Zamri, S.M., and Chen, X. (1999). Histopathology and cytopathology of white spot syndrome virus (WSSV) in cultured *Penaeus monodon* from peninsular Malaysia with emphasis on pathogenesis and the mechanism of white spot formation. *Dis Aquat Organ* 39 (1), 1-11.
- Wang, Z., Chen, Y.H., Dai, Y.J., Tan, J.M., Huang, Y., Lan, J.F., et al. (2015b). A novel vertebrates Toll-like receptor counterpart regulating the anti-microbial peptides expression in the freshwater crayfish, *Procambarus clarkii*. *Fish Shellfish Immunol* 43 (1), 219-229.
- Wu, J., and Chen, Z.J. (2014). Innate immune sensing and signaling of cytosolic nucleic acids. *Annu Rev Immunol* 32, 461-488.
- Wyban, J. (2007). Thailand's White Shrimp Revolution. *Global Aquaculture Advocate*.
- Xiao, J., Liu, L., Ke, Y., Li, X., Liu, Y., Pan, Y., et al. (2017). Shrimp AHPND-causing plasmids encoding the PirAB toxins as mediated by pirAB-Tn903 are prevalent in various *Vibrio* species. *Sci Rep* 7, 42177.
- Yan, M., Li, C., Su, Z., Liang, Q., Li, H., Liang, S., et al. (2015). Identification of a JAK/STAT pathway receptor domeless from Pacific white shrimp *Litopenaeus vannamei*. *Fish Shellfish Immunol* 44 (1), 26-32.
- Yang, C., Zhang, J., Li, F., Ma, H., Zhang, Q., Jose Priya, T.A., et al. (2008). A Toll receptor from Chinese shrimp *Fenneropenaeus chinensis* is responsive to *Vibrio anguillarum* infection. *Fish Shellfish Immunol* 24 (5), 564-574.
- Zhang, R., Liu, R., Wang, W., Xin, L., Wang, L., Li, C., et al. (2015). Identification and functional analysis of a novel IFN-like protein (*CgIFNLP*) in *Crassostrea gigas*. *Fish Shellfish Immunol* 44 (2), 547-554.
- Zhang, Z., Yuan, B., Bao, M., Lu, N., Kim, T., and Liu, Y.J. (2011). The helicase DDX41 senses intracellular DNA mediated by the adaptor STING in dendritic cells. *Nat Immunol* 12 (10), 959-965.
- Zhu, X., Wang, D., Zhang, H., Zhou, Y., Luo, R., Chen, H., et al. (2014). Molecular cloning and functional characterization of porcine DEAD (Asp-Glu-Ala-Asp) box polypeptide 41 (DDX41). *Dev Comp Immunol* 47 (2), 191-196..



จุฬาลงกรณ์มหาวิทยาลัย
CHULALONGKORN UNIVERSITY

REFERENCES



จุฬาลงกรณ์มหาวิทยาลัย
CHULALONGKORN UNIVERSITY



จุฬาลงกรณ์มหาวิทยาลัย
CHULALONGKORN UNIVERSITY

VITA

NAME Suthinee Soponpong

DATE OF BIRTH 22 Sep 1990

PLACE OF BIRTH Bangkok, Thailand

HOME ADDRESS 36/538 Mathurose Home 11, Soi Pibulsongkram
22,
Pibulsongkram Road, Bangkhen, Muang
Nonthaburi,
Nonthaburi, 11000

PUBLICATION

1. Soponpong S, Amparyup P, Kawai T and Tassanakajon A (2019) A Cytosolic Sensor, PmDDX41, Binds Double Stranded-DNA and Triggers the Activation of an Innate Antiviral Response in the Shrimp *Penaeus monodon* via the STING-Dependent Signaling Pathway. *Front. Immunol.* 10:2069. doi: 10.3389/fimmu.2019.02069
2. Soponpong S, Amparyup P and Tassanakajon A (2018) A cytosolic sensor, PmDDX41, mediates antiviral immune response in black tiger shrimp *Penaeus monodon*. *Dev. Comp. Immunol.* 81:291-302. doi: 10.1016/j.dci.2017.12.013